SMAD1 IN THE TRANSFORMING GROWTH FACTOR - β SIGNALLING PATHWAY

BY

MOHAMMED HADI

A thesis submitted to the Faculty of Graduate Studies in partial fulfilment of the requirements for the degree of

MASTER OF SCIENCE

Department of Biochemistry and Molecular Genetics

UNIVERSITY OF MANITOBA

THE UNIVERSITY OF MANITOBA

FACULTY OF GRADUATE STUDIES

*****

COPYRIGHT PERMISSION PAGE

SMAD1 in the Transforming Growth Factor - ß Signalling Pathway

BY

Mohammed Hadi

A Thesis/Practicum submitted to the Faculty of Graduate Studies of The University of Manitoba in partial fulfillment of the requirements of the degree of

MASTER OF SCIENCE

DEDICATION

To my parents who encouraged me to study medicine

ACKNOWLEDGMENTS

I wish to thank my supervisor, Dr. Yuewen Gong for his guidance and support in this project. Special thanks are due to Dr. Hong Shen for isolating and providing me with rat hepatic stellate cells the use of which is described in this thesis.

I would like to acknowledge my academic committee advisors, Dr. Gerry Minuk, and Dr. Gilbert Arthur, for their critical assessment of this thesis.

TABLE OF CONTENTS

LIST OF FIGURES

LIST OF TABLES

ABSTRACT

We examined the relationship between Smad1 gene transcription and the transformation of hepatic stellate cells (HSC) into myofibroblast-like (MFBL) cells. We specifically aimed to determine the expression of Smad1 mRNA with regard to the transformation of the hepatic stellate cell, and whether Smad1 transcription is abated in response to signalling events that favour signalling by Smad2. We describe the cloning of rat Smad1 cDNA, and our attempt to clone the rat Smad1 5'-flanking region.

Smad1 mRNA expression in primary HSC cultures was shown to increase after 3 days, prior to transformation at day 6, and remain elevated after 9 days. A 1625bp nucleotide sequence of Smad1 cDNA was cloned and was shown to contain 4 amino acid substitutions over the published sequence. When used to analyze mRNA in HSC extracts that were treated with 2ng/ml and 5ng/ml TGF-β1, a decline in Smad1 mRNA levels was observed at 3 hours, followed by an increase to control levels thereafter. The cloning of the rat Smad1 5'-flanking region gave a 1078bp nucleotide sequence that aligns between exon1 and exon2 of rat Smad1 cDNA sequence revealing an exon splicing site at position 138.

Our results suggest a positive correlation between Smad1 transcription and the transformation of HSC into MFBL cells. Furthermore, Smad1 is down-regulated in TGF-β1 induced cells, indicating a possible control mechanism whereby the Smads regulate themselves.

I. REVIEW OF THE LITERATURE

1.1. Liver anatomy and cell morphology

The liver is the largest and metabolically most complex organ in mammals, and occupies a central role in metabolism. It is unique in that it has a dual blood supply through the *portal vein* and *hepatic artery*. The portal vein brings blood from the intestines and spleen, and the hepatic artery supplies the liver with arterial blood. Both vessels enter the liver through a fissure called the *porta hepatis* [1], where they branch to the right and left lobes. Anatomically, the liver is described in terms of *portal triads*, where each triad consists of the *portal vein radicle*, the *hepatic arteriole*, and *bile duct*. A functional division envisages a series of *acini*, each centred on the portal triad with its terminal branch of portal vein, hepatic artery, and bile duct. Small branches of each vessel, the *terminal portal venule* and *terminal hepatic arteriole* enter each acinus at the portal triad, where the pooled blood then flows through sinusoids between plates of hepatocytes. There is an exchange of nutrients across the *spaces of Disse*, which separates hepatocytes from the porous sinusoidal lining. The blood from the sinusoids in adjacent acini then merges at terminal hepatic venules, which eventually form the hepatic vein. All efferent blood drains into the *inferior vena cava*. Interference in hepatic blood supply is commonly seen in the manifestation of many liver diseases, including fibrosis and cirrhosis, and is often manifested by portal hypertension [2].

The *hepatocytes* are the parenchymal cells of the liver, and make up its bulk. They are polygonal in shape and contain three surfaces: the first faces and lies next to the

blood filled sinusoids and *space of Disse*, the second faces the *canaliculus,* and the third faces neighbouring hepatocytes. Hepatocytes are responsible for the liver's central role in metabolism, which includes the formation and excretion of bile, control of cholesterol metabolism, regulation of carbohydrate homeostasis, lipid biosynthesis and secretion of plasma lipoproteins, formation of urea, serum albumin, clotting factors, enzymes, and numerous other proteins, and metabolism or detoxification of drugs and other foreign substances [2].

The non-parenchymal cells surrounding the hepatocytes are the cells that line the sinusoids, and comprise at least four types: *endothelial cells*, *Kupffer cells*, *hepatic stellate cells (HSC)*, and *pit cells*. Endothelial cells lack a basement membrane and contain numerous pores (*fenestrae*), which permit the exchange of nutrients and macromolecules from the blood with the hepatocytes across the spaces of Disse. Endothelial cells also endocytose various molecules and particles, synthesize extracellular matrix molecules, and play a role in liver metabolism. The Kupffer cells are the resident macrophages of the liver, and are spindle-shaped cells that play an important part in the reticuloendothelial system. They originate from bone marrow precursors and become prominent in wound-healing during injury [3, 4]. Major functions include phagocytosis of foreign particles, removal of endotoxin and other noxious substances, and modulation of the immune response. Because of its Kupffer cells and rich blood supply, the liver is often secondarily involved in infections and other systemic disorders [2]. The third cell-type, the HSC, are also known as *lipocytes*, *perisinusoidal cells*, *fat-storing cells*, and *Ito* cells. They store vitamin A

and are involved in the synthesis of various matrix proteins. They are believed to be the major source of the hepatic fiber [2]. Finally, pit cells are believed to be tissue lymphocytes with natural killer cell functions. Their role in hepatic disorders is unknown.

The extracellular matrix (ECM) of the liver includes the organ's reticulin framework. The ECM is composed chiefly of collagens (predominantly types I, III, and IV), as well as non-collagenous proteins, such as glycoproteins (*fibronectin, laminin*) and proteoglycans (*heparan sulfate, chondroitin sulfate, dermatan sulfate, hyaluronate*), with the hepatocytes and sinusoids distributed within [1, 2]. Fibroblasts are found only in the portal tracts, and produce the ECM molecules required by the liver [2].

1.2. Liver fibrosis and the hepatic stellate cell

Fibrosis manifests itself when the liver is subjected to chronic injury. Injury may arise from excessive alcohol consumption, persistent viral and helminthic infections, and hereditary metal overload. The cellular mechanisms of fibrosis are shared among these insults [1, 5, 6]. The liver engages in "wound healing" [4, 5], during which excessive amounts of type I collagen is produced and deposited [7, 8], resulting in *scarring* [9]. Scarring is prominent when fibril-forming collagens (types I and II) are synthesized in place of basement membrane type IV collagen [7, 8, 10-12], and excess glycoconjugates, including proteoglycans, fibronectin, and hyaluronic acid are deposited within the space of *Disse*, but also when there is a reduced degradation of existing collagens and other extracellular matrix molecules. The resulting scar is an accumulation of fibrous tissue around the sinusoids, hepatic venules and the portal

tracts, and the loss of endothelial fenestrae, causing the obstruction of the free passage of substances from the blood to the hepatocytes through the space of Disse [13]. Hepatocyte microvilli begin to degrade, impairing the ability of these cells to perform the key functions of the liver.

While the mechanisms of fibrosis in early and advanced (cirrhotic) stages of liver disease are similar, early changes are reversible, whereas longstanding injury characterized by cross-linked collagen and regenerative nodules (cirrhosis) is not. For this reason, it is important to understand the mechanisms underlying the early fibrosing injury [1], and the regulatory factors involved in the various pathobiological conditions associated with excessive cellular proliferation. Numerous experimental and clinical studies have identified the presence of activated HSC that increase in number, surround the developing hepatic nodules, and infiltrate them with interstitial collagen [1-4, 6, 8, 9, 11, 13-18]. In normal livers, HSC are thought to be responsible for low-grade ECM synthesis in order to maintain the architectural framework of the liver [17], however in fibrosis, they are characterized by producing excessive ECM. Precisely what triggers HSC activation has yet to be identified, but *transforming growth factor (TGF)-β* derived from Kupffer cells [3, 5, 16], and the HSC itself [14, 16, 19] may play regulatory roles [15, 22], as well as initiating factors from other sources, such as hepatocytes [20], platelets and lymphocytes [1].

1.3. Model for hepatic stellate cell activation

HSC are precursors of fibroblasts, capable of proliferating and producing an excess of extracellular matrix [3, 4, 9]. In normal liver they are the major storage site of

retinoids, giving the morphological characteristic of cytoplasmic lipid droplets [23]. They contain *actin* and *myosin*, contract in response to *endothelin-1* and *substance P*, and express *desmin*, a cytoskeleton intermediate filament characteristic of muscle cells.

As a consequence of liver injury, normal (quiescent) HSC transform *into myofibroblasts-like (MFBL)* cells [21], a cell type that exhibits the phenotype of both myocytes (smooth muscle) and fibroblasts [4], and is common to wound healing in general [9]. The transformation of HSC into MFBL cells accompanies the *de novo* expression of smooth muscle *α-actin* [21, 24, 25]. *Endothelin-1* is synthesized which can stimulate reversible cell contraction [9], thus they may also have a role in blood flow regulation [9, 13]. The transformation of HSC into MFBL cells accompanies an active secretory apparatus for proteins [23]. The ECM molecules produced include at least three types of collagens (type I, III, IV), heparan sulfate, laminin, cellular fibronectin, tenasin, decorin, and biglycan. HSC and Kupffer cells [4] also release matrix proteinases and inhibitory molecules of matrix proteinases (*tissue inhibitors of metalloproteinases*, *TIMP*) [1, 4].

The process of HSC activation *in vivo* has been well characterized and includes the following four features: cell enlargement, local proliferation, enhanced fibrogenesis, and expression of smooth muscle-like features [1]. Activation occurs in two stages: the *initiation* stage, where cells enlarge and become more responsive to proliferative and fibrogenic cytokines through the up-regulation of receptors, notably TGF-β1; and

the *perpetuation* stage, reflecting the cellular response to these cytokines, which collectively enhance scar formation [5, 8]. New matrix produced by the transformed HSC perpetuates the activated phenotype, as well as cytokines secreted from the HSC itself that act in an autocrine manner [8, 16]. Initiation events are largely paracrine, occurring in response to early matrix changes [5]. Models of HSC activation emphasize both cell proliferation and increased fibrogenesis as the main event in fibrosis (Figure 1).

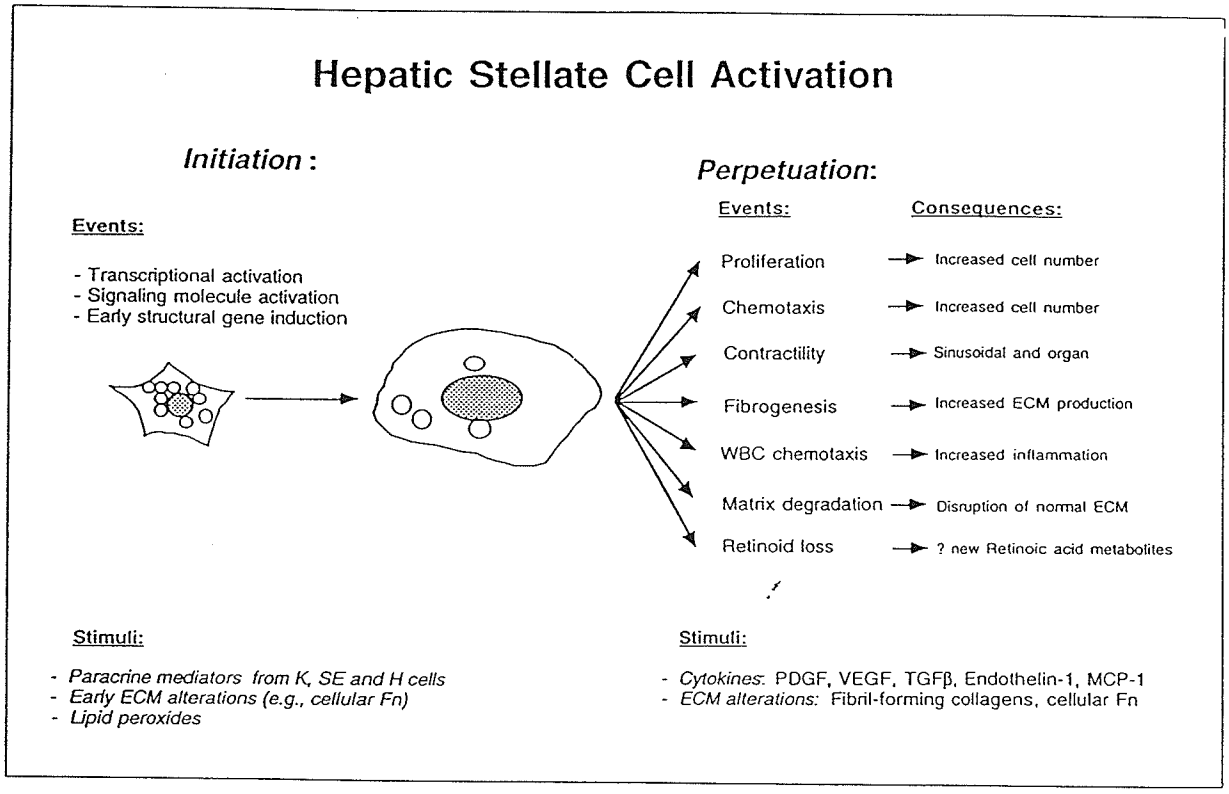

Figure 1:A model of hepatic stellate cell activation.
PDGF = platelet growth factor; VEGF = vascular endothelial growth factor; TGF-β1 = transforming growth factor-β1; MCP-1 = monocyte chemotactic peptide-1; ECM = extracellular matrix; K cells= Kupffer cells; SE cells = sinusoidal endothelial cells; H cells = hepatocytes; Fn = fibronectin. Figure from *Friedman* [5].

Kupffer cells are thought to be critical in the initial stages of HSC activation [14]. Along with activated macrophages, they produce inflammatory cytokines, some of which have a proliferative effect on HSC, such as *platelet-derived growth factor* (*PDGF*) [26], while others like TGF-β stimulate fibrogenesis thereby increasing collagen synthesis and perpetuating cellular atrophy [21, 27]. Numerous other growth factors and cytokines from hepatocytes, monocytes, and platelets can also affect the activation of HSC, including *fibroblast growth factor* (*FGF*), *interleukin-1*, *epidermal growth factor* (*EGF*), and *tumour necrosis factor-α* [28, 29]. In addition, thrombin and lipid peroxidation (from exposure to ethanol) may also be involved in this process [8].

Activation depends on changes in the cell's microenvironment. Changes in the activities of Kupffer cells, HSC, and endothelial cells may lead to decreased ECM degradation, as these cells are important in the degradation of extracellular components [30]. The metalloproteinases are involved in regulation of ECM, and consist of three main groups: *collagenases, gelatinases (type IV)* and *stromelysins*. These enzymes are synthesized primarily by Kupffer cells and activated HSC. The normal hepatic microenvironment may be disrupted when they release inhibitory molecules of matrix proteinases (*tissue inhibitor of metalloproteinases, TIMP*). As part of this process, activated HSC progressively replace the normal low-density matrix with one rich in fibril-forming collagens, which tends to perpetuate the activated phenotype. The relationship among the matrix metalloproteinases, their

inhibitors, and their substrate or substrates *in vivo* however has not yet been clarified [1].

1.4. The transforming growth factor (TGF) - β cytokine

The *transforming growth factor (TGF)-β* family members, which include the *TGF-βs, activins, bone morphogenic proteins (BMPs), Müllerian inhibiting substances, nodal, glial-derived neurotrophic factor, Lefty*, and others, are structurally related, secreted cytokines found in many invertebrate and vertebrate species ranging from worms and insects to mammals [31-34]. In mammals, the TGF-β superfamily consists of about 30 proteins, including 3 isoforms of TGF-β itself (TGF-β_{1-3}), 3 forms of activin, and over 20 BMPs [32, 35]. The name TGF-β was based on the growth factor's ability to stimulate fibroblast growth in soft agar, but TGF-β is actually a potent inhibitor of epithelial cell proliferation [36]. Every cell in the body produces both TGF-β ligands and its cognate receptors: functionally, they are microenvironmental regulatory molecules that signal cell cycle arrest, and have emerged as a major source of signals that control cell growth and differentiation [35]. Unlike classical hormones however, members of the TGF-β family produce different effects that depend on the type and state of cell [37].

1.5. Effect of TGF-β on target cells

TGF-β can often induce several effects on the same cell, depending on its location in organs [37]. This finding has suggested that different TGF-β polymorphisms may result in different signalling events [35]. A wide spectrum of cellular functions are

ascribed to these growth factors, such as cell proliferation, apoptosis, differentiation, migration, and wound healing [31, 32, 35]. They play a critical role during embryonic development by specifying developmental cell fate [35], and are involved in maintaining tissue homeostasis during adult life [31, 32]. Deregulation of TGF-β family signalling has been reported in auto-immune and vascular diseases [31], and their role in the life and death of cancer cells has been documented [38].

Some contradictory evidence exists regarding the effect TGF-β has on cell growth. Because cultured epithelial cells show an arrest in growth in response to TGF-β, it was initially identified as a potent growth inhibitor for many cell types [37]. It can inhibit cell growth through several mechanisms, including induction of G_1 arrest, promotion of terminal differentiation, and activation of apoptosis [39]; these growth inhibitory properties led researchers to speculate its involvement in cancer cells. In other cells, TGF-β appears to stimulate rather than inhibit cell growth. Besides growth, TGF-β regulates cell differentiation [40]. It can noticeably induce the synthesis of extracellular matrix in cells that are responsible for wound healing.

1.6. Secretion and binding of TGF-β ligands to type II and type I cell surface receptors

TGF-β isoforms are each encoded by a specific gene and are expressed in a tissue-specific fashion. They show strong homology to each other, and in the case of human TGF-β, are 70 – 80% homologous. Different isoforms are expressed in different cells, and have different binding affinities for TGF-β receptors [35, 41]. Structurally,

the family members are synthesized as large precursor molecules that contain a propeptide region in addition to the TGF-β ligand itself [34, 42]. After it has been secreted, most protein is stored in the extracellular matrix as a complex of TGF-β, the propeptide, and a protein called the *latent TGF-β binding protein (LTBP)* [35, 42]. The attachment of TGF-β to the LTBP prevents it from binding to its receptors. There are four LTBPs in total, each encoded by a distinct gene and expressed in a tissue-specific fashion [43]. The propeptide portion of the molecule has to be proteolytically cleaved to form biological active TGF-β capable of binding to receptors [34, 35, 44, 45]. The ligand can be activated by *thrombospondin –1 (TSP-1)*, a glycoprotein secreted by most cells and incorporated into the extracellular matrix [46, 47]. Once TGF-β is secreted, it interacts with a growing array of extracellular matrix proteins, some of which bind the ligand and make it unavailable for binding to receptors, while others may facilitate its binding [44]. If released, it elicits a cellular response through the formation of a heteromeric complex with specific *type I* and *type II* serine / threonine kinase receptors [31]. Three major classes of receptors have been identified: five different type II receptors, seven type I receptors (also known as *activin receptor-like kinases, ALK 1-7*) [31, 32], and a multitude of *type III* receptors [35]. Type III receptors are most abundant, and are not directly involved in signalling. Their function is to bind the TGF-β ligand and transfer it to the type II and type I receptors [35]. The dimeric ligand first binds to the type II receptor through its transmembrane domain, then recruits the type I receptor to form a heteromeric complex. The active complex must include both receptors for

proper activation and downstream signalling, presumably due to the dimeric nature of the ligand [44].

Cell signalling cascades involve phosphorylation events. The type II receptor is a constitutively active kinase [28], which upon ligand-binding trans-phosphorylates particular serine and threonine residues in the type I receptor juxtamembrane region, also known as the *GS box* [48]. The phosphorylation of the GS-box activates the type I receptor serine / threonine kinase activity, which in turn initiates downstream signalling by phosphorylating intracellular proteins called the *Smads* [31, 32, 48, 49]. Type I receptors thus act downstream of type II receptors, and determine signal transduction specificity within the heteromeric receptor complex.

1.7. Receptor specificity and ligand binding

Receptors show ligand-binding specificity, which determines the nature of signalling. Of the type I receptors, ALK-4 and ALK-5 are activin and TGF-β type I receptors, respectively. ALK-1 was recently identified as an endothelial specific TGF-β type I receptor. ALK-3 and ALK-6 are BMP type I receptors. ALK-2, initially implicated as a type I receptor for activin and TGF-β, is now regarded most important for BMP signal transduction. The ligand for ALK-7 remains to be identified [31, 32].

There are fewer receptor family members than there are ligand family members: this would suggest that multiple ligands share a given receptor. In addition, type II and type I receptors bind different ligands [44]. As a result, the TGF-β family members

often bind to more than one type II and type I receptor combination. Various combinations of ligand-receptor binding will determine the specificity of signalling [58] (Figure 2).

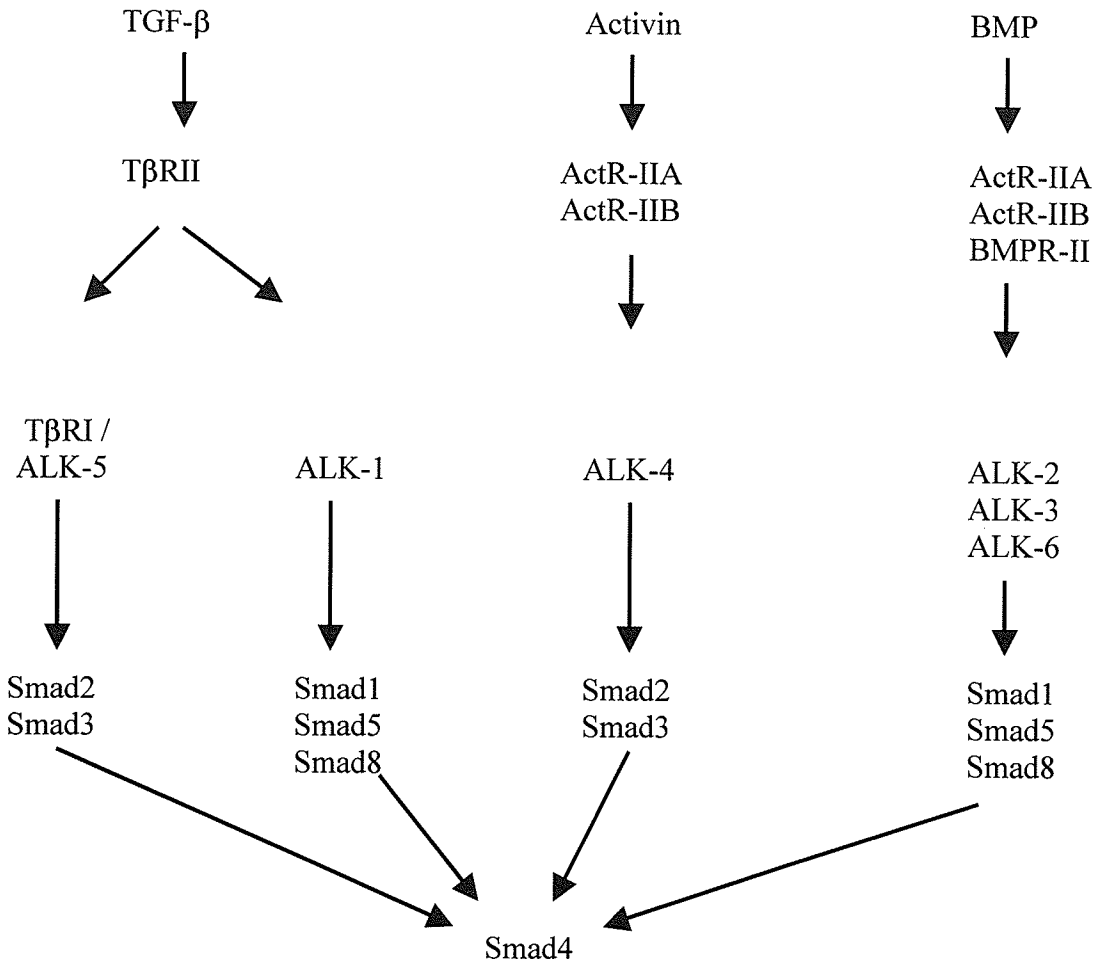

Figure 2: TGF-β signal transduction through type I and II receptors. Figure from *Susumu Itoh et al* [32].

1.8. Downstream signalling events: from type II / I receptors to the Smads

The *Smads* were discovered through genetic studies in *Drosophilia melonogaster* and *Caenorhabditis elegans*, and are pivotal intracellular mediators of TGF-β family members [31, 44, 59]. Shortly after cloning of TGF-β1 and activin in vertebrates [50], the first invertebrate member of the TGF-β superfamily, the *Drosophila decapentaplegic (dpp)* was identified [60, 61]. Genetic screens in *Drosophilia* identified the "*mothers against dpp" Mad* protein [62], which shared homology to three predicted polypeptides from the *C. elegans* genome [44, 63, 64]. The *C. elegans* sequences were subsequently found to correspond to three *Sma* genes (*Sma1*, *Sma2*, *Sma3*) [59]. At the same time, vertebrate Mad-related proteins were identified and shown to be implicated in BMP, activin, and TGF-β signal transduction. To avoid confusion with similar named proteins, the *Smad* moniker was adopted. It originates from a fusion between *Drosophilia "Mad"* and *C. elegans "Sma"* [31, 40, 65]. Subsequently, multidisciplinary efforts in *Drosophilia*, *C. elegans*, *Xenopus laevis* [66], and mammalian tissue culture have culminated in a molecular model for Smad-mediated signal transduction for two groups of TGF-β family ligands, one comprising the dpp / BMP2 / BMP4 subfamily, and a second comprising the activins / TGF-βs.

Eight Smads have been identified in mammals, and the family can be divided into three distinct subfamilies based on their structure and function in the TGF-β pathway:

receptor-regulated Smads (R-Smads), *common-partner Smads* (*Co-Smads*), and *inhibitory Smads* (*I-Smads*). The R-Smads can be further subdivided: those activated in response to TGF-β and activin type I receptors are designated Smad2 and Smad3 [67], while those activated by BMP type I receptors are named Smad1, Smad5, and Smad8 [31, 32, 41, 48, 68]. It has been suggested that the BMP-type Smads may also act indiscriminately with TGF-β receptors in addition to BMP receptors [32, 69]. Figure 3 shows the relative homology of the three Smad families.

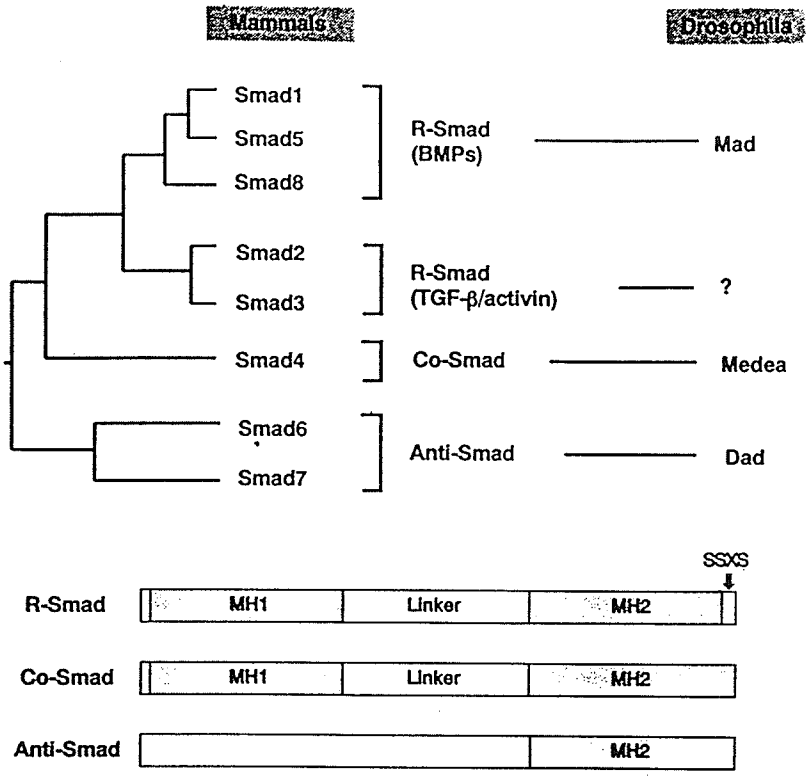

Figure 3: Classification and structures of Smads.
Smads are grouped into three classes depending on their structure and functions. Mammalian and *Drosophilia* Smads are listed. The I-Smads are also known as the antagonistic *anti-Smads.* Figure from *Masahiro Kawabata et al* [65].

1.9. Mechanism of action of the receptor-regulated and common-mediator Smads

R-Smads

Following the binding of the TGF-β ligand to type II and type I receptors on the cell surface, the activated type I receptor complex recruits and phosphorylates its designated Smad molecule. The *L45 loop* within the type I receptor kinase domain determines the specificity of Smad isoform activation [31, 70]. This interaction is specifically targeted and transient in nature [31, 65], and has been mapped to the "*L3 loop*" region in the C-terminal domain of the R-Smad protein [65, 70]. The amino acid sequence of the L3 loop is highly conserved, except for two amino acids between the TGF-β regulated Smads and the BMP-responsive Smads (Smad1, 5, 8). Exchange of these two amino acids switches the signalling specificity, including receptor interaction and phosphorylation [65]. After phosphorylation, the activated R-Smads recruits the common-mediator Smad4, and the heteromeric Smad complex translocates to the cell nucleus [71]. The nuclear Smad complex binds to DNA directly and / or indirectly through other DNA-binding proteins, where they regulate the transcription of target genes.

Co-Smad

Only one Co-Smad (Smad4), has been identified in mammals, although two isoforms, *Smad4α* and *Smad4β* (also known as Smad10) have been described in *Xenopus*. Co-Smads act by forming heteromeric complexes with all phosphorylated R-Smads, and

are thus shared components in TGF-β, activin, and BMP signal transduction [72]. They do not appear to have specificity for different ligand signals [44].

1.10. Structure and activation of R- and Co-Smads

Smads are molecules of relative molecular mass ranging from 42K to 60K [41]. The R- and Co-Smads have highly conserved amino-acid sequences at their N- and C-termini, which are termed *Mad homology* MH1 and MH2 domains, respectively. The two domains are connected to a less conserved, divergent proline-rich linker region of variable length [31, 41, 65] (Figure 4).

MH1 domain

The MH1 domain of the R-Smads and Co-Smad4 (except for Smad2) can bind to specific DNA sequences. For the interaction of Smad1 with ALK-1 or ALK-2 receptors, in addition to the L3 loop in the MH1 domain, an *α-helix (H1)* domain in MH2 is also required (Figure 4). The MH1 domain of Smad2 contains structural differences to the MH1 domain of other R-Smads, including the absence of a nuclear localization signal.

MH2 domain

The MH2 domain of the R-Smads determines the specificity of the interaction with type I receptors. They are distinguished from the MH2 domains of the other two Smad classes by an SSXS motif at the C-terminal end, which is the region of transient interaction with the type I cell receptor. Phosphorylation of the last two serines allows for the oligomerization with the common-mediator, Smad4 [65, 72].

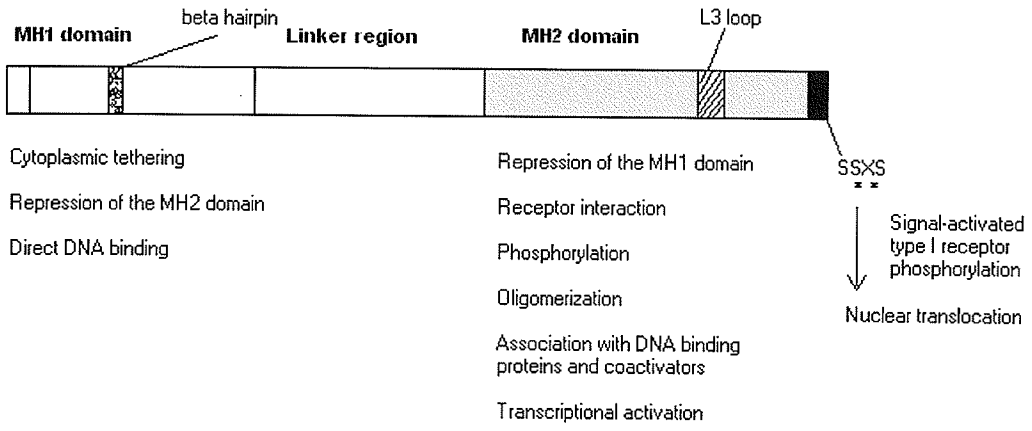

Figure 4: Functions of the MH1 and MH2 domains of R-Smads.
The functions of the MH1 and MH2 domains are summarized. The regions repress each other through intramolecular interactions. The last two serines (with asterisks) of the SSXS motif are phosphorylated by type I receptors. Figure adapted from *Laurel A. Raferty* [44] and *Masahiro Kawabata* [65].

The heteromeric complex becomes capable of translocating to the nucleus [32]. Smad4 contains MH1 and MH2, domains, but not the SSXS motif, and is therefore not a phosphorylation target by type I receptors.

Interaction of MH1 with MH2

In their normal, resting cytoplasmic form, the MH1 and MH2 domains interact with one another, rendering the Smad molecule inactive. Removal of the MH1 domain induces transactivation by the MH2 domain [41]. The MH2 domain on the other hand represses the DNA binding activity of the MH1 domain. Thus the two domains interact to repress each other [65]. Phosphorylation of the SSXS motif on the MH2 domain induces a conformational change in the protein structure, which results in the activation of the Smad protein and relieves mutual repression.

Cytoplasmic and nuclear forms of Smads

All three classes of Smads including the R-Smads, Co-Smads, and I-Smads exist as monomers in the absence of ligand [65]. TGF-β stimulation induces homo-oligomerization of the R-Smads with Smad4 [72]. Two lines of evidence indicate that Smads function as oligomeric complexes. The first line is the signal-dependent association of Co-Smads with R-Smads. The second line is based on crystal and solution structure analysis of the isolated C-terminal MH2 domain of vertebrate Smad4, where it has been shown to have the ability to form trimers [44, 65], thus it is believed the homo- and hetero-oligomerization of Smads function in trimeric form.

All Smads share the ability to form trimers, as the amino acids of the homomeric contact faces are highly conserved. R-Smads and Co-Smads alter amino acids on this contact face. Thus the capability to form trimers appears to be essential for function [44]. It has been suggested that both R-Smads and Co-Smads normally exist as homotrimers and that signal-dependent Smad complexes are heterohexamers [44]. In contrast, the requirement for three Smad proteins in each of the two *C. elegans* TGF-β family signal transduction pathways has been interpreted to indicate that Smads function in heteromeric complexes of three different Smad proteins. Other studies have found that R-Smads exist as monomers in the absence of the TGF-β signal and only associate in homomeric complexes in the presence of signal [44].

Smad anchor for receptor activation (SARA), a member of the membrane-associated FYVE-domain-containing proteins, has been shown to present Smad2 and Smad3 to the activated type I receptor [73]. The FYVE domain in SARA, which consists of two zinc-finger motifs, may bind to phosphatidylinositol-3-phosphate and thereby tether SARA at endosomal membranes. SARA interacts with the R-Smads and the TGF- β receptor through its *Smad binding domain (SBE)* and C-terminal region of SARA, respectively. Upon C-terminal phosphorylation of Smad2 and Smad3, the affinity decreases between type I receptor and Smad, as well as between Smad and SARA, and results in the dissociation of the complex between TGF-β receptor, activated R-Smad and SARA. Binding of R-Smad to SARA or Smad4 is mutually exclusive; after heteromeric complex formation of Smads, SARA is available for recruitment of other Smads for their activation [31]. Recently, microtubules were

identified as another subcelluar regulator for Smads. Immunofluorescence microscopy and biochemical studies showed that Smad2, Smad3, and Smad4 co-localize and interact with β-tubulin [31, 74].

1.11. Regulation of the subcellular distribution of R- and Co-Smads

Regulated translocation to the nucleus is a key event for induction of gene expression [44]. The R-Smads and Co-Smad4 are cytoplasmically localized in tissue culture in the absence of signal [31], but are predominantly located in the nucleus in the presence of actively signalling receptors. Whereas ligand-induced nuclear accumulation of R-Smads is not dependent on expression of Co-Smads, Co-Smads require association with activated R-Smads to enter the nucleus [31, 44, 65]. Thus the driving force for nuclear accumulation of the Smads lie with the R-Smads.

An N-terminal, basic, *nuclear localization-like sequence* (*NLS-like*; lys-lys-leu-lys), that is conserved among all R-Smads, was shown to be required for TGF-β-induced nuclear import of Smad3 [65, 75]. In another report [76] however, deletion of the MH1 domain and linker region caused nuclear accumulation of Smad2 [65]. It has been suggested that the MH2 domain may contain the signal for nuclear transportation, and / or the MH1 domain may be responsible for cytoplasmic retention [65]. A functional leucine-rich *nuclear export sequence (NES)* was identified in Smad4 that ensures cytoplasmic localization in unstimulated cells [31]. TGF-β induced heteromeric complex formation of Smad4 with R-Smads was found to inactivate the NES of Smad4. The nuclear entry of the Smad4 / R-Smad complex may be stimulated upon unmasking of the NLS on R-Smad upon their heteromeric complex formation [31].

1.12. Smad binding to DNA and nuclear function

The MH1 domain of Smad3 and Smad4 has the ability to bind to a specific DNA consensus binding sequence (5'-AGAC-3') also called the *Smad-binding element (SBE)* [65]. Whereas the full-length protein of Smad4 can bind SBE, Smad3 DNA binding requires the C-terminal phosphorylation by type I receptor kinase or an artificial truncation of the Smad3 protein removing its MH2 domain. SBEs have been found in multiple TGF-β responsive promoter regions, including *Smad7, Smad6,* the *plasminogen activator inhibitor-1 (PAI-1), JunB, type VI collagen, α2(I) procollagen,* the *germline immunoglobulin Iα region,* and *platelet derived growth factor-(PDGF)B chain* [31, 82]. Smad4 has been shown to bind directly to a specific sequence around an AP-1 site in the collagenase promoter [65].

The crystal structure of the Smad3 MH1 domain with SBE has revealed a conserved β-hairpin structure that is embedded in the major groove of the target DNA that is responsible for direct DNA contact. The β-hairpin is conserved among R-Smads and Co-Smads. Smad3 and Smad4 have also been reported to bind to GC-rich sequences. This would suggest that the DNA binding specificity of β-hairpin loop of DNA is not so strict, or that there are possible multiple DNA interaction surfaces on Smads. Smad2 lacks the ability to bind to DNA, even though it shares 92% homology with Smad3 [77]. It contains a small exon upstream of the β-hairpin loop – removal of this exon confers the ability of Smad2 to bind to DNA. Smad1 can bind to DNA indirectly through Smad4 [31, 77].

1.13. Smad transcriptional co-activators and co-repressors

TGF-β signalling serves a broad range and multifunctional nature of cell activities. Members of the TGF-β family regulate the transcription of various genes, including cell cycle regulators, extracellular matrix adhesion molecules, homeobox genes, and ligands themselves. Smads are the messengers that convert the phosphorylation signal at the cell surface to gene expression in the nucleus, and therefore they serve as transcriptional regulators.

The structurally related *p300* and *CBP* co-activators were shown to interact in a ligand-dependent manner with R-Smads through the MH2 domain to induce gene expression [65]. p300 / CBP associates with various DNA binding proteins, including *c-Jun* and *c-Fos*, and may act as a bridging factor between Smads and other transcription factors [65, 78, 79]. They may promote transcription by facilitating the interaction of Smads with basal transcriptional machinery or through their intrinsic (or recruited) histone acetylase activity, which loosens chromatin structure. *MSG1*, a 27-kDa nuclear protein with strong transcriptional activity without the ability to bind directly to DNA, was found to stabilise the interaction of Smad4 with p300 / CBP, and acts as a Smad4 co-activator [31].

Smads have also been found to interact with transcriptional co-repressors. One such molecule is *TGIF*, a homeodomain protein that can bind histone deacetylases *(HDACs)*. The promoter to which the Smad-TGIF complex is targeted, may be inhibited through recruitment of HDACs [31].

Smad nuclear interacting protein (SNIP) 1 has been isolated as another repressor for TGF-β signalling. SNIP1 suppresses p300 / CBP-dependent TGF-β signalling through its interaction with p300 / CBP as well as Smad4 [31].

1.14. Transcriptional factors interacting with Smads

TGF-β family members may induce different gene responses in different cell types. The intrinsic DNA binding ability of Smads cannot explain how different target genes are selected in a cellular context-dependent manner. To provide target gene specificity, transcription factors must interact with Smads.

Recent work on the *Xenopus Mix2* early response gene has identified a novel transcription factor with a winged helix / forkhead motif, *FAST-1 Xenopus forkhead activin signal transducer (FAST)-1* was the first transcription factor partner for Smads to be identified. Nuclear FAST-1 binds the *activin response element (ARE)* in *Xenopus Mix2* promoter, but requires Smads for efficient DNA binding and activation gene transcription. SBEs are found in close proximity to FAST-1: Smad2 interacts directly with FAST-1, and Smad4 promotes this interaction. FAST-1 interacts directly with Smad2 in an activin-dependent manner. Smad4 is incorporated into the complex, and promotes DNA binding through its MH1 domain and activates transcription through its MH2 domain. The consensus sequence of human FAST-1 was shown to be TGT (G/T) (T/G) ATT and has been termed *FBE* (for *FAST-binding element*). Reporter genes with either a single FBE or SBE do not respond to TGF-β, however a reporter with a combination of FBE and SBE responds to TGF-β in the

presence of human FAST-1. These results indicate that both sites may be required for the activation of FAST-1 responsive genes [65]. A large number of transcription factors have been found to associate with Smads and regulate the transcriptional activity of TGF-β family members responsive genes. Regulation can be positive, or negative [31].

FAST-2 is another mammalian homolog of FAST-1, and is an activin-responsive gene. FAST-2, like FAST-1 interacts with Smad2 in a ligand-dependent manner. FAST-2 activates a reported gene with an activin responsive element in the presence of Smad2 and Smad4. The binding sites for FAST-2 and Smad4 were found to be AAT CCA CA on the activin-responsive gene, which is the sequence of the FBE found for FAST-1.

Smad4 binds to GC-rich sequences around FBE where four GCCG motifs exist. FAST-2 binds to DNA constitutively, whereas Smads require FAST-2 for DNA binding, suggesting that the affinity of Smads for DNA is relatively low. Thus, FAST-2 recruits that Smad complex to a specific site on the DNA and Smads activate transcription [65]

Smads are unique in DNA binding, as they are tethered to DNA not only via interaction with other DNA-binding proteins such as FAST-1, but also directly to specific DNA sequences. *Medea*, the *Drosophilia* Smad4 homolog, was also found to directly bind to DNA. Both have been found to bind to a consensus sequence of CGC

CGC (G/C)G(C/A) C on the *Drosophilia tinman* gene. In addition, an adjacent sequence GAATGT was found to be necessary for proper gene expression. This sequence is closely related to the FAST-1 binding site, suggesting the existence of another essential transcriptional cofactor [65].

1.15. Signalling cross talks through Smads

Members of the TGF-β superfamily act in environments where multiple signals interact, and are thus likely to cross-talk with other signalling pathways. *Calmodulin*, a central molecule in calcium signalling, interacts with Smads in a calcium-dependent manner [65]. EGF induces phosphorylation of the linker region of Smad1 through activation of *ERK kinase*, and inhibits its translocation from the cytoplasm to the nucleus. EGF may thus antagonize BMP signalling through Smad1.

Both synergistic and antagonistic regulations between the TGF-β superfamily and the *MAPK cascade* are known, and Smads may be the site of intersection [65].

1.16. Inhibitory Smads: the I-Smads

The first two classes of Smads, the R-Smads and Co-Smad, have central roles in signal transduction. The third class, the I-Smads, antagonizes signal transduction. The I-Smads lack the C-terminal MH2 phosphorylation site that is found in the R-Smads, and are not phosphorylated [32]. To date, two I-Smads have been identified in mammals, Smad6 and Smad7. These have been identified as inhibitors of the TGF-β, activin, and BMP signalling, and are believed to function in negative feedback loops since TGF-β, activin, and BMPs are all able to induce their expression [32, 80, 82].

I-Smads interact by complexing with activated type I receptors, thereby denying access to the receptor kinase for R-Smads phosphorylation and activation. Smad6 appears to inhibit the phosphorylation of BMP Smads [31], although this is controversial [32]. On the other hand, Smad7 interacts with all type I receptors and is considered a general inhibitor of TGF-β family signalling [31]. The WD-domain containing protein, *serine / threonine kinase receptor-associated protein (STRAP)*, interacts with Smad7 [35]. STRAP potentiates the inhibitory effects of Smad7 by recruiting Smad7 to the TGF-β receptor [31]. No molecules recruiting Smad6 to the activated type I receptor have been reported thus far [31]. Other than by competing with R-Smads for the activated receptor, other mechanisms have been proposed for the inhibitory effect of Smad6. One such mechanism is competitive inhibition of Smad6 for Smad4 heteromeric complex formation, thereby reducing its availability for complexing with activated Smad1 [31, 32]. Thus Smad6 may interfere with TGF-β family member signalling pathways at different levels in the signal transduction pathway.

Positive functions have been ascribed to I-Smads. Smad6 or Smad7 were found to enhance TGF-β induced adipocyte differentiation. In addition, up-regulation of Smad7 by TGF-β was shown to mediate apoptosis of prostate carcinoma cells; expression of anti-sense Smad7 mRNA inhibited TGF-β induced programmed cell death. The molecular mechanism by which these positive effector functions for I-Smads are achieved is unclear [31]. While Smad7 mRNA expression is rapidly up-

regulated by R-Smads, Smad6 mRNA is induced after several hours and is maintained for 48 hours or more [48].

In the absence of ligand stimulation, I-Smads are predominantly found in the nucleus. TGF-β stimulation was shown to result in an export of Smad7 from the nucleus. The MH2 domain of Smad7 is sufficient for ligand-induced nuclear export. The molecular mechanisms through which I-Smads are exported are unknown.

Smad6 and Smad7 mRNA are potently induced by TGF-β family members. I-Smads may thus act in an autocrine negative feedback loop to control intensity and duration of TGF-β signalling responses [82]. I-Smads are direct target genes; the promoters for Smad6 and Smad7 genes have been characterized and found to contain SBEs and other critical sequences that bind Smads. Thus I-Smads alone or together with other molecules can regulate signalling of TGF-β family members in a negative as well as positive manner [31].

A proposed model of Smad signalling involving the TGF-β cytokine and the inhibitory Smads has been described by *Chen et al* [82]. Here, an increase in the TGF-β cytokine causes the cell to regulate signalling events through direct binding of the Smad3 / Smad4 complex with the SBE sequence in the Smad7 promoter. In conjunction with the up-regulation of Smad7, it is stipulated that the binding of the Smad3 / 4 complex to the promoter region of Smad7 favours an increase in Smad7 mRNA synthesis resulting in a negative feedback loop that regulates the length and

intensity of TGF-β and activin signalling. Similar observations have been reported between BMP signalling and Smad1, Smad5, and Smad6 binding.

1.17. TGF - β1 ligand binding and liver fibrosis

The most potent fibrogenic mediator identified so far is TGF-β1 [4, 16]. In its latent form, it exists as a 390 – 391 amino acid propeptide that is incapable of binding to TGF-β receptors unless made active by proteolytically cleaving an arg-arg cleavage site between residues 278 – 279 [42, 45]. The mature form is a 25kDa homodimeric protein of 112 amino acids derived from the carboxy-terminus of the propeptide [42, 50, 51]. TGF-β1 is derived from various cell types, and has regulatory roles in cell growth and differentiation [3, 45]. In fibroblasts, it has been shown to stimulate the production of ECM such as collagen and fibronectin, and also inhibits their degradation [3, 45]. Addition of exogenous TGF-β1 results in proliferation of HSC in rats [52], promotes wound repair [3, 53, 54], and a localized fibrotic response [3]. TGF-β1 is probably the major inhibitor of hepatocyte proliferation and is strongly expressed in non-parenchymal cells during liver regeneration. Experimentally TGF-β1 exerts both positive and negative effects, depending on the cell type and culture conditions [1].

A model for studying liver fibrosis is the activation of cultures of HSC. Rat HSC *in vitro* undergo a transition into MFBL cells, which is paralleled by a drastic drop in retinyl ester content and a more than tenfold increase in collagen (mainly type I) [19, 55], events that closely mirror the hepatic fibrotic response *in vivo*. Typically

transformation occurs within 1 –2 weeks [55]. Using this model, experiments have shown that TGF-β stimulates collagen and proteoglycan synthesis, and that in acute liver injury induced by administrating carbon tetrachloride (CCl_4) to rats, the level of TGF-β mRNA rises significantly [28], along with an increase in smooth muscle α-actin expression [18]. An increase in collagen type IV and fibronectin mRNA levels in transformed HSC [56], strongly suggest a central role of TGF-β in hepatic fibrosis [57].

II. HYPOTHESIS

In this study, we attempted to examine the relationship between Smad1 transcriptional activity and the transformation of hepatic stellate cells into myofibroblast-like cells. We hypothesize that the transcriptional activity of Smad1 increases in hepatic stellate cells prior to their transformation into myofibroblast-like cells, and that a regulatory process exists among the Smads in which the transcription of Smad1 is down-regulated in response to events that favour signalling by Smad2. Furthermore, we attempt to clone the rat Smad1 5'-flanking region, as we predict that the regulation of Smad1 transcription is a key event in liver fibrosis.

Our objectives are as follows:

1. To examine the expression levels of Smad1 mRNA in rat hepatic stellate cells before and after the transformation into myofibroblast-like cells.
2. To clone rat Smad1 cDNA.
3. To study the effect of the TGF-β1 cytokine on the expression of Smad1 mRNA in rat hepatic stellate cells, a condition that favours intracellular signalling by Smad2.
4. To clone the 5'-flanking region of the rat Smad1gene.

III. METHODS

3.1. PCR analysis of Smad1 expression during activation of HSC

3.1.1. Isolation of hepatic stellate cells from rat liver

The method of HSC isolation was adapted from Friedman SL (Hepatology 1992 Feb; 15(2): 234-43). A brief description follows: to isolate HSC, the liver of an an-aesthetized Sprague-Dawley male rat was cannulated and perfused for 10 minutes at 37^0C in a buffer containing 0.015% collagenase H, 0.2% pronase, and 0.001% DNase (all from Boehringer Mannheim, Indianapolis, IN) in 300ml of Gey's balanced salt solution (GBSS). After sufficient perfusion, as determined by the tenderness and colour of the liver (typically 10 – 20 minutes), the liver was removed from the rat and placed in a sterile plastic dish, where it was stroked to disperse the cells. The cell tissue extract was transferred to 200ml of incubation buffer (identical to the perfusion buffer) and incubated for 30 minutes at 37^0C under constant stirring. This was filtered through sterile gauze to remove undispersed tissue and other material, and HSC were isolated and purified from other tissue components and foreign cells using a density centrifugation method that employs a gradient of 11.3% Nycodenz with NaCl. This method has been shown to give cultures of HSC of consistent quality, free from other cell types and contaminants. The cells once isolated and purified, were seeded at a concentration of $3x10^6$ / ml in 100mm sterile, plastic-coated dishes (Corning, New York, NY), and assessed by light microscopy for purity and viability.

3.1.2. Cell Culture

The primary culture HSC used in this experiment were cultivated by placing the cell

dishes in an incubator at 37^0C saturated with 95% O_2 / 5% CO_2. Cells were cultivated in DMEM with 10% cool-calf serum and were examined under a phase-contrast microscope. Culture medium was replaced every two days. The culture medium for this cell type was prepared by dissolving 13.5g of Dulbecco's Modified Eagle Medium ("DMEM" from GibcoBRL, supplied by Life Technologies, Rockville, MO) powder in 920ml ddH_2O and 10ml HEPES saline buffer (0.283M NaCl, 0.023M HEPES acid, 1.5mM Na_2HPO_4, diluted to 2 litres in ddH_2O). The pH when measured was determined to be between 7.2 and 7.3. 50ml of 10% cool calf serum (Cool Calf 2, Sigma, St. Louis, MO), 10ml of 1x Penicillin-Streptomycin (GibcoBRL, Life Technologies, Rockville, MO) and 10ml of L-glutamine (Sigma, St. Louis, MO) were added to give a final volume of 1000ml. The solution was filtered through a 0.2μ sterile filter, and stored at 4^0C until use. At the end of the experiment, all culture medium was drained from the dish, and the dish was stored at -70^0C until RNA could be isolated from the cells.

3.1.3. Isolation of RNA from HSC

Total RNA was isolated from primary HSC using the Trizol-LS reagent (Life Technologies, Rockville, MO) as follows: each cell culture-dish was incubated for ten minutes with 2.5ml of Trizol-LS at room temperature under mild agitation. The red reagent - cell extract from each plate was transferred to separate plastic tubes and shaken vigorously by hand for 15 seconds with 0.67ml chloroform, followed by incubation at room temperature for 10 minutes. The tubes were centrifuged for 15 minutes at 12,000g, after which the colourless, upper phase was removed, transferred

to a different tube, mixed with 1.67ml isopropanol, incubated at room temperature for 10 minutes, and then centrifuged for 15 minutes at 12,000g. The clear liquid was drained, leaving behind a small, white pellet. After air-drying for 10 minutes, the pellet in each tube was dissolved in two volumes of 15µl sterile water, and transferred to separate, sterile 1.5ml Eppendorf tubes. RNA samples were quantitated by spectrophotometry at 260nm using the BioRad SmartSpec 3000 spectrometer (BioRad, Hercules, CA). In total, three RNA samples were available from the cell-extracts of primary HSC that were in culture for 1, 3, and 9 days. These were labelled P1, P3, and P9, respectively. Samples were stored at -70^0C until further use.

3.1.4. 1st Strand Synthesis

The Advantage RT-PCR Amplifier Kit (CLONTECH Laboratories, Palo Alto, CA) was used to synthesize 1st strand cDNA from total RNA samples described above. A brief description of the method is given here: 1µg of each RNA sample (P1, P3, P9) was mixed with 1µl 20mM random hexamer primer in a thin-walled 200µl PCR tube, and heated for 2 minutes at 70^0C. To each of the three tubes (P1, P3, P9) were added 4µl 5x Reaction buffer (250mM Tris-HCl pH 8.3, 375mM KCl, 15mM $MgCl_2$), 1µl 10mM dNTP mix, 0.5µl recombinant RNA inhibitor, and 1µl Moloney-Murine Leukaemia Virus (MMLV) reverse transcriptase (200units/µl). The tube contents were mixed, and incubated at 42^0C for 1 hour, followed by brief immersion into a hot-water bath at 94^0C to stop the cDNA synthesis reaction, and to destroy DNase activity. The single-stranded DNA samples were diluted to 100µl by adding 80µl diethylpyrocarbonate (DEPC)-treated water. Samples were stored at -70^0C until

further use.

3.1.5. Polymerase Chain Reaction

5µl of each single-strand cDNA sample (P1, P3, P9) were used in PCR under cycling conditions described in Table 1. PCR was performed in 200µl thin-walled tubes using the Eppendorf Scientific Mastercycler (Brinkmann Instruments, Westbury, NY). PCR mixtures were prepared by pipetting into a 1.5ml tube 36µl ddH_2O, 5µl 10x Advantage 2 PCR buffer, 1µl 50x dNTP mix, 1µl 50x Advantage 2 Polymerase mix, and 1µl of each sense and anti-sense Smad1 primer. Primers are described in Table 2 and Section 3.2.1. Controls were employed to determine whether each sample contained equal amounts of 1^{st} strand DNA, thus enabling us to compare the relative expression of Smad1 among the three samples. Control reactions were made up as above, but by substituting 2µl of 10mM premixed human G3PDH primers (supplied in the Advantage RT-PCR kit) in place of the two Smad1 primers. Additional reactions using 10µl of the RNA sample were carried when the intensity of G3PDH expression (indicative of RNA sample quality) was not consistent among the samples. All reaction products were stored at -4^0C until further analysis.

3.1.6. Analysis of PCR products

PCR products from all samples were analysed on a 1.2% agarose / ethidium bromide (EtBr) gel under short-wave ultraviolet light, and the gel was photographed using a Polaroid camera. The photographs were scanned into a Power Macintosh computer using the Hewlett Packard HP 6100 C high-resolution scanner. The densitometric

Table 1: PCR reaction conditions for Smad1 cDNA cloning

NAME	CYCLES	DENATURATION	ANNEALING	EXTENSION
SMAD1	31	94^0C, 1 minute	59.5^0C, 30 seconds	72^0C, 4 minutes

Start: 94^0C, 2 minutes

End: 72^0C, 8 minutes

Table 2: PCR primer design for amplifying Smad1 cDNA

NAME	SEQUENCE	START SITE
GSP-1C	5'-TCC TAC CTT TCC GAA CCG AAG A-3'	179 - 201
GSP-2C	5'-GAG GTC AAG TAT CAC GGA TCC TTT AC-3'	1778 - 1804
Product length: 1625bp		

values obtained from both Smad1 and G3PDH expression were determined by the NIH-Image computer-imaging program (NIH-Image 1.61 download from <*http://www.info.nih.gov/nih-image*>), and were used for quantifying rat Smad1 cDNA expression. To obtain maximum resolution, the images of the bands (white) were inverted with the background (black), and a filter was employed to subtract background noise. The values of expression of Smad1 mRNA, as given by its cDNA expression, were represented as a graph of corrected expression intensity against the number of days of HSC incubation.

3.2. The cloning of rat Smad1 cDNA and the analysis of Smad1 in HSC

The polymerase chain reaction (PCR) cloning of Smad1

3.2.1. PCR primer design

Two primers were designed for the amplification of rat Smad1 cDNA using the Oligo Primer Analysis Software (Version 5.1, National Biosciences Inc, Plymouth, MN), and the published rat Smad1 cDNA sequence as the template for primer design (GenBank Accession Number U66478). Primers were designed for optimal PCR conditions, which include a minimum annealing temperature of 70^0C, a primer length of no less than 22 nucleotides, a GC content ranging between 45 – 60 %, and 3'-terminal ends that are not complementary to each other, and do not contain more than three GC nucleotides in the last six positions of the 3'-end. Primers were chosen to encompass the longest, continuous reading frame for the Smad1 gene, which was determined to be from position 316 to 1722 by using the GeneJockey Sequence

Processor software (Biosoft, Cambridge, UK) (Figure 5). The sequence of the designed primers and length of the predicted PCR product is listed in Table 2.

Primers were synthesized by GibcoBRL Custom Primers (Life Technologies, Burlington, ON) in lyophilised form, and were reconstituted with TE buffer (10mM Tris-Cl, 1mM EDTA, pH 8.0) to a concentration of 100μM, then diluted further with TE to 10μM for direct use in PCR. The optimal annealing temperature of the primer pair was determined to be 59.5°C.

3.2.2. PCR Protocol

PCR reagents chosen for this experiment were the Advantage 2 PCR System and rat-brain Marathon cDNA template, both supplied by Clontech Laboratories, Palo Alto, CA. PCR was performed on both the MJ Research Minicycler (MJ Research, Waltham, MA) as well as the Eppendorf Mastercycler (Brinkmann Instruments, Westbury, NY). The cycling protocol used is given in Table 1. Each reaction was prepared in 200μl thin-walled PCR reaction tubes contained 36μl PCR-grade water, 5μl 10x Advantage 2 PCR buffer, 1μl 50x dNTP mix, 1μl of each 10mM custom primer, and 1μl 50x Advantage 2 Polymerase mix, initially prepared as a Master Mix sufficient for three reactions. Two aliquots of 49μl each were pipetted into separate tubes; to the first, 5μl of rat Marathon cDNA were added, to the second, 5μl of PCR-grade water.

3.2.3. Analysis of Smad1 PCR products

Figure 5: Open-reading frame for rat Smad1

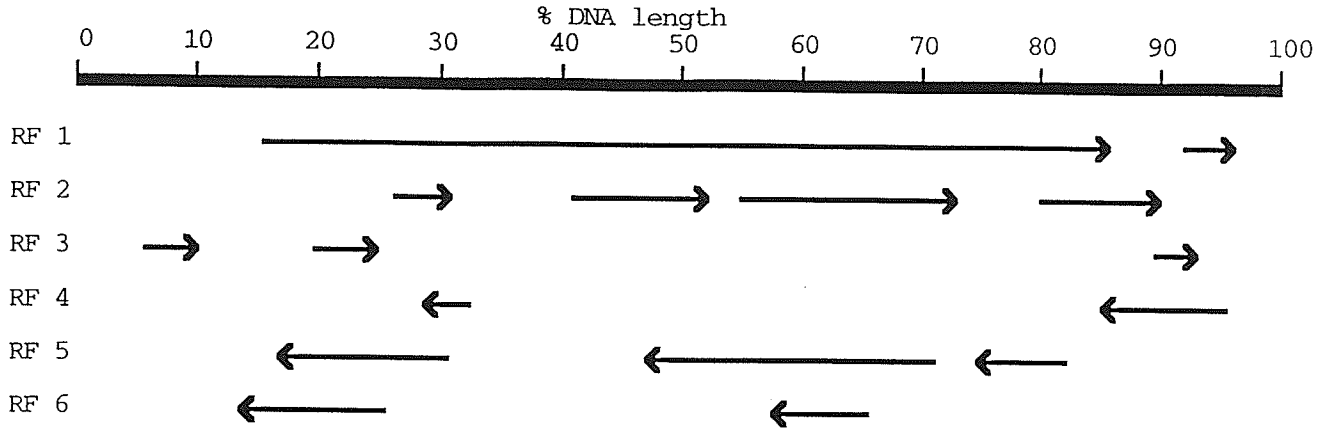

Figure 5: RF 1 represents the longest, continuous reading frame for the Smad1 gene and occurs from position 316 to 1722 of the sequence. PCR was designed to clone a product that encompasses this sequence.

The initial analysis of the amplified PCR products was performed by electrophoresis of 5µl of each tube contents on a 1.2% agarose / ethidium bromide (EtBr) gel in TBE buffer (108g Tris base, 55g boric acid, 40ml 0.5M EDTA pH 8, dissolved in H_2O to a total volume and diluted 10x). A 1kb DNA ladder (Promega, Madison, WI) was used as a DNA size reference.

3.2.4. Subcloning of the Smad1 PCR products

To clone the PCR product, the Zero Blunt TOPO PCR cloning kit (Invitrogen, Carlsbad, CA) was used. This kit makes use of the pCR-Blunt II-TOPO plasmid vector to clone blunt-ended PCR products. The linearized vector is supplied with the *Vaccinia* virus topoisomerase I enzyme covalently bound to the 3'-end of each DNA strand, which allows for the insertion of the PCR product without the use of a ligase. In addition, the vector contains the M13 Forward and M13 Reverse priming site for sequencing of the 5'- and 3'-ends of the ligated product, as well as a kanamycin-encoding gene for selection of positive, recombinant products. The cloning reaction was performed by placing 3µl of each PCR product in a 200µl plastic tube, along with 1µl of salt solution (1.2M NaCl, 0.06M $MgCl_2$), and 1µl of ddH_2O. 1µl of the TOPO vector was added to the tube to bring the final volume to 6µl. The tube was incubated for 5 minutes at room temperature, after which 2µl of the tube contents were pipetted into a single vial of One Shot TOP10 Competent *E.Coli* cells (Invitrogen, Carlsbad, CA), and incubated for 5 minutes on ice. The vial was heat-shocked at 42^0C for 30 seconds, placed immediately on ice, mixed with 250µl of SOC medium (2% tryptone, 0.5% yeast extract, 10mM NaCl, 2.5mM KCl, 10nM $MgCl_2$, 10mM $MgSO_4$, 20mM

glucose), and left for one hour on a horizontal shaker set at 200rpm and 37^{0}C. Twenty to one hundred microlitres of the vial contents were streaked on six pre-warmed LB Agar plates containing 50μg/ml kanamycin (Sigma, St. Louis, MO), and the plates were left overnight in an incubator at 37^{0}C. Ten bacterial colonies from the selective plates were picked and cultured in LB medium on a small-scale for further analysis.

3.2.5. Small-scale culture and restriction enzyme analysis of Smad1 cDNA

Small-scale cultures were prepared by cultivating the bacterial colonies overnight at 37^{0}C on a horizontal shaker at 300rpm in separate tubes, each containing 2 ml LB medium with 50μg/ml kanamycin. The following morning, 1.5ml of each culture were used for plasmid isolation using a mini-preps procedure, while the remaining 0.5ml was stored at 4^{0}C for potential large-scale cloning. Once the plasmids had been isolated, each was dissolved in 20μl of TE buffer at pH8, and its concentration measured at 260nm using the BioRad SmartSpec 3000 spectrophotometer (BioRad, Hercules, CA). A restriction enzyme digest was set up to identify false-positives and other PCR contaminating products that may have been ligated into the TOPO vector during the cloning procedure. The digest contained 5μg plasmid DNA in each tube, 2μl of the optimal restriction enzyme buffer (supplied with the restriction enzyme), and enough ddH_2O to give a final volume of 19μl. The tubes were briefly centrifuged, and 1μl of either the *EcoRI* or *SacI* restriction enzymes (both from Promega, Madison, WI) was added to the contents. The digest was incubated at 37^{0}C in a hot water-bath for 1 hour in the case of the *EcoRI* enzyme, or 16 hours in case of

the *SacI* enzyme. 5µl of the contents from each tube were analysed by electrophoresis on a 1.2% agarose gel / EtBr gel in TBE buffer. The gel was visualized under short-wave UV light, and photographed with a Polaroid camera.

3.2.6. Large-scale cloning reactions

The remaining 0.5ml bacterial LB-kanamycin culture, which had been stored at 4^0C, was used for large-scale cloning in 150mL LB medium containing 50µg/ml kanamycin. Two cultures were cultivated containing the vector of interest. The two culture flasks were placed overnight in a 300rpm shaker at 37^0C, and the plasmids isolated using the commercial Maxi / Midi plasmid isolated kit available from Qiagen, Valencia, CA. The isolated plasmids were dissolved in 300µl sterile TE buffer at pH8, and their concentrations determined by spectrophotometry at 260nm. Both plasmids were stored at -20^0C.

3.2.7. Sequencing of Smad1 cDNA

The sequencing mix was prepared by adding 200ng of the vector-ligated Smad1 PCR product and 5pmol of the sequencing primer to a 200µl PCR tube while on ice. The total reaction volume was adjusted to 3µl with ddH_2O. Samples were then submitted to the sequencing facility at the Manitoba Institute of Cell Biology.

The 5'- and 3'-ends of the vector-Smad1 construct were sequencing by using the M13 Reverse and M13 Forward (-20) primers described in Table 3. These primers, which were supplied in the Zero Blunt pCR-Blunt II-TOPO cloning kit, ligate to complementary DNA sequences on the vector and lie close to the cloning site of the

Table 3: Sequencing primers for rat Smad1 DNA

NAME	SEQUENCE
M13R (-20)	5'-CAG GAA ACA GCT ATG AC-3'
M13F (-20)	5'-GTA AAA CGA CGG CCA G-3'
X1	5'-GCC GCT ATG AAT GTG ACC AG-3'
X2	5'-CTG CGA GTT CCC ATT TGG TT-3'
X3	5'-CTG GCA GCA GCA GCA GCA CCT AC-3'
X4	5'-AAT GTT AAC CGG AAC TCC ACT ATT G-3'
X5	5'-CAA CAA CCA AGA GTT CGC TCA G-3'
Y1	5'-GCC TTT AAG ACA CCG ACG AAA TA-3'
Y2	5'-CCT CCG ACG TAA TAA AGG TGG AC-3'
Y3	5'-TCG CCC ACA CGG TTG TTG AGC-3'

Primers: X denotes forward primers, Y denotes reverse primers.

Smad1 PCR product. M13F (supplied as 385pMoles in 0.1μg/μl of TE buffer) and M13R (supplied as 407pM) primers were used in the sequencing reaction by mixing 0.25μl of either primer with 0.20μl of the plasmid sample, and 2.55μl of water on ice.

To fully characterize the Smad1 cDNA product, several primers were designed using the OLIGO 5.1 primer design program and the published rat Smad1 cDNA sequence as a template for primer design. The designed primers were custom-made by GibcoBRL, as described in Section 3.2.1. Sequencing primers are given in Table 3. Primers were supplied in lyophilised form and reconstituted to a concentration of 100μM with TE buffer at pH8. Primers were then diluted 20 fold and 1μl (5pmol) of each was used in the sequencing reaction mix.

The analysis of Smad1 in hepatic stellate cells

3.2.8. Isolation of hepatic stellate cells from rat liver

The isolation of HSC from rat liver is described in Section 3.1.1. This method has been shown to give cultures of HSC free from contaminants. The cells once isolated and purified from the rat liver were seeded in 100mm sterile, plastic-coated dishes (Corning, New York, NY) in DMEM with 10% cool-calf serum, and assessed by light microscopy for purity and viability.

3.2.9. Cell Culture

The primary culture HSC were cultivated by placing the cell dishes in an incubator at 37^0C saturated with 95% O_2 / 5% CO_2 until 70 - 80% confluent. Confluence was

assessed by visual inspection using light microscopy, and was typically accomplished after 2 – 4 days after isolation from the rat. Cell culture medium was prepared by dissolving 13.5g of Dulbecco's Modified Eagle Medium powder (DMEM from GibcoBRL, supplied by Life Technologies, Rockville, MO) in 920ml ddH_2O and 10ml HEPES saline buffer (0.283M NaCl, 0.023M HEPES acid, 1.5mM Na_2HPO_4, diluted to 2 litres in ddH_2O). The pH when measured was determined to be between 7.2 and 7.3. The solution was divided into two fractions: the first fraction, labelled "serum-free medium", consisted of 490ml of DMEM medium to which were added 5ml of 1x Penicillin-Streptomycin (GibcoBRL, Life Technologies, Rockville, MO) and 5ml of L-glutamine (Sigma, St. Louis, MO) to a final volume of 500ml. This solution was filtered through a 0.2μ sterile filter, stored at 4^0C, and was used for incubating cells when treated with TGF-β1. To the second fraction, consisting of 440ml DMEM solution, were added 50ml of 10% cool calf serum (Cool Calf 2, Sigma, St. Louis, MO), 5ml of 1x Penicillin-Streptomycin, and 5ml of L-glutamine, giving a final volume of 500ml. This solution was filtered, stored at 4^0C, and used for culturing cells prior to treatment with TGF-β1. In all 12 dishes of cells were made available, which were divided into two sets consisting of six dishes each.

3.2.10. Treatment of HSC with TGF-β1

To maintain cell viability prior to treatment with TGF-β1, culture medium in each cell-dish was replaced every two days with the serum-containing DMEM. To treat cells with TGF-β1, a sterile solution of 2ng/ml TGF-β1 was prepared. The TGF-β1 stock reagent (human TGF-β1 from R & D Systems, Minneapolis, MN) was supplied

in lyophilised form, and reconstituted as follows: 5ml of 4mM HCl containing 1mg/ml BSA was filtered through a 0.22μ filter (Millipore, Bedford, MA). 1ml of the filtered HCl solution was added directly to 1μg TGF-β1 reagent and mixed. The bottle contents were then divided into 4 separate fractions of 250μl each, and were stored in 1.5ml Eppendorf tubes at -70^0C until needed. After it had been determined that all cell dishes were 70 – 80% confluent, all culture medium was removed from the dishes by suction in a sterile cell culture hood, and 3ml of 1x PBS (137mM NaCl, 2.7mM KCl, 4.3mM $Na_2HPO_4 \bullet 7H_2O$, 1.4mM KH_2PO_4, pH 7.3) were added to the dishes to remove all traces of the serum-containing culture medium. The PBS was completely removed by suction, and replaced with 8ml of serum-free DMEM. The two sets of cells were divided into two groups and labelled to receive either 2ng/ml or 5ng/ml TGF-β1 for 1, 3, 6, 12, or 24 hours each, and incubated for 24-hours in preparation for treatment with TGF-β1. Two dishes were labelled as "control", which were destined not to receive the TGF-β1 reagent.

To add 2ng/ml TGF-β1 to the first set of six cell-dishes, 8μl of the 2ng/ml stock TGF-β1 were pipetted into the DMEM medium of each cell culture dish for the indicated time period, starting with the 24-hour group. The experiment was designed such that all cells could be harvested at the end of a 24-hour period. The 5ng/ml TGF-β1 cell group received 20μl of the 2ng/ml TGF-β1 stock reagent per dish for the indicated time period. The control set were treated in the same manner as the other cell dishes, with the exception that they received no TGF-β1. All cells were incubated in 95% O_2 / 5% CO_2 at 37^0C during TGF-β1 treatment. After the incubation period had elapsed,

the culture medium from each dish was removed completely by suction, and the cells dishes were transferred to a -70^0C freezer for storage until isolation of RNA could be accomplished.

3.2.11. Isolation of RNA

RNA was isolated using the Trizol-LS reagent (Life Technologies, Rockville, MO) as follows: each stored cell-culture dish was incubated for ten minutes with 2.5ml of Trizol-LS at room temperature under mild agitation to ensure complete dispersion of the reagent to all cells. The red reagent - cell extract from each plate was transferred to separate plastic tubes, 0.67ml chloroform was added to each, and the tubes were shaken vigorously by hand for 15 seconds, followed by incubation at room temperature for 10 minutes. The tubes were centrifuged for 15 minutes at 12,000g, after which the colourless, upper phase transferred to a clean tube and mixed with 1.67ml isopropanol, followed by incubation for 10 minutes at room temperature. Finally, the tubes were centrifuged for 15 minutes at 12,000g, and the clear liquid was drained leaving behind a small, white pellet. The pellet was air-dried for 10 minutes, and dissolved in two volumes of 15µl sterile water, then transferred to a sterile 1.5ml Eppendorf tube for storage. RNA concentration was quantified at 260nm using the BioRad SmartSpec 3000 spectrometer. Samples were stored at -70^0C.

3.2.12. Agarose gel electrophoresis

A formaldehyde agarose gel (agarose, 10x MOPS, 37% formaldehyde solution) was made to contain 6 wells on the left side and 6 wells in the centre of the gel. The

2ng/ml TGF-β1 set of RNA samples were loaded in the left wells, starting from the control sample (2ng/ml-C) in the uppermost well, and ending with the 24-hour treated sample (2ng/ml-24hr) in the bottom well. The 5ng/ml TGF-β1 set of RNA samples were loaded in the centre wells, with the control (5ng/ml-C) at the top, and the 24-hour treated sample (5ng/ml-24hr) at the bottom. To load samples, each RNA sample was thawed on ice, and 15ng of each were placed in separate tubes containing 17μl of formaldehyde loading buffer (0.2ml 0.5M EDTA, 0.1% (w/v) bromphenol blue, 0.1% (w/v) xylene cyanol, 10ml formamide). The samples were incubated at 60^0C in a water bath for 20 minutes, then briefly centrifuged, and loaded onto a formaldehyde agarose gel as described. The gel was then completely covered with 1x MOPS buffer (0.2M MOPS sodium salt, 100nM acetate, 10nM Na_2EDTA, then diluted 10x with ddH_2O), and 100V was applied through the electrophoresis tank for 2 hours, until the 18S and 28S rRNA bands were sufficiently separated. The separation of bands was determined by interrupting the electrophoresis process and visualising the gel under a short-wave UV lamp. Once separation was judged to be sufficient, the gel was then photographed under UV light using a Polaroid camera.

3.2.13. RNA membrane transfer

To transfer the separated RNA from the agarose gel to a nylon membrane, a plastic tank was filled with 300ml of 10X SSC solution (175.3g NaCl, 88.2g Na-citrate, diluted 2x in H_2O), and a glass bridge with a rectangular piece of Whatman filter paper (Maidstone, UK) was placed on top of the tank, such that the filter paper extended into the solution in the tank at both ends. The gel was carefully placed onto

the centre of the bridge with the wells facing down, and a nylon membrane (Zeta Probe GT Genomic Tested Blotting Membrane, Hercules, CA) was placed on the topside of the gel, taking care to eliminate air bubbles. Two more pieces of filter paper that completely covered the gel were placed on top the membrane, and the contraption was soaked with 10x SSC solution. The sides and edges of the gel that did not make contact with the membrane were covered with plastic foil to prevent the sideward movement of RNA. Finally, a large wad of paper towels and a small 500ml bottle were placed over the gel construct, and left overnight to allow the transfer of the RNA to the membrane to take place. The following day, the membrane was baked for 2 minutes at 150mJ in the GS GeneLinker UV Chamber crosslinker (BioRad, Hercules, CA) to attach the RNA permanently to the membrane.

3.2.14. ^{32}P Hybridisation

To reduce non-specific binding, the membrane was incubated at 42^0C for 3 hours in 10ml hybridisation buffer (5x SSC, 5x Denhardt's solution, 50% (w/v) deionised formamide, 7% SDS, and 100μg/ml denatured sheared salmon sperm (from Life Technologies, Rockville, MA). The cloned Smad1 cDNA described in Section 3.2.1, was used as a probe to detect Smad1 mRNA on the membrane. For this purpose, the cDNA had to be radioactively labelled. This was accomplished by mixing 200ng of the cDNA probe in 11μl ddH_2O in a 1.5mg Eppendorf tube, boiling for 5 minutes in a water bath to denature the cDNA, and immediately placing it on ice to prevent renaturation. To the tube contents were added 4.5μl Oligolabelling buffer solution ("OLB solution" used in random labelling reaction; available commercially and

mixed with Pd(N)6 oligonucleotide in a 2:1 ratio (Amersham Pharmacia Biotech AB), 0.5µl (<1 unit) of Klenow (large fragment of DNA polymerase I, 100U, GibcoBRL, Gaithersburg, MD), and 3µl of the radioactive ^{32}P dCTP isotope (ICN Radiochemicals, Costa Mesa, CA). The solution was incubated for 2 hours at room temperature to allow for the incorporation of the isotope, then passed through a G-50 Sephadex NICK column (G-50 DNA grade, Amersham Pharmacia Biotech AB, Uppsala, Sweden) that had been previously washed with 4ml TE pH 8. Two volumes of 500µl TE buffer were passed through the column, and the two fractions were collected in separate tubes. The second fraction, containing the radioactive Smad1 cDNA probe, was boiled for 5 minutes in a hot water bath, immediately placed on ice, then added to the hybridisation tube containing the membrane and hybridisation buffer, and left overnight at 42^0C, while the tube was being continuously rotated.

Following hybridisation, the membrane was washed twice at room temperature with 65ml of the 1st wash solution (2x SSC, 0.1% SDS, for 5 and 15 minutes), followed by washing at 42^0C with two volumes of 65ml of the 2nd wash solution (0.5x SSC, 0.1% SDS, for 5 minutes and 15 minutes). The membrane was wrapped in plastic foil and placed in an autoradiography cassette. To visualize, a Kodak X-OMAT Scientific film (Sigma, St. Louis, MO) was placed above the membrane, the cassette closed and placed for 30 minutes at -70^0C. The film was developed, and new film was placed in the cassette and developed at different time intervals, until a sufficiently strong image, free from background distortion could be obtained. To correct for inconsistencies in the amount of RNA loading onto the formaldehyde gel, as well as

sample degradation, a control using an 18S rRNA probe (obtained from the lab, and radioactively labelled as described above) was used. To this end, the membrane had to be stripped of the Smad1 probe by placing it twice in a tank at 65^0C in 300ml of boiling RNA stripping buffer (0.1x SSC, 0.5%SDS) for 20 minutes. The membrane was treated as before, but with the 18S rRNA probe in place of the Smad1 cDNA probe.

3.2.15. Computer Analysis

To determine the effect of 2ng/ml and 5ng/ml TGF-β1 on Smad1 mRNA levels with time, the X-ray film was scanned into a Power Macintosh computer using the HP 6100 C high-resolution scanner. The densitometric values obtained from Smad1 mRNA and the 18S rRNA bands were determined by the NIH-Image computer-imaging program. A filter was employed to subtract background noise. Calculated values were expressed as a graph of expression intensity of Smad1 mRNA against hours of incubation with TGF-β1.

3.3. Cloning of the rat Smad1 Promoter

3.3.1. Genome Walker PCR theory

To clone the promoter of the rat Smad1 gene, use was made of the "Genome Walker Kit" (Clontech Laboratories, Palo Alto, CA). The kit contains four tubes, each containing genomic rat DNA treated with one of four restriction enzymes, *EcoRV*, *DraI*, *SspI*, and *PvuII* (the DNA "libraries"), to which a unique adaptor had been ligated to the 5'- and 3'-of the cleaved DNA fragments (Figure 6). The adaptor intro-

duces a known priming site on unknown genomic DNA sequences. To clone unknown promoter sequences, PCR is used to "walk" towards the 5'-end, by using the AP1 / AP2 adaptor primers supplied in the kit, and user-designed primers. The protocol calls for two amplifications per DNA library: the primary PCR reaction uses the outer adaptor primer AP1, and the user specified gene- specific primer (GSP1). The primary PCR product is diluted, and a secondary, nested PCR is performed using the inner, adaptor primer AP2, and a nested, user-specified, gene-specific primer (GSP2). Both gene-specific primers were designed by using the published Smad1 cDNA sequence as a template (GenBank Accession Number U66478). The resulting PCR fragments can be cloned and analysed for novel sequences.

PCR is performed simultaneously with all four genomic DNA libraries, along with positive and negative controls. Positive controls make use of any one of the four libraries, and the supplied primer mix to produce a fragment of known size. Positive controls when analysed on an agarose / EtBr gel should give a fragment length of 1.5kb for the EcoRV library; 1.2kb for DraI, 0.7kb for PvuII, and 1.0kb for the SspI library.

3.3.2. Primer design

Primers were designed according to recommended parameters in the Genome Walker kit user manual. Conditions for optimal primers design call for a primer length of 25 – 28 nucleotides, a GC content of 40 –60%, and a $T_m > 67^0$ C. Two primers were designed using the Oligo Primer Analysis Software (Version 5.1, National

Figure 6: Structure of the "Genome Walker" adaptor and adaptor primers

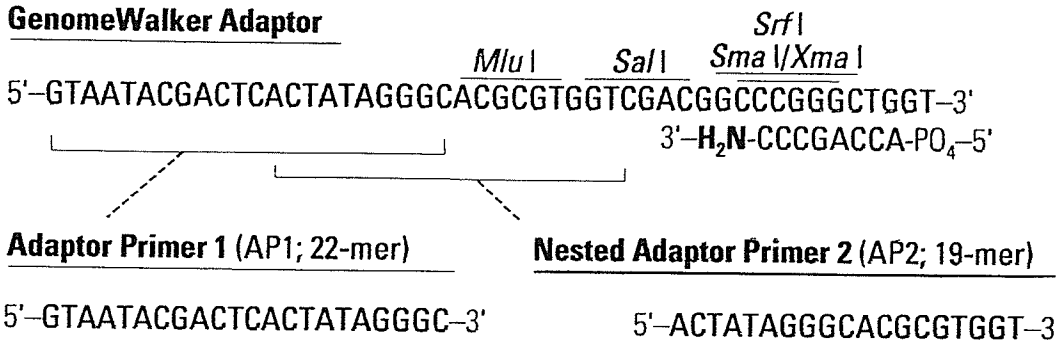

Figure 6: Structure of the Genome Walker adaptor and adaptor primers.
The adaptor has been ligated to both ends of the genomic DNA fragments in all four Genome Walker "libraries" supplied in the kit. The amine group on the lower strand of the adaptor blocks extension of the 3'-end of the adaptor-ligated genomic fragments, and thus prevents formation of an AP1 binding site on the general population of fragments. Adapted from the *Clontech Genome Walker User Manual (PT1116-1, 11/10/1999, page 8),*
< http://www.clontech.com/techinfo/manuals/PDF/PT1116-1.pdf>

Biosciences Inc, Plymouth, MN), and the published rat Smad1 cDNA sequence as the template (GenBank Accession Number U66478). The outer primer used in conjunction with AP1, was labelled GSP-2A, and the nested primer used in conjunction with AP2, labelled NGSP-1A. Together AP1 / GSP-2A had an optimal annealing temperature of 59.5^0 C, while the AP2 / NGSP-1A pair had an optimal annealing temperature of 62.5^0 C. Primer sequences are given in Table 4.

3.3.3. Polymerase Chain Reaction (PCR)

The Advantage Genome PCR kit (Clontech), which contains the Advantage Genome Polymerase mix and all other reagents needed for PCR, was used for "Genome Walking". Primary PCR reactions mixtures were made up in 200µL thin-walled PCR tubes that contained 49µl of Master Mix (consisting of 37.8µl sterile water, 5µl 10x *Tth* PCR reaction buffer, 1µl 10mM dNTP, 2.2µl 25mM $Mg(OAc)_2$, 1µl 10µM AP1 primer, 1µl 10µM GSP-2A, 1µl 50x Advantage Genomic Polymerase mix), and 1µl of one of the four DNA libraries. The four reaction tubes were labelled 1A, 3A, 4A, and 5A, and contained the EcoRV, DraI, PvuII, and SspI DNA libraries, respectively. A sixth tube, labelled 6A, contained PCR-grade water instead of DNA, and functioned as a negative control, while a seventh tube, labelled 7A, contained the positive control primer pair with either one of the four DNA libraries. PCR reactions were performed on the Eppendorf Mastercycler (Brinkmann Instruments, Westbury, NY). The cycling protocol is given in Table 5. The reaction mixture for nested PCR was identical to that of primary PCR, but employed the primary PCR product as the

Table 4: PCR primer design for amplifying the Smad1 promoter region

NAME	SEQUENCE	START SITE
GSP-2A	5'-TGC AAA GCC AAC AGA GAT TTC AG-3'	231
AP1	5'-GTA ATA CGA CTC ACT ATA GGG C-3'	1
NGSP-1A	5'-TTG GTC TTC GGT TCG GAA AGG TA-3'	195
AP2	5'-ACT ATA GGG CAC GCG TGG T-3'	13

Table 4: The GSP-2A and AP1 primers are used for primary PCR reactions. GSP-2A was designed as a 23-mer, and has an annealing temperature 69.5^{0}C, and a GC content of 43.5%. The primer was designed at position 231 of the Smad1 cDNA sequence. The supplied AP1 primer is 22bp in length, and had an annealing temperature of 59^{0}C. Together the two primers give an optimal PCR annealing temperature of 59.5^{0}C, with a difference in Tm of 0.7^0 C as determined by the Oligo 5.1. Primer Analysis software.

The inner, nested primer NGSP-1A was designed as a 23-mer, having an optimal annealing temperature of 72.2^{0}C, a GC content of 47.8%, and is identical with the rat Smad1 cDNA sequence at position 195. AP2 is a 19-mer, with an optimal annealing temperature of 71^{0}C. Optimal PCR annealing for the pair occurs at 62.5^{0}C, with a difference of T_m = 1.1^{0}C

Table 5: Primary PCR reaction conditions for promoter cloning

NAME	CYCLES	DENATURATION	ANNEALING / EXTENSION
1^0 PCR	7	94^0C, 25 seconds	72^0C, 4 minutes
	32	94^0C, 25 seconds	65^0C, 4 minutes
	1	-----	65^0C, 4 minutes

template for amplification. Each of the six primary PCR products was diluted 50x in sterile PCR-grade water, and 3µl were used as a template for each reaction. Tubes were labelled as 1B, 3B, 4B, 5B, 6B, and 7B, corresponding to the primary PCR labelling scheme. PCR was performed on the Eppendorf Mastercycler. The cycling protocol is given in Table 6.

3.3.4. Analysis of PCR products

8µl of the primary PCR reaction products were analysed on a 1.5% agarose / EtBr gel, while 5µl of the secondary PCR products were analysed on a 1.2% agarose / EtBr gel in TBE, along with 1kb DNA ladder (Promega, Madison, WI). Each gel was visualized under short-wave UV light and photographed. If clearly separated bands (no smears) were obtained for the primary PCR reaction, nested PCR was performed.

3.3.5. Subcloning and plasmid isolation

3µl of each nested PCR reaction product were cloned into the Zero Blunt pCR-Blunt II-TOPO plasmid vector (Invitrogen, Carlsbad, CA). The cloning procedure is described in Section 3.2.4. For each PCR reaction three pre-warmed LB Agar - kanamycin (50µg/ml) plates were streaked with 20, 50, or 100µl *E.Coli*, and incubated overnight at 37^0C. From the selective culture plates, 4 colonies from the DraI library, 6 from the PvuII library, and 11 from the SspI library were cultured in 2ml of LB medium containing 50µg/ml kanamycin. After 11 hours, 1.5ml from each bacterial culture tube was used to isolate the plasmid-PCR vector using a minipreps plasmid isolation procedure. The remaining tubes containing the 0.5ml bacterial

Table 6: Secondary PCR reaction conditions for promoter cloning

NAME	CYCLES	DENATURATION	ANNEALING / EXTENSION
2^0 PCR	5	94^0C, 25 seconds	72^0C, 4 minutes
	22	94^0C, 25 seconds	67^0C, 4 minutes
	1	------	67^0C, 4 minutes

cultures were stored at 4^0C for potential use in large-scale cloning. The isolated plasmid-PCR vector was quantified at 260nm using the BioRad SmartSpec 3000 spectrometer.

3.3.6. Restriction enzyme analysis of cloned PCR products

Once plasmids were isolated, a restriction enzyme digest for each isolated plasmid was done to ensure that identical and unique products in each DNA library could be identified. The restriction enzyme *EcoRI* was used. The restriction enzyme digest set-up is described in Section 3.2.5. Ten microlitres were analysed on a 1.2% agarose / EtBr gel, and visualized under short-wave UV light.

3.3.7. Large-scale cloning reactions

Based on the analysis of the small-scale culture described in Section 3.3.6, five products were chosen for large-scale cloning and further analysis: one product from the DraI library was labelled 3A, two products from the PvuII library (#1 and #6) were labelled 5-1 and 5-6, and two products from the SspI library (#1 and #3) were labelled 3-1 and 3-3. All five were cloned on a large scale by placing the stored 0.5ml bacterial culture into five media flasks containing 150ml LB broth with 50μg/ml kanamycin in a shaker at 37^0C overnight. Plasmids were isolated the following day using the commercial Maxi / Midi plasmid isolation kit (Qiagen, Valencia, CA). Concentrations of each were determined using the BioRad SmartSpec 3000 spectrophotometer. All plasmids were stored at -20^0C.

A restriction enzyme digest was set up using *EcoRI* and *AvaI* restriction enzymes (both from Promega, Madison, WI) to determine that each plasmid obtained was in fact that identical to that of the small-scale culture. Details of the restriction enzyme digest method are described in Section 3.2.5. Restriction enzyme products were analysed on a 1.2% agarose / EtBr gel. Based on the results of the restriction enzyme digest, three plasmids were submitted for sequencing: 3A (DraI), 3-1 (SspI), and 5-1 (PvuII).

3.3.8. Sequencing

The M13F (-20) and M13R (-20) primers (Table 7) supplied with the Zero Blunt pCR-Blunt II-TOPO plasmid kit were used to sequence the 5'- and 3'- ends of each of the three PCR – plasmid products (3A, 3-1, and 5-1). Priming sites for these two primers exist close to the cloning site of the vector, thus allowing for sequencing of the 5'-and 3'- ends of the cloned PCR product. The sequencing reaction set-up is described in Section 3.2.7. Tubes were labelled as 31R, 31F, 51R, 51F, 3AR, 3AF, where *R* and *F* represent the position of the primer (R = M13 Reverse primer, F = M13 Forward primer).

Primers used for sequencing the full-length of the cloned promoter are described in Table 7, and were designed using the OLIGO 5.1 primer software. Primers were designed such that the sequences obtained would overlap with new sequences that were submitted. Primers were supplied by GibcoBRL, and were prepared for the sequencing reaction as described in Section 3.2.7.

Table 7: Sequencing primers for the rat Smad1 promoter region

NAME	SEQUENCE
M13R (-20)	5'-CAG GAA ACA GCT ATG AC-3'
M13F (-20)	5'-GTA AAA CGA CGG CCA G-3'
B1	5'- CGG GCT GGT ATT TCA TCT CTA -3'
B2	5'- ACG TCG AGT TGC CTG CCC TGG -3'
B3	5'- TGT CGG CTC CTG TGT ATC AGT C -3'
B4	5'- GGA TTC TGT GCC CGA AAC ACT C -3'

3.3.9. Analysis of the promoter sequence

The putative promoter sequence was constructed from overlapping sequences using the GeneJockey Sequence Processor (Biosoft, Cambridge, UK) computer software. The sequences were aligned against the known rat Smad1 cDNA sequence (GenBank Accession Number U66478), to identify novel sequences, as well as against each other to identify overlapping regions. A putative promoter region was constructed.

IV. RESULTS

4.1. PCR analysis of Smad1 expression during activation of HSC

To demonstrate a relationship between Smad1 and the transformation of HSC into MFBL cells, changes in Smad1 mRNA expression were determined before and after HSC transformation. A *reverse transcriptase polymerase chain reaction* (RT-PCR) was performed on RNA extracted from rat HSC that had been cultured for 1, 3, and 9 days. HSC are completely undifferentiated at day 1, show a change in morphology typical of MFBL cells at day 6, are and completely transformed at day 9. By measuring the level of Smad1 mRNA at day 3, it can be determined whether increased Smad1 transcription is an event that precedes the transformation of HSC, and therefore whether it is an initiating factor in cell transformation.

The reverse RT-PCR method involves two stages; in the first, RNA is reversely transcribed into single-stranded cDNA by AMV reverse transcriptase. Random hexamer primers allow the entire population of mRNA molecules to be converted into single-stranded cDNA. In the second stage, gene-specific primers are used to prime the single-stranded cDNA by conventional PCR in order to obtain double-stranded cDNA molecules.

The experiment was designed to be semi-quantitative. Total RNA would be isolated from primary HSC cultures. 1st strand synthesis would be performed to obtain the pool of single-stranded DNA. Equal amounts of single-stranded cDNA would be used in PCR with Smad1 specific primers. Equal amounts of the PCR products are

analysed on an agarose / EtBr electrophoresis gel, and visualized under UV light. The gel would be photographed, and the expression of Smad1 PCR products quantified by computer-imaging. To ensure consistency in the amount of single-stranded cDNA used in the PCR reaction, controls would be employed using the housekeeping enzyme *glyceraldehyde 3-phosphate dehydrogenase* (G3PDH). G3PDH has been shown to be present in equal amounts in most cell types of the body, including HSC. By performing PCR on 1st strand cDNA using G3PDH primers, and analysing the products by electrophoresis, obtaining equal amounts of G3PDH in each of the samples would suggest that equal amounts of single-stranded cDNA had been available for each PCR reaction, making a comparison among Smad1 cDNA levels possible.

4.1.1. RT-PCR for Smad1 expression in HSC

Figure 7 shows the RT-PCR results for Smad1 cDNA and G3PDH for P1, P3, and P9. The gel reveals a PCR fragment in each lane of approximately 1000bp, which represents the G3PDH control, and a second, longer fragment of approximately 1625bp, which is the Smad1 cDNA product. When scanned for intensity of expression, the G3PDH control shows approximately equal intensity for P3 and P9 (9234 and 9312 units respectively), while a lower intensity of 7590 units is observed for P1. The depressed value in P1 indicates that less the single-strand cDNA was available for PCR than in samples P3 and P9.

To correct for the lower P1 value, additional PCR reactions were performed to

Figure 7: RT-PCR products for Smad1 and G3PDH

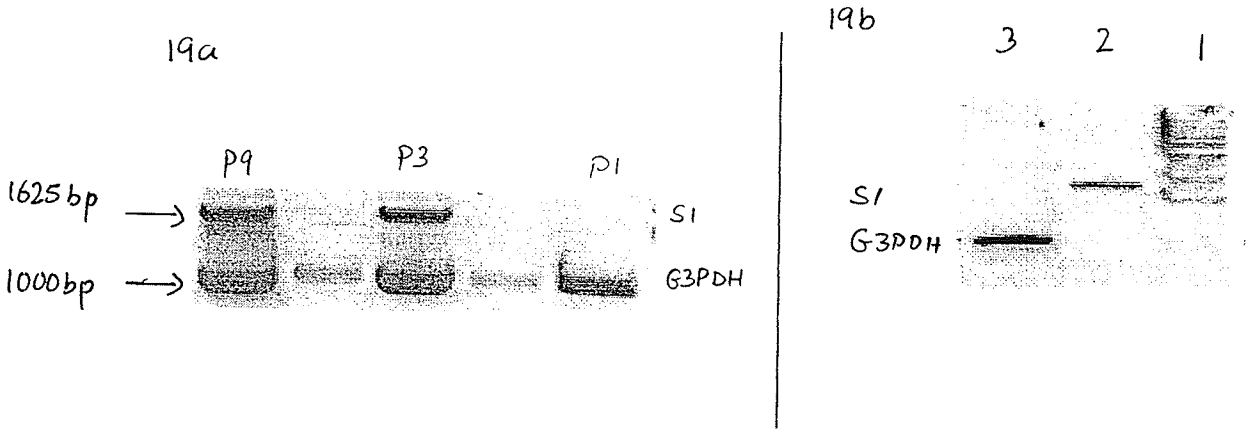

Figure 7a: **RT-PCR results for Smad1 and G3PDH in samples P3 and P9.** Smad1 product at 1625bp; G3PDH product at 1000bp. Legend: P1: RNA extract from primary culture HSC after 1 day; P3: RNA extract from primary culture HSC after 3 days cell culture; P9: RNA extract from primary culture HSC after 9 days of cell culture. HSC are completely transformed into MFBL cell at day 9; the differentiation point at which cells start to undergo a change in morphology to resemble MFBL cells is day 6.

Figure 7b: **RT-PCR results for Smad1 and G3PDH in sample P1**. Screening for Smad1 and G3PDH. Legend: Lane 1: 1kb DNA ladder; lane 2: Smad1 product; lane 3: G3PDH control.

achieve an intensity of G3PDH close to P3 and P9 values. The intensity of G3PDH in P1, when corrected for background noise is 9590 units, which is in the range of P3 and P9. Results of the intensity of expression of G3PDH and Smad1 cDNA for all three samples are given in Table 8.

Figure 8 shows a plot of the expression of Smad1 cDNA against the number of days of HSC incubation. Expression values were corrected by dividing the absolute expression of Smad1 cDNA against the expression of the G3PDH control. An increase in Smad1 mRNA expression is observed at day 3.

4.2. The cloning of rat Smad1 cDNA and the analysis of Smad1 in HSC

The PCR cloning of Smad1

Rat Smad1 cDNA was cloned to aid in the analysis of Smad1 mRNA in HSC. To clone Smad1, the polymerase chain reaction (PCR) was employed, as this procedure allows for the amplification of high quality cDNA in the shortest time span. To clone the desired sequence, rat-brain and rat-liver Marathon cDNA (both from Clontech Laboratories, Palo Alto, CA) were chosen as the template for the PCR reaction. Rat DNA was chosen over human DNA as the template of choice, since subsequent experiments make use exclusively of HSC that have been isolated from rat livers. The region to be cloned was chosen to encompass the open reading frame (ORF) of the Smad1 cDNA sequence published in GenBank under Accession Number U66478 (<*http://www.ncbi.nlm.nih.gov*>). The ORF was determined by using the

Table 8: Intensity of expression of Smad1 and G3PDH cDNA as determined by RT-PCR in HSC

Smad1-G3PDH expression in hepatic stellate cells

Sample	P1	P3	P9
Smad1 expression (Absolute values)	3268	9583	10029
G3PDH expression (Absolute values)	9590	9234	9312
Smad1 / G3PDH	**0.34**	**1.03**	**1.07**

Table 8: Expression of Smad1 cDNA in hepatic stellate cells, as determined by the intensity of bands on an agarose gel loaded with equal amounts of the PCR product. P1: primary culture HSC at day 1; P3: primary culture HSC at day 3; P9: primary culture HSC at day 9. Units are arbitrary.

Figure 8: RT-PCR expression of Smad1 cDNA in HSC

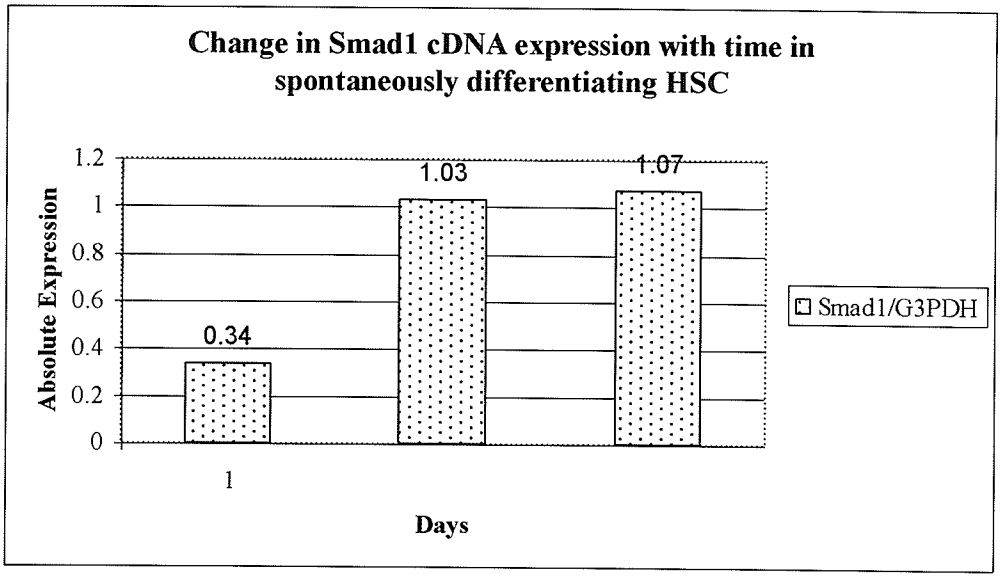

Figure 8: **RT-PCR expression of Smad1 cDNA in HSC cell extract.** Day 1: completely undifferentiated HSC; day 3: a rapid increase in Smad1 mRNA is observed. It can be inferred that the increase in Smad1 transcription is an initiating event for the transformation into MFBL cells; day 9: HSC that have been completely transformed into MFBL cells show a steady expression of Smad1.

GeneJockey computer software (Biosoft, Cambridge, UK), and consists of the largest, continuous fragment extending from position 316 to 1722 of the published sequence. Using the known rat Smad1 cDNA sequence, two gene-specific primers were designed to encompass a region ranging from 179 – 1804.

The PCR reaction was followed by the small-scale cloning of the PCR product in a bacterial vector, and restriction enzyme analysis of isolated plasmids to identify ligated PCR products representative of Smad1 in size and orientation. An *EcoRI* digest allows for the complete excision of the Smad1 PCR product from the vector, and the identification of false-positives. The two *EcoRI* restriction sites are located at positions -11, and +7 from the cloning site of the vector, while the cloned Smad1 cDNA does not contain *EcoRI* restriction sites. A *SacI* digest, on the other hand, allows for the distinction of sense- and anti-sense cloned PCR products. Since the pCR-Blunt II-TOPO vector employed contains blunt ends, it would not allow for the distinction between the 5'- and 3'- ends of the PCR product, which can orient itself in either in the forward (sense) or backward (anti-sense) position. *SacI* cleaves the Smad1 product at one known site only, and an analysis of the size of the fragments obtained from the digest would allow for the identification of orientation. Once appropriate vector products were identified, a large-scale cloning reaction and verification procedure were carried out, and the products were submitted for full-length sequencing.

4.2.1. Analysis of PCR products

The Smad1 PCR product, when loaded onto a 1.2% agarose / EtBr gel and photographed under short-wave UV light, shows a single band of approximately 1636bp in length, as determined by DNA size-markers (Figure 9). The fragment length is in agreement with the theoretically expected PCR length of 1625bp.

4.2.2. Analysis of plasmids containing the Smad1 insert by *EcoRI* and *SacI*

Figure 10 shows a photograph of a 1.2% agarose / EtBr gel visualized under short wave UV light, and containing 10µl of the *EcoRI* digested recombinant plasmid in each lane. Lane 1 shows that the undigested vector-Smad1 recombinant plasmid exceeds 3000bp (theoretical length of the construct is 5144bp), while lanes 2 – 11 shows ten samples which all contain the expected Smad1 fragment at 1636bp. The second, larger fragment at >3000bp is the remainder of the pCR-Blunt II-TOPO vector, which has a size of 3519bp.

Figure 11 shows the results from the *SacI* restriction digest. 10µl of each of the ten restriction samples were loaded onto a 1.2% / EtBr gel and visualized under UV light. The *SacI* restriction site exists in the vector at the –20 position from the 5'-end of the cloning site, and in the cloned Smad1 product at position 1156 of the published sequence. The PCR product (1625bp) and the vector (3519bp) give a construct of total length of 5144bp. Plasmids that contain Smad1 inserted in the *sense orientation*, when digested by *SacI*, should give two fragments, one totalling 997bp in length (20bp vector + 977bp Smad1), and the other totalling 4147bp (5144 – 997). Products in lanes 2, 6, 8, 10, and 12 in Figure 11 match this prediction. For products

Figure 9: Agarose gel of Smad1 PCR product

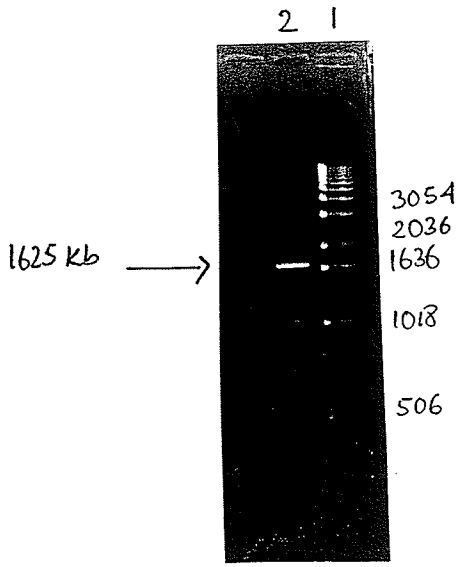

***Figure 9*: Rat Smad1 PCR product.** Lane 1: 1kb DNA ladder; lane 2: Smad1 PCR fragment.

Figure 10: *EcoRI* restriction enzyme analysis for the small-scale Smad1 cloning reaction

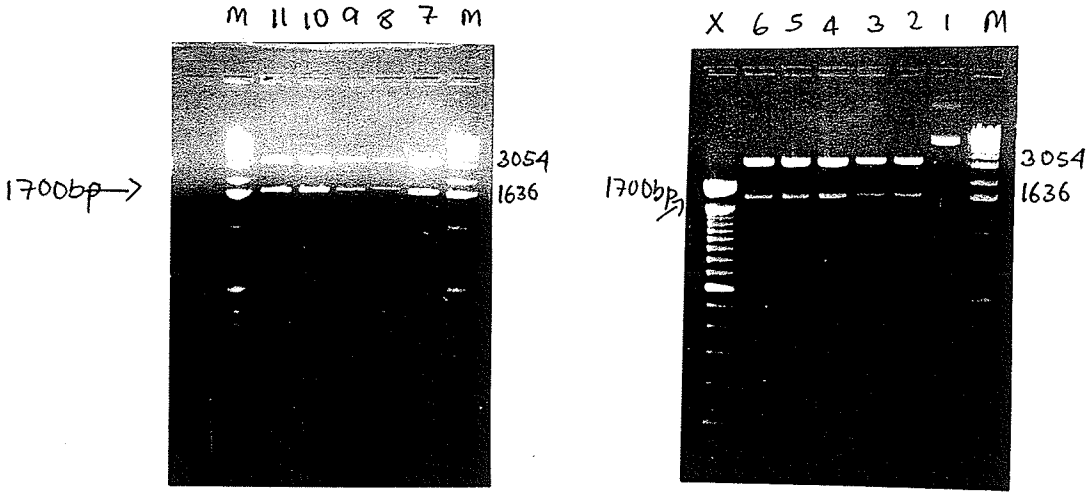

Figure 10: **Products from the *EcoRI* restriction enzyme digest.** The Smad1 PCR product was cloned into the Zero Blunt pCR-Blunt II-TOPO plasmid vector then excised by *EcoRI* to identify positive cloning products. *Legend:* Lanes "M": 1kb DNA ladder; lane 1: control, undigested recombinant Smad1 vector; lanes 2 - 11: fragment at 1636bp represents the cloned Smad1 PCR product that had been ligated into the plasmid vector. The lane marked "X" is a 100bp DNA ladder.

Figure 11: *SacI* restriction enzyme analysis for the small-scale Smad1 cloning reaction

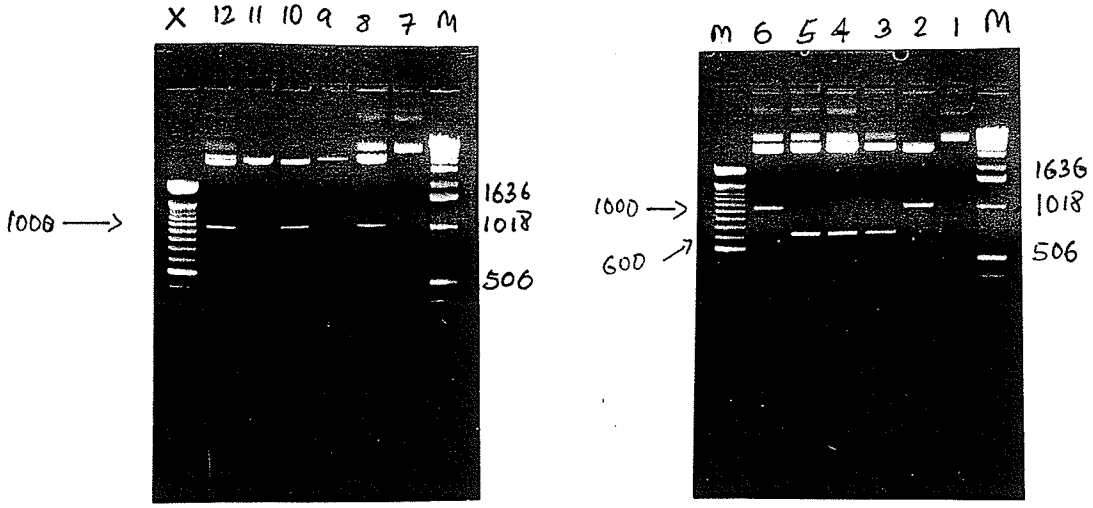

Figure 11: **Products from the *SacI* restriction enzyme digest.** The Smad1 PCR product was cloned into the Zero Blunt pCR-Blunt II-TOPO plasmid vector then excised by SacI to identify the orientation of ligation of the PCR product into the blunt vector. Two cleavage products are possible depending on the direction of orientation. *Legend:* Lane "M": 1kb DNA ladder; lanes 1 and 7: undigested recombinant Smad1 vector; lanes 2, 6, 8, 10, 12: the fragment at approximately 1000bp represents the remnants of the cloned Smad1 PCR product ligated in the sense-orientation. Lanes 3, 4, 5, 9, and 11: anti-sense Smad1 products.

ligated in an *anti-sense* fashion, fragments of sizes 668bp (20 + 648bp Smad1) and 4147bp (remainder of vector) are expected. Products in lanes 3, 4, 5, 9, and 11 in Figure 11 reveal this pattern.

4.2.3. Analysis of plasmids containing Smad1 cDNA cloned on a large-scale

Bacterial colonies representing digests 2 and 6 in Figure 11 were chosen for large-scale cloning. The large-scale cloning reaction was performed to obtain plasmids of sufficient quality and concentration deemed necessary for sequencing, and for future experiments. Figure 12 shows the *EcoRI* restriction enzyme analysis of isolated plasmids of both bacterial colonies on a 1.2% agarose / EtBr gel. Lanes 1 and 2 both show a fragment of approximately 1636bp, which is the expected size for the Smad1 cDNA product (1625bp). The plasmid of product 1 was submitted for full-length sequencing.

4.2.4 Rat Smad1 cDNA sequencing results

The complete cDNA sequence of the cloned rat Smad1 cDNA product is shown in Figure 13. The sequence was constructed from overlapping fragments, and was checked for accuracy by the use of overlapping primers, sequencing of cDNA templates from both cloned products described in Section 4.2.3, and by sequencing each DNA fragment two or more times. Figure 14 shows the protein sequence of ORF "RF 1" translated from the nucleotide sequence using the GeneJockey analysis tool. When aligned against the published rat Smad1 cDNA sequence (GenBank Accession Number U66478), six differences in nucleotides are observed (Figure 15).

Figure 12: *EcoRI* restriction enzyme analysis for the large-scale Smad1 cloning reaction

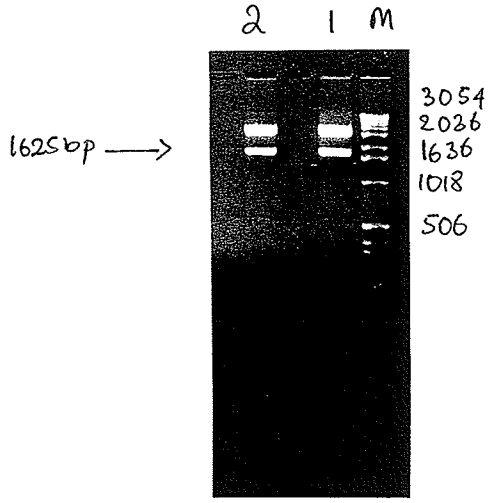

***Figure 12: EcoRI* digest of Smad1 product ligated into the Zero Blunt pCR-Blunt II-TOPO plasmid vector.** Legend: Lane "M": 1kb DNA ladder; lanes 2 and 3: fragment at approximately 1635bp represents the excised Smad1 PCR product.

Figure 13: Nucleotide sequence of cloned rat Smad1 cDNA

```
   1    ACCAAGGCGA GGCCAGGGCC GAGGCGCGGG GACGGCGGCC GAGAGCTAAG
  51    CGACGTGGGA CGGTGACTGG GAACGGATCG GAGCGCGGGA CCCGGCCCGG
 101    GTCTCGTGCG TCCCCGCCGA TGGGCCTCCG CCGAGCCGGT GCTAACTGGG
 151    TCTTCCCTGA AGCAGAAGGA ACAGTATTTC CTACCTTTCC GAACCGAAGA
 201    CCAAGAAGCT AGAGAATCTA TGTAAATAAA CTGAAATCTC TGTTGGCTTT
 251    GCACCCCACC CCGGAGCCGT CACTTTTACC TGGTCTGAGG AGCGTGTAGA
 301    CCTCGGCCAG CCGCTATGAA TGTGACCAGC TTGTTTTCAT TCACAAGCCC
 351    AGCTGTGAAG AGACTCCTTG GGTGGAAACA GGGCGACGAA GAAGAGAAAT
 401    GGGCGGAGAA GGCTGTGGAC GCTTTGGTGA AGAAACTGAA GAAGAAGAAA
 451    GGGGCCATGG AAGAGCTGGA GAAGGCCCTG AGCTGCCCCG GGCAGCCCAG
 501    TAACTGTGTC ACCATTCCTC GCTCCCTGGA TGGCAGGTTG CAGGTGTCCC
 551    ACCGGAAGGG ACTGCCTCAT GTCATTTATT GCCGCGTGTG GCGCTGGCCC
 601    GACCTCCAGA GCCATCATGA ACTAAAGCCT CTGGAATGCT GCGAGTTCCC
 651    ATTTGGTTCC AAGCAGAAGG AAGTCTGCAT CAATCCCTAC CACTATAAGC
 701    GAGTGGAGAG CCCCGTTCTC CCACCGGTGC TGGTTCCGAG GCACAGCGAG
 751    TACAACCCTC AGCACAGCCT TCTGGCTCAG TTCCGAAACC TGGGACAAAA
 801    TGAGCCCCAC ATGCCACTGA ATGCCACGTT CCCCGACTCC TTCCAGCAGC
 851    CACACAGCCA CCCGTTTCCC CAGTCCCCCA ACAGCAGCTA CCCCAACTCT
 901    CCTGGCAGCA GCAGCAGCAC CTACCCTCAC TCCCCGACCA GCTCAGACCC
 951    GGGCAGCCCT TTTCAGATGC CAGCCGACAC ACCCCCGCCT GCTTACCTGC
1001    CTCCTGAAGA CCCCATGGCC CAGGATGGCT CTCAGCCTAT GGACACGAAC
1051    ATGACGAACA TGACGGCACC GACACTGCCC GCGGAGATCA ATAGAGGAGA
1101    TGTTCAAGCA GTTGCTTACG AGGAACCAAA ACACTGGTGC TCTATTGTGT
1151    ACTATGAGCT CAACAACCGT GTGGGCGAAG CGTTCCATGC CTCCTCCACC
1201    AGCGTGTTGG TGGATGGTTT CACCGATCCT TCCAACAATA AGAACCGATT
1251    CTGCCTTGGG CTGCTCTCCA ATGTTAACCG GAACTCCACT ATTGAAAATA
1301    CCAGGCGACA CATCGGGAAA GGAGTCCACC TTTATTACGT CGGAGGAGAG
1351    GTGTATGCGG AGTGCCTCAG TGACAGCAGC ATCTTCGTGC AGAGTCGGAA
1401    CTGCAACTAC CACCATGGCT TTCATCCCAC CACGGTCTGC AAGATCCCCA
1451    GCGGGTGCAG CTTGAAAATC TTCAACAACC AAGAGTTCGC TCAGCTACTG
1501    GCGCAGTCTG TGAACCATGG GTTCGAGACA GTGTATGAAC TCACCAAAAT
1551    GTGCACTATT CGAATGAGCT TCGTGAAGGG CTGGGGAGCG GAGTACCACC
1601    GGCAGGATGT CACTAGCACC CCCTGCTGGA TTGAGATACA CCTGCATGGC
1651    CCTCTCCAGT GGCTGGATAA AGTCCTTACC CAGATGGGTT CGCCCCACAA
1701    CCCTATTTCG TCGGTGTCTT AAAGGCCCTC GGCTTCTGTC TCTTGCAAAC
1751    TATTGGGCCT TGCAGTACTT GAAGGACGGA GAAGTCAGAC AGGATGGGGA
1801    GCTGTAAAGG AGCCGTGATA CTTGACCTCT GTGACCAACC GTTGGATGGA
1851    GAAGCTGACA GGCCTTGGTA ACAAGCTGTT GATATCAAGA ACCCGCTTAG
1901    TTTACATTGT GACATTCTGT TGTAAAATCA ACTAAAATGC TGACTTTTAG
1951    CAGGACTTTG TGAATAGTTA GAAAAGAGAT GGCCAAGCCA GGGGCAAATT
2001    AT
```

Figure 14: Open-reading frame and translated sequence of cloned rat Smad1 cDNA

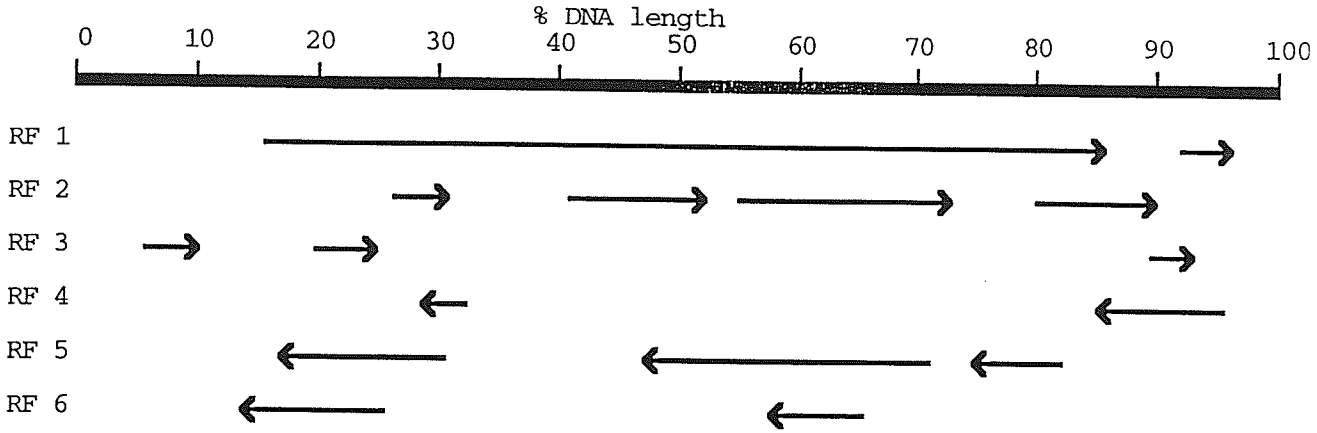

rat Smad1 cloned seq translated from 316 to 1722

```
  1    MNVTSLFSFT SPAVKRLLGW KQGDEEEKWA EKAVDALVKK LKKKKGAMEE
 51    LEKALSCPGQ PSNCVTIPRS LDGRLQVSHR KGLPHVIYCR VWRWPDLQSH
101    HELKPLECCE FPFGSKQKEV CINPYHYKRV ESPVLPPVLV PRHSEYNPQH
151    SLLAQFRNLG QNEPHMPLNA TFPDSFQQPH SHPFPQSPNS SYPNSPGSSS
201    STYPHSPTSS DPGSPFQMPA DTPPPAYLPP EDPMAQDGSQ PMDTNMTNMT
251    APTLPAEINR GDVQAVAYEE PKHWCSIVYY ELNNRVGEAF HASSTSVLVD
301    GFTDPSNNKN RFCLGLLSNV NRNSTIENTR RHIGKGVHLY YVGGEVYAEC
351    LSDSSIFVQS RNCNYHHGFH PTTVCKIPSG CSLKIFNNQE FAQLLAQSVN
401    HGFETVYELT KMCTIRMSFV KGWGAEYHRQ DVTSTPCWIE IHLHGPLQWL
451    DKVLTQMGSP HNPISSVS•
```

Figure 15: Alignment of the published Smad1 nucleotide sequence (top) against the cloned sequence (bottom)

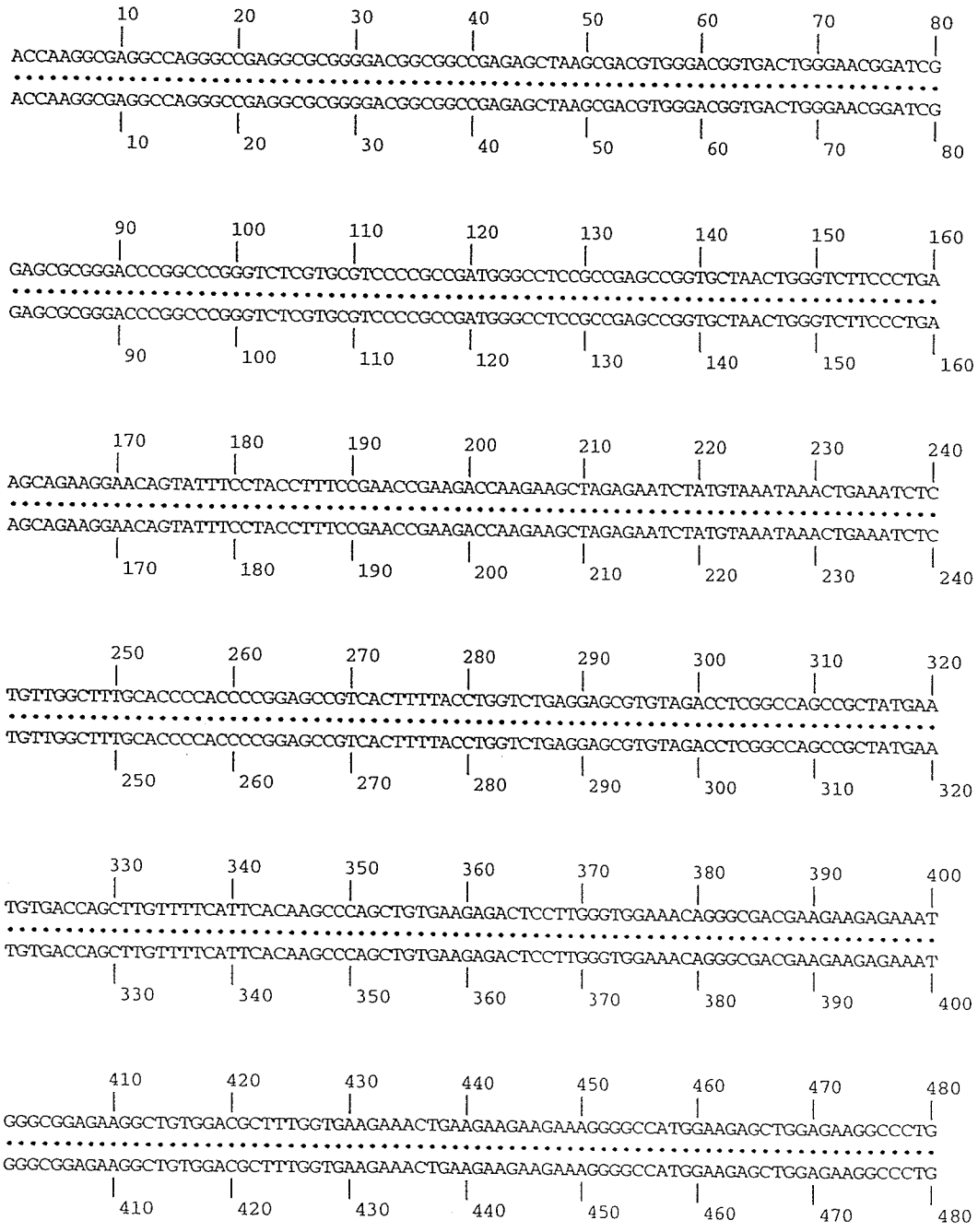

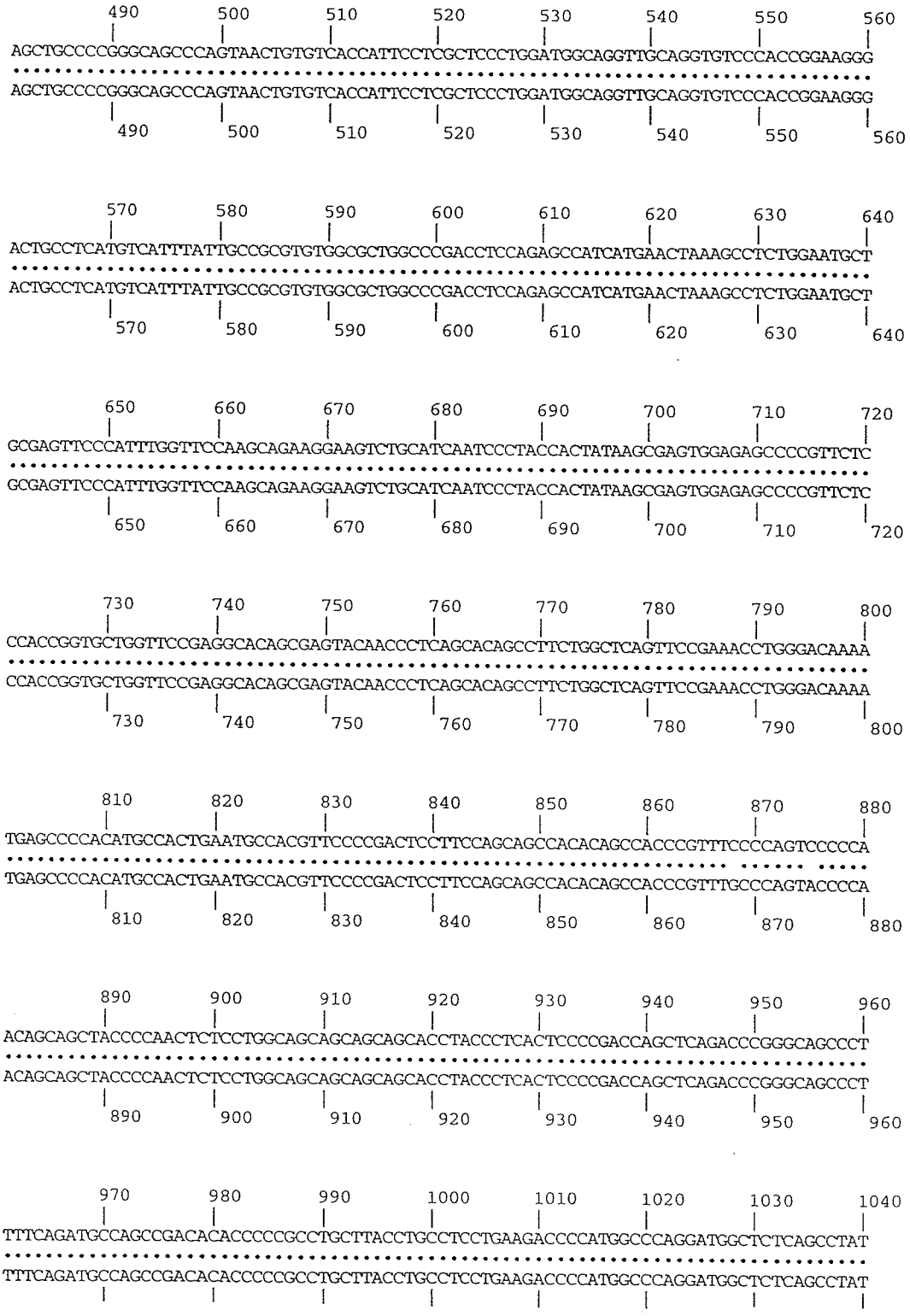
490 500 510 520 530 540 550 560
AGCTGCCCCGGGCAGCCCAGTAACTGTGTCACCATTCCTCGCTCCCTGGATGGCAGGTTGCAGGTGTCCCACCGGAAGGG
AGCTGCCCCGGGCAGCCCAGTAACTGTGTCACCATTCCTCGCTCCCTGGATGGCAGGTTGCAGGTGTCCCACCGGAAGGG
490 500 510 520 530 540 550 560
570 580 590 600 610 620 630 640
ACTGCCTCATGTCATTTATTGCCGCGTGTGGCGCTGGCCCGACCTCCAGAGCCATCATGAACTAAAGCCTCTGGAATGCT
ACTGCCTCATGTCATTTATTGCCGCGTGTGGCGCTGGCCCGACCTCCAGAGCCATCATGAACTAAAGCCTCTGGAATGCT
570 580 590 600 610 620 630 640
650 660 670 680 690 700 710 720
GCGAGTTCCCATTTGGTTCCAAGCAGAAGGAAGTCTGCATCAATCCCTACCACTATAAGCGAGTGGAGAGCCCCGTTCTC
GCGAGTTCCCATTTGGTTCCAAGCAGAAGGAAGTCTGCATCAATCCCTACCACTATAAGCGAGTGGAGAGCCCCGTTCTC
650 660 670 680 690 700 710 720
730 740 750 760 770 780 790 800
CCACCGGTGCTGGTTCCGAGGCACAGCGAGTACAACCCTCAGCACAGCCTTCTGGCTCAGTTCCGAAACCTGGGACAAAA
CCACCGGTGCTGGTTCCGAGGCACAGCGAGTACAACCCTCAGCACAGCCTTCTGGCTCAGTTCCGAAACCTGGGACAAAA
730 740 750 760 770 780 790 800
810 820 830 840 850 860 870 880
TGAGCCCCACATGCCACTGAATGCCACGTTCCCCGACTCCTTCCAGCAGCCACACAGCCACCCGTTTCCCCAGTCCCCCA
TGAGCCCCACATGCCACTGAATGCCACGTTCCCCGACTCCTTCCAGCAGCCACACAGCCACCCGTTTGCCCAGTACCCCA
810 820 830 840 850 860 870 880
890 900 910 920 930 940 950 960
ACAGCAGCTACCCCAACTCTCCTGGCAGCAGCAGCAGCACCTACCCTCACTCCCCGACCAGCTCAGACCCGGGCAGCCCT
ACAGCAGCTACCCCAACTCTCCTGGCAGCAGCAGCAGCACCTACCCTCACTCCCCGACCAGCTCAGACCCGGGCAGCCCT
890 900 910 920 930 940 950 960
970 980 990 1000 1010 1020 1030 1040
TTTCAGATGCCAGCCGACACACCCCCGCCTGCTTACCTGCCTCCTGAAGACCCCATGGCCCAGGATGGCTCTCAGCCTAT
TTTCAGATGCCAGCCGACACACCCCCGCCTGCTTACCTGCCTCCTGAAGACCCCATGGCCCAGGATGGCTCTCAGCCTAT

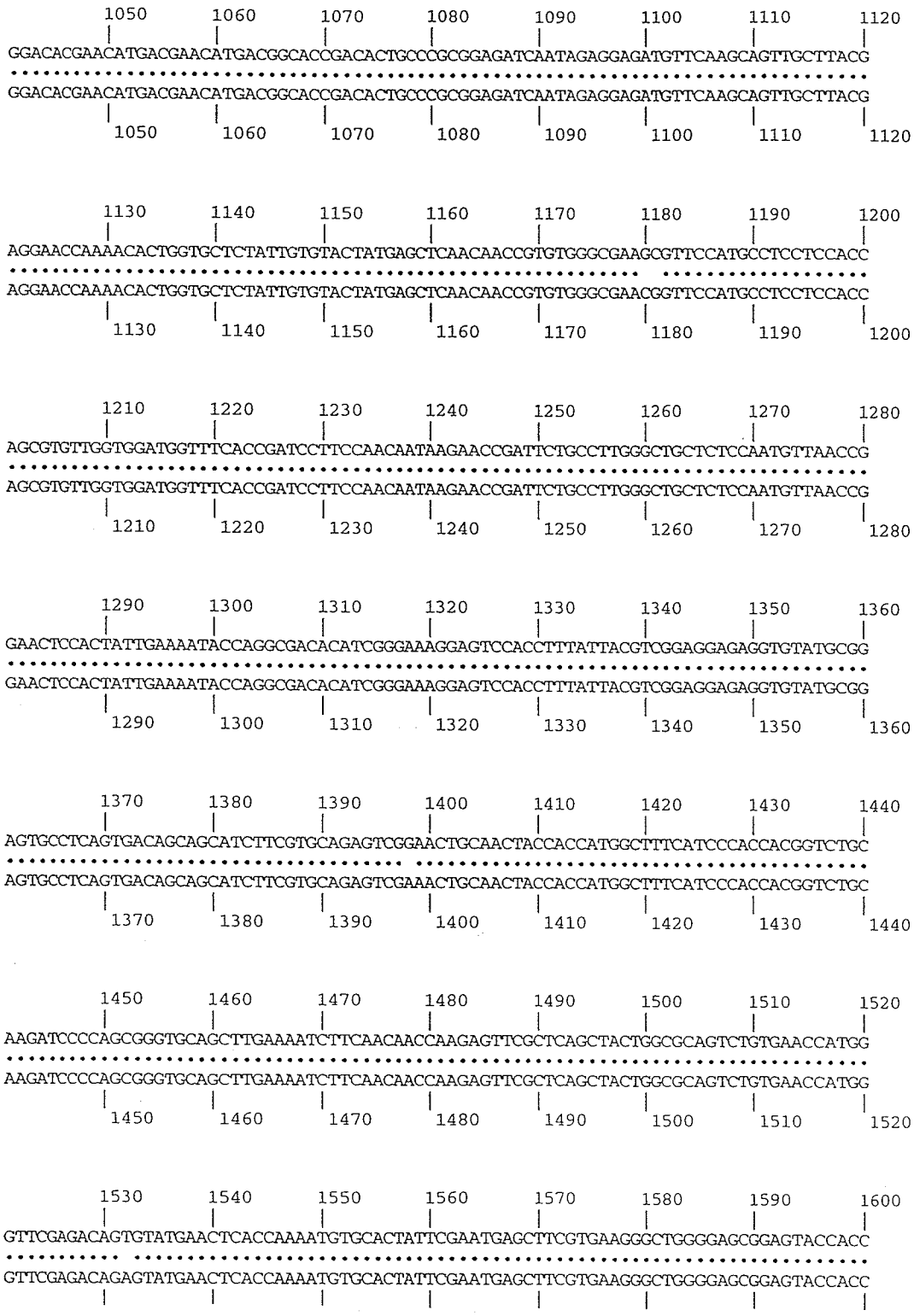
1050 1060 1070 1080 1090 1100 1110 1120
GGACACGAACATGACGAACATGACGGCACCGACACTGCCCGCGGAGATCAATAGAGGAGATGTTCAAGCAGTTGCTTACG
GGACACGAACATGACGAACATGACGGCACCGACACTGCCCGCGGAGATCAATAGAGGAGATGTTCAAGCAGTTGCTTACG
1050 1060 1070 1080 1090 1100 1110 1120
1130 1140 1150 1160 1170 1180 1190 1200
AGGAACCAAAACACTGGTGCTCTATTGTGTACTATGAGCTCAACAACCGTGTGGGCGAAGCGTTCCATGCCTCCTCCACC
AGGAACCAAAACACTGGTGCTCTATTGTGTACTATGAGCTCAACAACCGTGTGGGCGAACGGTTCCATGCCTCCTCCACC
1130 1140 1150 1160 1170 1180 1190 1200
1210 1220 1230 1240 1250 1260 1270 1280
AGCGTGTTGGTGGATGGTTTCACCGATCCTTCCAACAATAAGAACCGATTCTGCCTTGGGCTGCTCTCCAATGTTAACCG
AGCGTGTTGGTGGATGGTTTCACCGATCCTTCCAACAATAAGAACCGATTCTGCCTTGGGCTGCTCTCCAATGTTAACCG
1210 1220 1230 1240 1250 1260 1270 1280
1290 1300 1310 1320 1330 1340 1350 1360
GAACTCCACTATTGAAAATACCAGGCGACACATCGGGAAAGGAGTCCACCTTTATTACGTCGGAGGAGAGGTGTATGCGG
GAACTCCACTATTGAAAATACCAGGCGACACATCGGGAAAGGAGTCCACCTTTATTACGTCGGAGGAGAGGTGTATGCGG
1290 1300 1310 1320 1330 1340 1350 1360
1370 1380 1390 1400 1410 1420 1430 1440
AGTGCCTCAGTGACAGCAGCATCTTCGTGCAGAGTCGGAACTGCAACTACCACCATGGCTTTCATCCCACCACGGTCTGC
AGTGCCTCAGTGACAGCAGCATCTTCGTGCAGAGTCGAAACTGCAACTACCACCATGGCTTTCATCCCACCACGGTCTGC
1370 1380 1390 1400 1410 1420 1430 1440
1450 1460 1470 1480 1490 1500 1510 1520
AAGATCCCCAGCGGGTGCAGCTTGAAAATCTTCAACAACCAAGAGTTCGCTCAGCTACTGGCGCAGTCTGTGAACCATGG
AAGATCCCCAGCGGGTGCAGCTTGAAAATCTTCAACAACCAAGAGTTCGCTCAGCTACTGGCGCAGTCTGTGAACCATGG
1450 1460 1470 1480 1490 1500 1510 1520
1530 1540 1550 1560 1570 1580 1590 1600
GTTCGAGACAGTGTATGAACTCACCAAAATGTGCACTATTCGAATGAGCTTCGTGAAGGGCTGGGGAGCGGAGTACCACC
GTTCGAGACAGAGTATGAACTCACCAAAATGTGCACTATTCGAATGAGCTTCGTGAAGGGCTGGGGAGCGGAGTACCACC

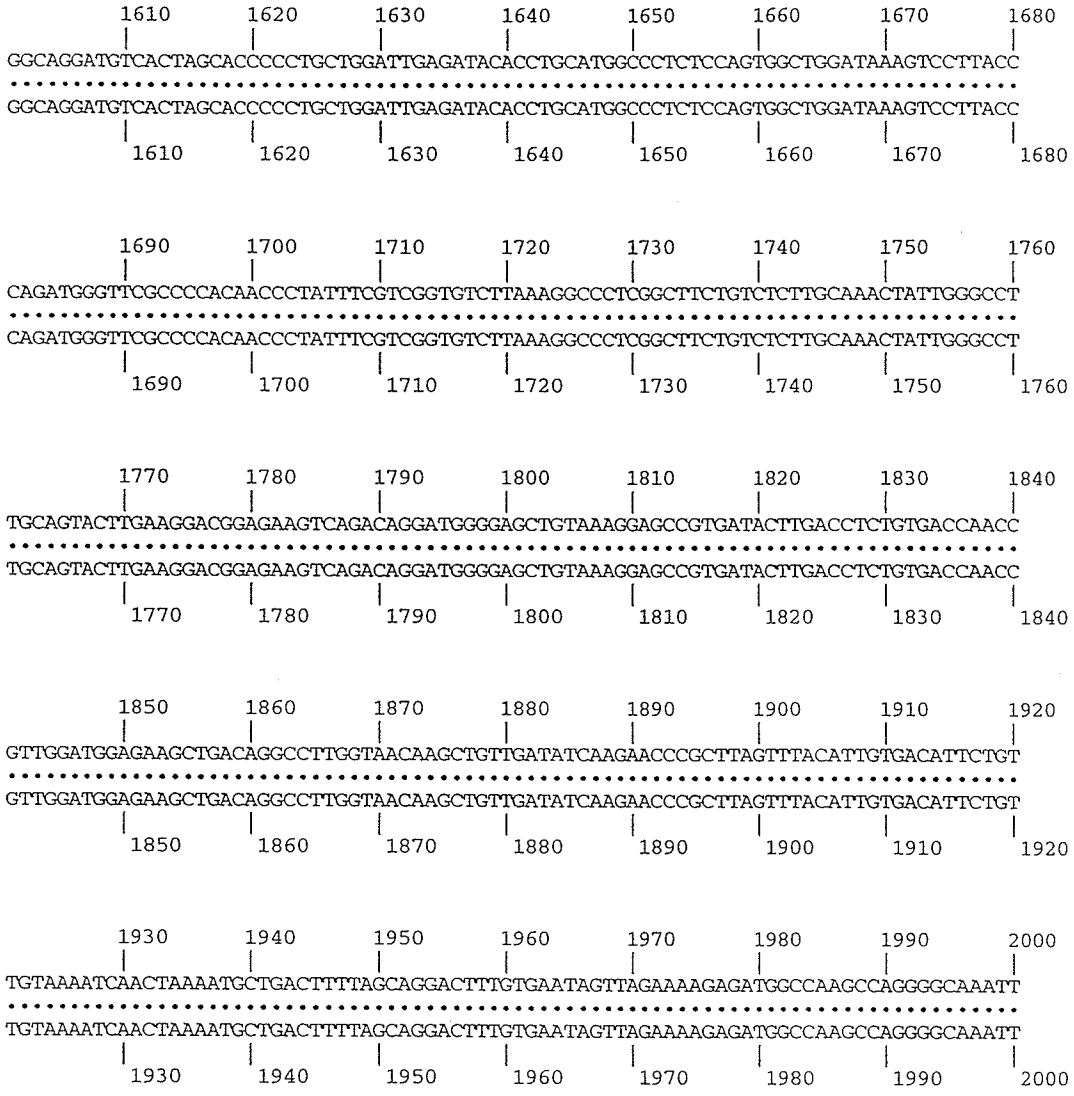
1610 1620 1630 1640 1650 1660 1670 1680
GGCAGGATGTCACTAGCACCCCCTGCTGGATTGAGATACACCTGCATGGCCCTCTCCAGTGGCTGGATAAAGTCCTTACC
GGCAGGATGTCACTAGCACCCCCTGCTGGATTGAGATACACCTGCATGGCCCTCTCCAGTGGCTGGATAAAGTCCTTACC
1610 1620 1630 1640 1650 1660 1670 1680
1690 1700 1710 1720 1730 1740 1750 1760
CAGATGGGTTCGCCCCACAACCCTATTTCGTCGGTGTCTTAAAGGCCCTCGGCTTCTGTCTCTTGCAAACTATTGGGCCT
CAGATGGGTTCGCCCCACAACCCTATTTCGTCGGTGTCTTAAAGGCCCTCGGCTTCTGTCTCTTGCAAACTATTGGGCCT
1690 1700 1710 1720 1730 1740 1750 1760
1770 1780 1790 1800 1810 1820 1830 1840
TGCAGTACTTGAAGGACGGAGAAGTCAGACAGGATGGGGAGCTGTAAAGGAGCCGTGATACTTGACCTCTGTGACCAACC
TGCAGTACTTGAAGGACGGAGAAGTCAGACAGGATGGGGAGCTGTAAAGGAGCCGTGATACTTGACCTCTGTGACCAACC
1770 1780 1790 1800 1810 1820 1830 1840
1850 1860 1870 1880 1890 1900 1910 1920
GTTGGATGGAGAAGCTGACAGGCCTTGGTAACAAGCTGTTGATATCAAGAACCCGCTTAGTTTACATTGTGACATTCTGT
GTTGGATGGAGAAGCTGACAGGCCTTGGTAACAAGCTGTTGATATCAAGAACCCGCTTAGTTTACATTGTGACATTCTGT
1850 1860 1870 1880 1890 1900 1910 1920
1930 1940 1950 1960 1970 1980 1990 2000
TGTAAAATCAACTAAAATGCTGACTTTTAGCAGGACTTTGTGAATAGTTAGAAAAGAGATGGCCAAGCCAGGGGCAAATT
TGTAAAATCAACTAAAATGCTGACTTTTAGCAGGACTTTGTGAATAGTTAGAAAAGAGATGGCCAAGCCAGGGGCAAATT
1930 1940 1950 1960 1970 1980 1990 2000

Observed changes are at positions 868 (C instead of G), 875 (C instead of A), 1180 (G instead of C), 1181 (C instead of G), 1398 (G instead of A), and 1532 (T instead of A), over the published sequence. None of these changes however, introduce a stop codon. The longest protein open-reading frame (RF-1, Figure 14) has a start /stop site at position 316 / 1722, totalling 1406bp nucleotides in length, and encodes for a protein of 468 amino acids with a calculated molecular weight of 52kDa. This data is in accordance with the published sequence. The amino acid substitutions in RF-1 are illustrated in Figure 16, in which the translated published sequence is aligned against the translated cloned sequence.

The analysis of Smad1 in hepatic stellate cells

The analysis of Smad expression in HSC attempts to study how the Smads regulate themselves. The experiment aims to study the effects of different concentrations of TGF-β1 on Smad1 mRNA expression, as well as its effect over a 24-hour period. For this purpose, the cultures of freshly isolated rat HSC are induced with 2ng/ml and 5ng/ml of the TGF-β1 in serum-free medium. A 24-hour incubation period was chosen to study the effects of TGF-β1, since the viability of cells in the absence of serum-containing medium could not be guaranteed. In addition, mRNA synthesis and degradation typically occurs over a short time span, and a 24-hour period was deemed to be sufficient for the study of Smad1 mRNA expression in this experiment. Smad1 mRNA expression was measured by Northern blotting, which involves transferring RNA to a synthetic membrane, and detection of the RNA of interest with a radioactive, single-stranded, complementary DNA probe. The Smad1 cDNA clone

Figure 16: The amino acid sequence of the published, translated RF1 (top) aligned against the cloned, translated RF1 (bottom)

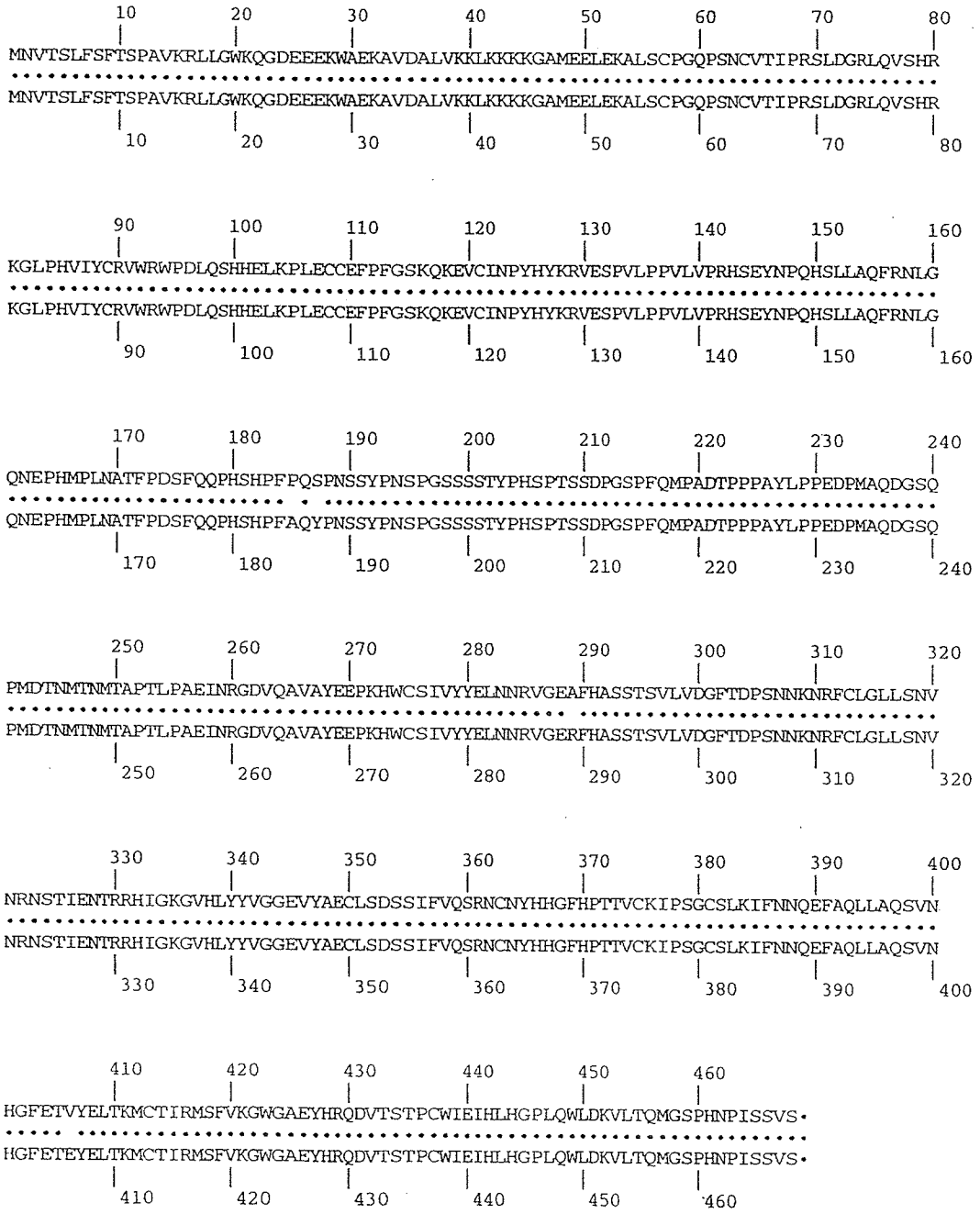

described in Section 4.2.2 was radioactively labelled, and used as the probe. In addition, a control was performed to measure 18S rRNA, in order to able to correct for potential errors in sample loading and concentration, thus enabling a comparison of the differences in expression of Smad1 mRNA among samples.

4.2.5. Northern blot agarose gel electrophoresis

The agarose / EtBr gel shows a clear separation of the 18S and 28S bands for both the 2ng/ml (left) and 5ng/ml samples (centre) (Figure 17), which is indication of sufficient sample separation for analysis of the mRNA of interest. The 5ng/ml samples show clean bands with no sample degradation. Since the 2ng/ml samples are obstructed by excess EtBr, it was unclear at this stage whether these samples were of sufficient quality for Northern blot analysis.

4.2.6. Northern blot visualization

The results of the transfer of the RNA to a membrane, its subsequent probing with the 18S rRNA and the Smad1 probe, and its visualization by autoradiography on an X-ray film, are shown in Figures 18 and 19. The exposure of the membrane to a film was performed numerous times to obtain the best image / background noise ratio, and to properly visualize the 18S rRNA and the Smad1 mRNA labelled samples. The images used were of sufficient intensity to allow for semi-quantitative analysis.

4.2.7. Analysis of Smad1 mRNA and 18S rRNA expression

The intensity of expression of each band on the X-ray film was determined by the

Figure 17: Agarose gel electrophoresis of RNA isolated from hepatic stellate cells

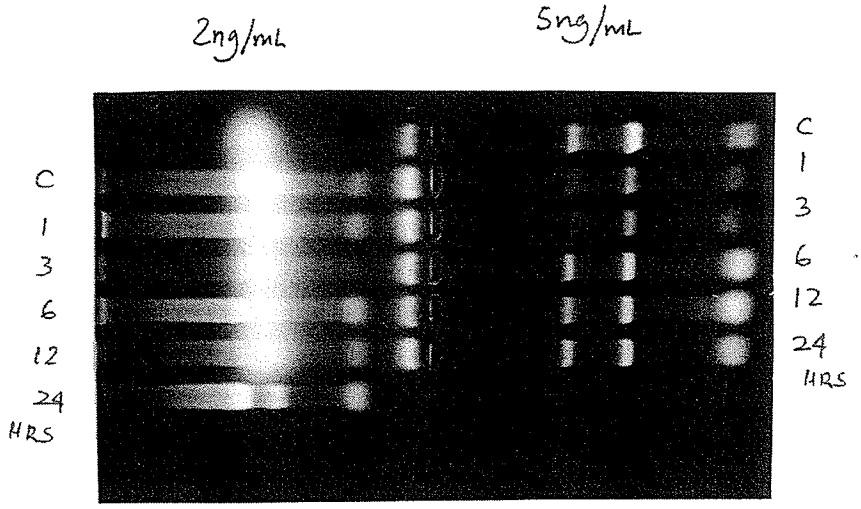

Figure 17: 18S and 28S bands for both the 2ng/ml (left) and 5ng/ml TGF-β1 treated samples (right). C = control; 1=1 hour TGF-β1 treated sample; 3 = 3 hours TGF-β1 treated; 6 = 6 hours; 12 = 12 hours; 24 = 24hours TGF-β1 treated sample.

Figure 18: Autoradiography of TGF-β1 treated HSC using 18S rRNA as a probe

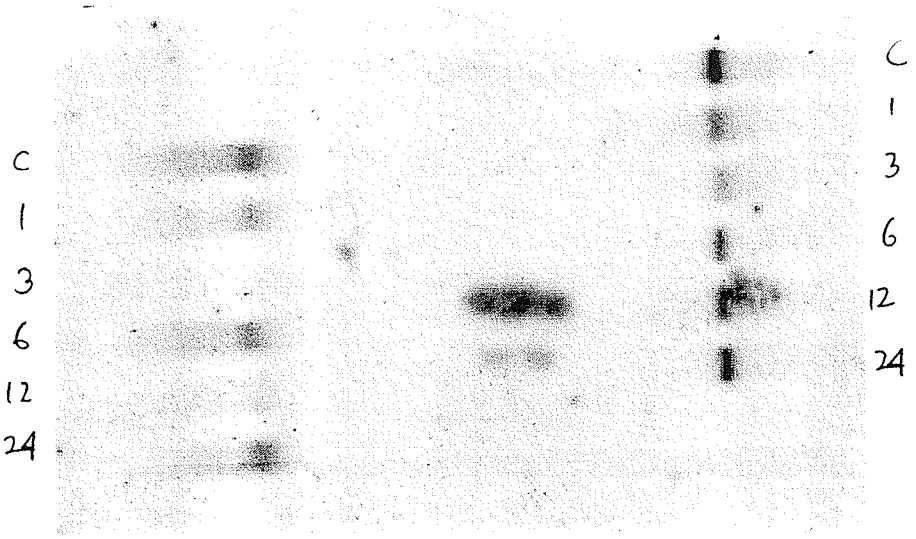

Figure 18: Dark bands show regions of high 18S rRNA concentration. 2ng/ml-TGF-β1-induced samples are shown the left side of the membrane, and 5ng/ml-induced samples are in the centre. The order of sample loading from top to bottom is: control, 1-hour TGF-β1 treated, 3-hour, 6-hour, 12-hours, 24-hour treated cells.

Figure 19: Autoradiography of TGF-β1 treated HSC using Smad1 cDNA as a probe

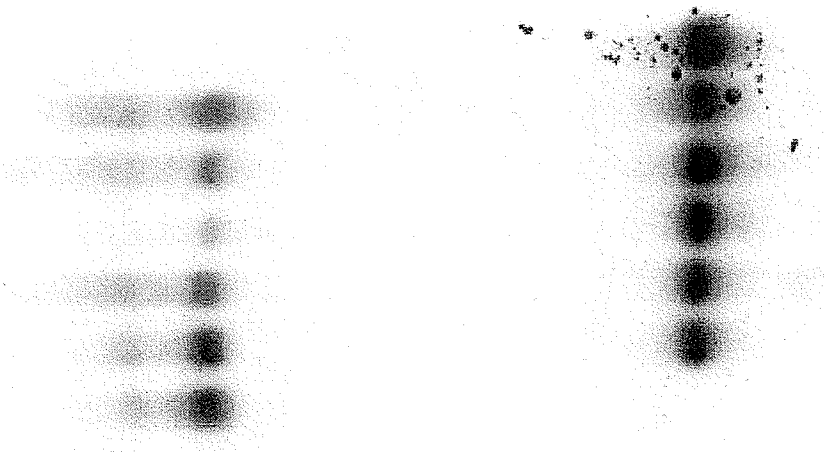

Figure 19: Dark bands show regions of high Smad1 mRNA concentration. 2ng/ml-TGF-β-induced samples are shown the left side of the membrane, and 5ng/ml-induced samples are in the centre. The order of sample loading from top to bottom are control, 1-hour TGF-β1 treated, 3-hour, 6-hour, 12-hours, 24-hour treated cells.

Table 9: Intensity of expression of Smad1 mRNA and 18S rRNA in TGF-β1 treated HSC

18S rRNA control

Time / TGF-β1 concentration	Control	1 hour	3 hours	6hrs	12hrs	24hrs
2ng/ml TGF-β1	10717	8282	3557	9438	13273	13820
5ng/ml TGF-β1	15557	15712	16795	14771	12387	10854

Smad1 mRNA

Time / TGF-β1 concentration	Control	1 hour	3 hours	6 hrs	12 hrs	24hrs
2ng/ml TGF-β1	10383	6597	1759	7750	3635	10840
5ng/ml TGF-β1	12568	10343	8582	9245	8944	10780

NIH-Image 1.61 imaging software, and is given in Table 9. To allow for possible errors in the quantity of RNA sample loaded onto the gel, as well as for sample degradation during the storage of samples and electrophoresis, the expression of Smad1 mRNA recorded on the film had to be corrected against the 18S rRNA control sample. The corrected results are tabulated in Table 10. The corrected expression of Smad1 mRNA in TGF-β1-induced HSC for both 2ng/ml and 5ng/ml treated samples were plotted against the time of cell induction with TGF-β1. Plots are shown in Figure 20 and 21.

Both the 2ng/ml and 5ng/ml TGF-β1 groups show a decrease of Smad1 RNA expression after 1 hour, reaching a maximum depression after 3 hours. In both, there is an increase in Smad1 mRNA expression after 3 hours, to approximate control levels at 24 hours.

4.3. Cloning of the rat Smad1 Promoter

The goal of this section was to clone the 5'-flanking region of the rat Smad1 gene. The method selected for promoter cloning involves nested PCR, using commercial genomic DNA that has ligated to its 5'-ends specific adaptor oligomers of known sequence, thus enabling the cloning of the 5'- region by the use of adaptor specific primers and the primers designed along the Smad1 cDNA sequence. The rat was chosen over the human as the species from which the 5'-flanking region was to be identified, as the intent of the cloning and identification of the Smad1 promoter region was to study its interaction in cells isolated from rats.

Table 10: Corrected values for the intensity of Smad1 mRNA expression in TGF-β1 treated HSC

Time / TGF-β1 concentration	Control	1 hour	3 hrs	6 hrs	12 hrs	24 hrs
2ng/ml TGF-β1	0.97	0.80	0.49	0.82	0.27	0.78
5ng/ml TGF-β1	0.81	0.65	0.51	0.62	0.72	1.00

Expression of Smad1 mRNA =
expression of Smad1 mRNA when exposed to x hours TGF-β1 /
expression of 18S rRNA for the same sample

Figure 20: Change in Smad1 mRNA expression with time in HSC that were treated with 2ng/ml TGF- β1

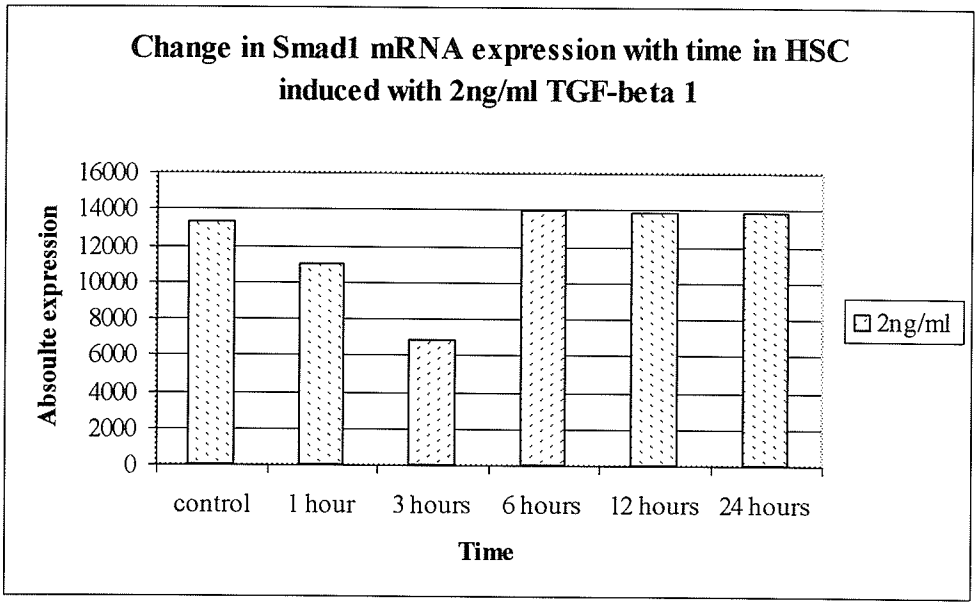

Figure 20: Changes in Smad1 mRNA expression in rat HSC. Control group: HSC that were incubated for a period of 24 hours in serum-free DMEM without TGF-β1 treatment. Arbitrary units.

Figure 21: Change in Smad1 mRNA expression with time in HSC that were treated with 5ng/ml TGF- β1

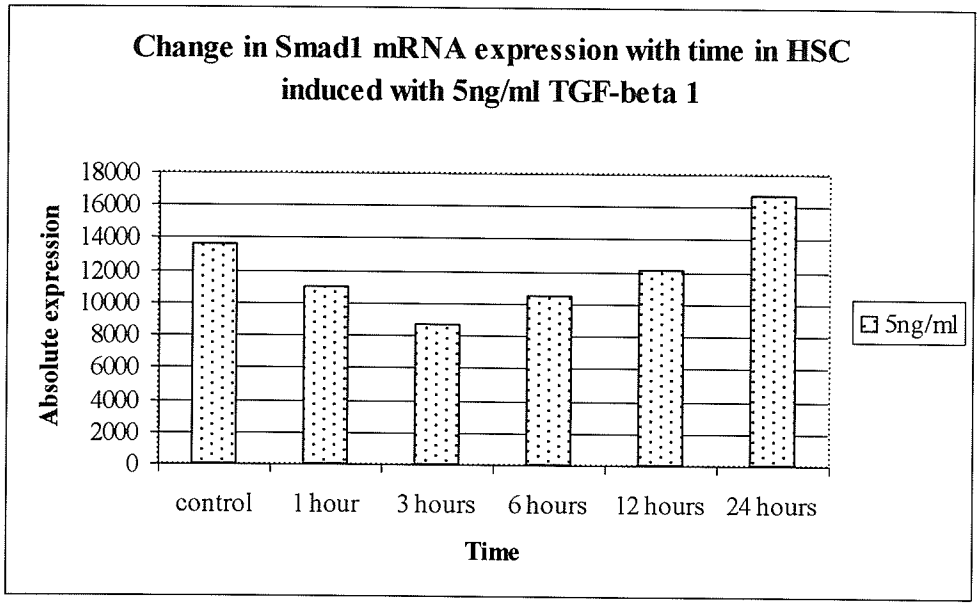

Figure 21: Changes in Smad1 mRNA expression in rat HSC. Control group: HSC that were incubated for a period of 24 hours in serum-free DMEM without TGF-β1 treatment. Arbitrary units.

To clone the 5'-flanking region, primary and secondary PCR were performed on all the four commercial genomic DNA templates. The products of the secondary PCR were ligated into the Zero Blunt pCRII TOPO vector and cloned in *E.Coli*, followed by analysis of the recombinant vector using the *EcoRI* restriction enzyme. While two restriction sites for *EcoRI* exist at the -11 and +7 sites surrounding the cloning site of the vector, it is not known if any restriction sites exist in the cloned PCR products. Therefore, the purpose of the restriction enzyme digest was to identical plasmids within each cloned DNA library. Large-scale cloning reactions were carried out for all unique recombinant plasmids, and partial sequencing was performed at the 5'- and 3'-ends of the inserted PCR product, using the priming sites of the Zero Blunt vector. From the initial partial sequences, identical PCR fragments could be identified, and the longest, continuous PCR fragment could be submitted for full-length sequencing.

4.3.1. Analysis of primary and secondary PCR products

Primary PCR

8µl of the primary PCR products were electrophoresed on a 1.5% agarose / EtBr gel in TBE buffer (Figure 22a). Several bands for each DNA library (EcoRV, DraI, PvuII, SspI) were observed. The EcoRV library shows multiple, non-specific weak bands, the DraI library a strong band at approximately 134 base-pairs, the PvuII library reveals two strong bands at approximately 800 and 1100bp, and finally the SspI library shows two strong, closely spaced bands of a size larger than 1100, but smaller than 1636bp. As expected, no PCR products were observed for the negative control. The positive control, employing the EcoRV library, gave the expected fragment at 1500bp.

Figure 22: Smad1 primary and secondary PCR promoter products

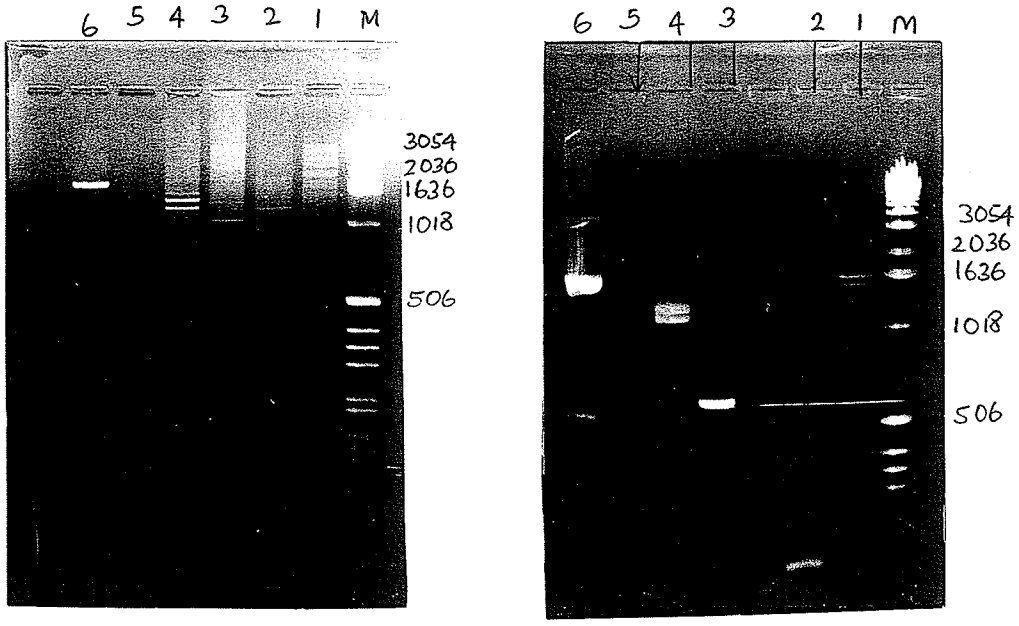

Figure 22a: **PCR products of the primary PCR reaction.** Legend: lane"M": 1kb DNA ladder; lane 1: EcoRV library; lane 2: DraI library; lane 3: PvuII library; lane 4: SspI library; lane 5: negative control; lane 6: positive control.

Figure 22b: **PCR products of the nested PCR reaction.** Legend: lane "M": 1kb DNA ladder; lane 1: EcoRV library; lane 2: DraI library; lane 3: PvuII library; lane 4: SspI library; lane 5: negative control; lane 6: positive control.

Secondary PCR

Figure 22b shows the results when 5µl of each secondary PCR product were subjected to electrophoresis on a 1.2% agarose/EtBr gel in TBE buffer. The EcoRV library shows weak bands of a non-specific nature. The DraI library gives one strong band at 134 base pairs, PvuII one product of approximately 800bp, and SspI lshows two strong, closely separated bands at approximately 1100bp each. As expected, no products were observed for the negative control. The positive control gave a 1.5kb product.

4.3.2. Subcloning and plasmid isolation

Cloning the secondary PCR products into the Zero Blunt pCR-Blunt II-TOPO plasmid vector in *E.Coli* was negative for the EcoRV product. Cloning of the products of the remaining three DNA libraries proved successful: from these, 4 plasmids from the DraI library, 11 from the PvuII library, and 5 from the SspI colony were isolated.

4.3.3. Small-scale restriction enzyme analysis of cloned PCR products

Figures 23 – 25 show the *EcoRI* restriction enzyme products. For the DraI library (Figure 23), lanes 1 – 3 gave fragments of about 134bp, which corresponds its PCR product in nested PCR. The PvuII library (Figure 24) reveals that 11 products contain a fragment of approximately 800bp length. Figure 25 shows the resulting restriction enzyme digest for the SspI library. Here all five lanes gave a fragment of the expected size of approximately 1100bp.

Figure 23: *EcoRI* restriction enzyme analysis for the DraI cloning reaction

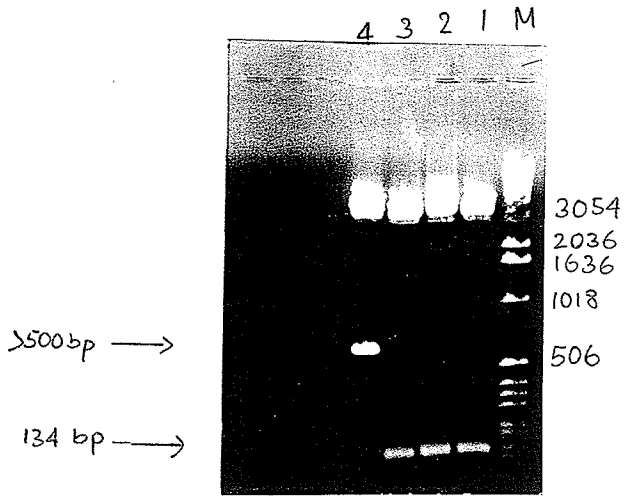

Figure 23: **Results of the *EcoRI* restriction enzyme digest for the DraI PCR products.** The secondary PCR product of the DraI DNA "library" was cloned into the Zero Blunt pCR-Blunt II-TOPO plasmid vector then excised by EcoRI to identify positive cloning products. *Legend:* lane "M": 1kb DNA ladder; lanes 1 – 3: fragment at approximately 134bp represents the cloned DNA PCR product; lane 4: unknown DNA product at approximately 500bp.

Figure 24: *EcoRI* restriction enzyme analysis for the PvuII cloning reaction

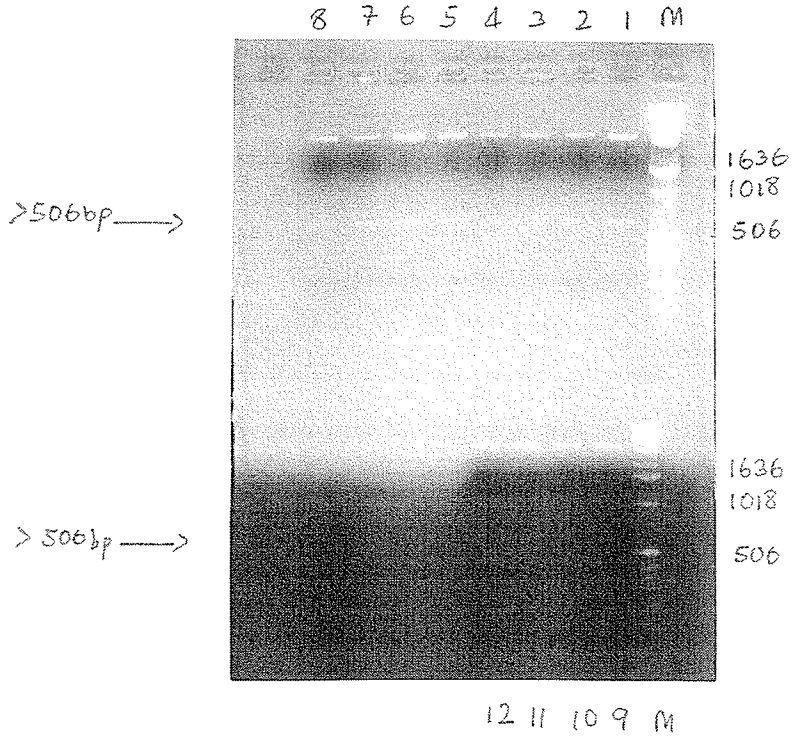

Figure 24: **EcoRI restriction enzyme digest for the PvuII PCR products.** The secondary PCR product of the PvuII DNA "library" was cloned into the Zero Blunt pCR-Blunt II-TOPO plasmid vector then excised by EcoRI to identify positive cloning products. *Legend:* lane "M": 1kb DNA ladder; lanes 1 – 12: fragment at approximately 500bp represents the cloned DNA PCR product.

Figure 25: *EcoRI* restriction enzyme analysis for the SspI cloning reaction

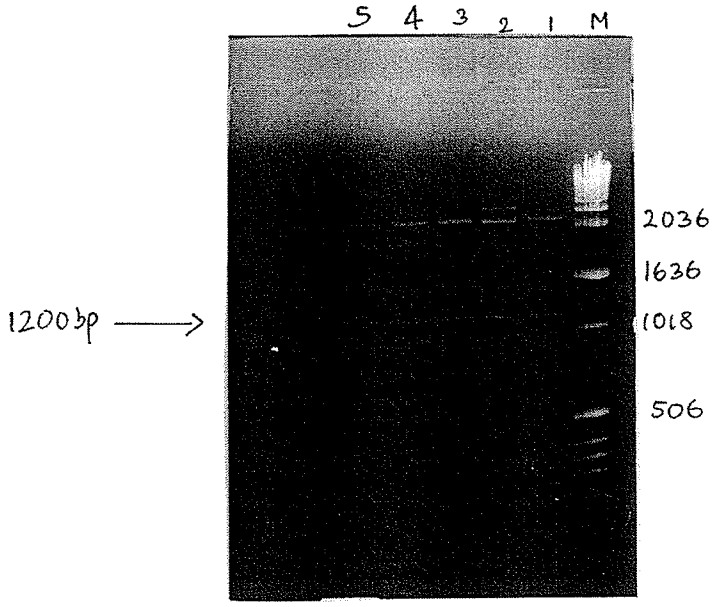

***Figure 25: EcoRI* restriction enzyme digest for the SspI PCR products.** The secondary PCR product of the SspI DNA "library" was cloned into the Zero Blunt pCR-Blunt II-TOPO plasmid vector then excised by EcoRI to identify positive cloning products. *Legend:* lane "M": 1kb DNA ladder; lanes 1 – 5: fragment at approximately 1100bp represents the cloned DNA PCR product.

4.3.4. Large-scale cloning and analysis

Five plasmids corresponding to the small-scale cultures were cloned on a large-scale. From each, samples were taken for analysis by *EcoRI* and *AvaI*. Figure 26 shows the gel from the *EcoRI* restriction digest for the PvuII and SspI samples. Lanes 3-1 and 3-3 reveal a fragment of 1100bp, which is indicative of the cloned SspI product. Similarly, lanes 5-1 and 5-2 show a fragment at 800bp, confirming the PvuII PCR product. Figure 27 shows the results of the *AvaI* restriction enzyme digest, which confirmed that the cloned products selected for further analysis were identical to each other.

4.3.5. Partial sequencing

Three PCR products were submitted for partial sequencing. The sequences obtained were aligned against the published rat Smad1 cDNA sequence (GenBank Accession Number U66478), using the GeneJockey Sequence Processor. All three products were found to be identical at the 3'- end, but different at the 5'- ends due to the differences in their lengths. For illustration, the following describes the alignment results of DraI (3A), SspI (3-1), and PvuII (5-1). The full-length sequence is described in Section 4.4.6.

5' end:

3AR: Aligns at positions 138 – 165 of Smad1. Total sequenced length of the product is 493bp.

3-1R: Aligns at positions 138 – 204 of the rat Smad1 gene. The total length of the sequenced product is 599bp.

Figure 26: *EcoRI* restriction enzyme analysis for the DraI and SspI large-scale cloning reaction

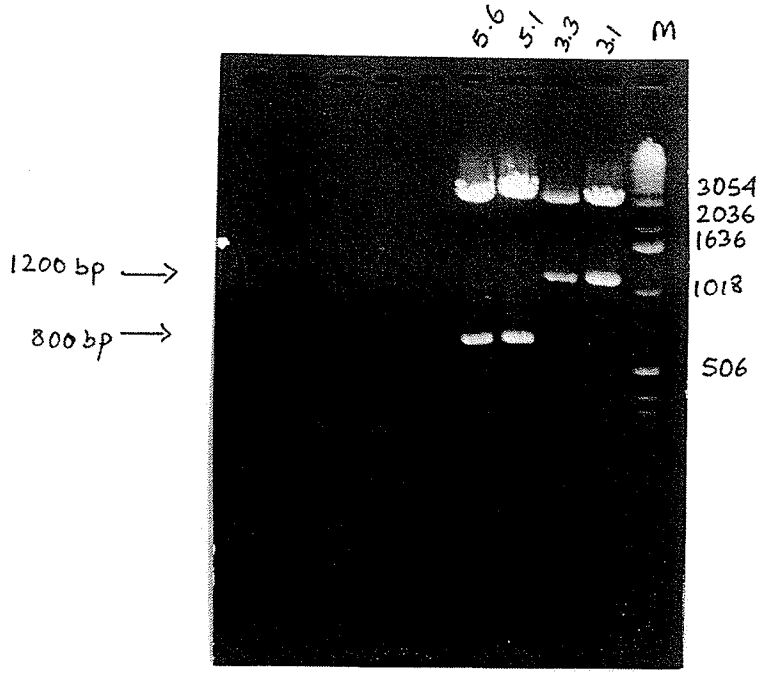

***Figure 26: EcoRI* restriction enzyme digest of the large-scale cloning reaction.** Large-scale cloning reaction from the bacterial cultures of the small-scale culture. 0.5ml of the remaining bacterial cultures were used to propagate the Zero Blunt pCR-Blunt II-TOPO plasmid vector with the ligated PCR product on a large-scale, then excised by *EcoRI* to identify cloned products. *Legend:* Lane "M" is the 1kb DNA ladder. 3-1 and 3-3 are the SspI plasmid products. The fragment at approximately 1100bp is consistent with that observed for the small-scale and nested PCR reaction; 5.1 and 5.6. show the PvuII plasmid fragment at approximately 800bp, again consistent with the observed product of nested PCR.

Figure 27: *AvaI* restriction enzyme analysis for the DraI and SspI large-scale cloning reaction

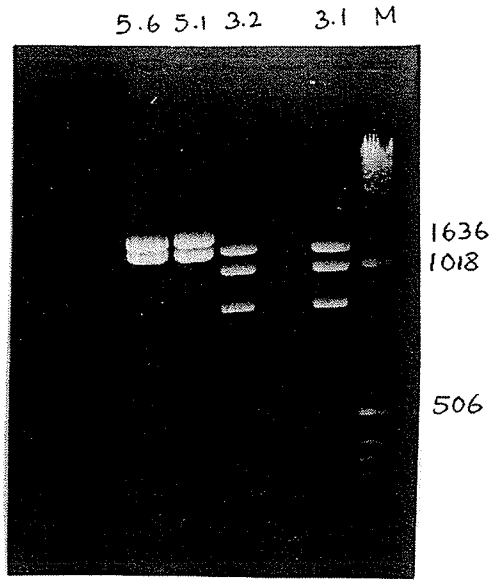

Figure 27: **AvaI restriction enzyme digest of the large-scale cloning reaction.** Large-scale cloning reaction from the bacterial cultures of the small-scale culture. 0.5ml of the remaining bacterial cultures were used to propagate the Zero Blunt pCR-Blunt II-TOPO plasmid vector with the ligated PCR product on a large-scale, then excised by *AvaI* to identify cloned products. *Legend:* Lane "M" is the 1kb DNA ladder. 3-1 and 3-3 are the SspI plasmid product. The three bands indicates that both products are identical to each other; 5.1 and 5.6. show two identical bands each, indicating that the PvuII plasmids cloned are indeed identical to each other.

5-1R: Aligns at positions 138 – 204 of the rat Smad1 gene. Total length of the sequenced product is 600bp.

3'-end:

3AR: No sequence information could be obtained.

3-1F: Perfect alignment at positions 138 –204 of the Smad1 gene. The total length of the sequenced product is 501bp.

5-1R: Perfect alignment at positions 138 - 204 of the Smad1 gene. The total length of the sequenced product is 493bp.

4.3.6. Full-length sequencing

Based on the length of the nested PCR products, the longest clone (Sample 3-1, of the SspI library) was submitted for sequencing with the appropriate primers. The full-length sequence was obtained by aligning the sequenced fragments against each other, as well as against the published Smad1 cDNA sequence to remove duplicate sequences. The total length of the sequence is 1078bp long, and aligns at position 138 of Smad1 cDNA. Figure 28 gives the sequence in full. Figure 29 shows the predicted location of the sequenced product, along with the location of the other PCR fragments from the Genome Walker libraries along the Smad1 gene. Based on this prediction, it is suggested that the cloned fragment represents part of intron 1 of the rat Smad1 gene.

Figure 28: Full-length sequence of the cloned Smad1 gene fragment

Contig of Contig Reverse 2(top), Contig Reverse 1(bottom)

```
       1  ACTATAGGGC ACGCGTGGTC GACGGCCCGG GCTGGTATTT CATCTCTACT
      51  GTAGTTTCCT CTTTGACTCG TGGTTAAAAT TATGGTTGTT TTCAACCCCA
     101  TATTATTGTT GATGTCTTAG TTATACTAAG GCCGAGGGGT CTTGGTTATT
     151  ACCATTTATT ATACGTTTAC ATGCAGCTAC GTGCACAGAC GTCGAGTTGT
     201  CTGCCCTGGT TGTTTGTTCA TTATGGAGAC AGGGTCTCTG GCTGACCTGA
     251  GCTTGCTAAT GAACTGGTCC AGCCAGCAAG TTCAGAGATC CGCCTGTGCC
     301  TTCTCAGAGT GGGCAGATAA GCACGGTCCG CTCAGTGTGG GCTCTGAGAA
     351  CGGGACGAGT GCCCTCAGGC TTCTGANGCA CTGAGCGGGC TCCTCCACCC
     401  ACAGGAGCTT ATCCTTCAAA TGATTTTCCT CTGTCACCAA AAACCTCTGG
     451  CTTTGCCGAT GAATTTGGTC GCATTTTTAC GCTGTAGTCT TCTGTACCTG
     501  TCGGCTCCTG TGTATCAGTC CATCTCCCTC CAGGAGTGTC GGTTGCTGGA
     551  GTGGTTTAGC TTCTTTGCAG TTTTGTGCTT GGTATCTGTT GGGGCTTGTC
     601  ACTTTCGTTT ACATATGAGG TGGTAATATG CAAATCAGCC AAGTGGATTT
     651  TTCTGTGCCC GAAACACTCG CATGACCTTT GTCCAGGGCT TGGGTGCTGT
     701  TGGGAGCAAT CTATTCCCTT CCTCTTGTAA AGCTGCCAAT CCTGTTGCCT
     751  CAAGCCCCAC CCACCCTTAT AATCTAACTT AACCCTAGTG AGTTACTTAG
     801  AGGCTCCAAG CCCAAATACC AGTCGGTCGC AGTGGGTGCT CTGCCTTTAA
     851  CTGGTGAACT TTAGGAGAAC GTAGCTCAGT TCCTGGTGTC ACAGGACACA
     901  AATGTTCATG AACTCAGCAT GGGGTTGCTC TCTAATGAAG TCACCGAATT
     951  GGTCTAAGCC AAGCGTGGAC CTCTACCACA GGGTCAGACT TAAGTAGTTA
    1001  GTACCTGGCA CGCACTAATT AGCTAATTGT GACGCAGTTA GAGTAATTTT
    1051  AAATCAGCTT CTTGTCTTTT CTTTCGCA
```

Figure 29: Alignment and prediction of the location of the cloned PCR fragments along the rat Smad1 gene

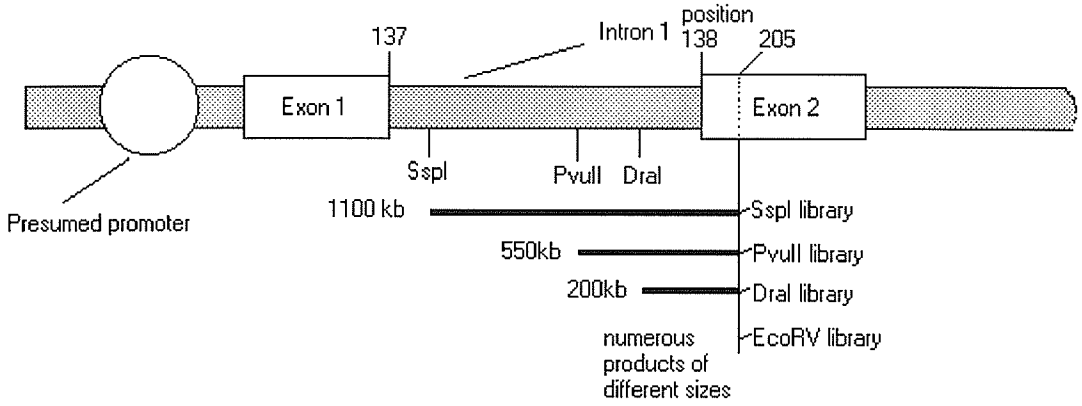

Adapted from the *Clontech Genome Walker User Manual (PT1116-1, 11/10/1999, page 8), < http://www.clontech.com/techinfo/manuals/PDF/PT1116-1.pdf>*

V. DISCUSSION

In this study we attempted to examine Smad1 transcriptional activity in hepatic stellate cells. We examined the mRNA levels of Smad1 under transforming conditions, as well as under conditions that favour signalling through Smad2. In addition, we have cloned the Smad1 cDNA sequence in the rat, and attempted to elucidate part of the 5'-flanking region in the same species. We suggest that Smad1 plays a significant role in HSC and it's transformation into MFBL cells, and is important in cellular events that lead to fibrosis of the liver.

5.1. Examination of Smad1 mRNA levels in rat hepatic stellate cells

The concentration of Smad1 mRNA was examined *in vitro* HSC cultures. In these cells, the transformation into the myofibroblast-like phenotype is typically observed after six days of culture, with complete transformation recorded after nine days. While elevated levels of the Smad1 protein has been observed in transforming cells, as well as the localization of phospho-Smad1 in the nuclear and peri-nuclear region of the cell [82], it is not known whether this increase is the result of increased translational or transcriptional activity. To answer this question, an experiment was designed to measure the concentration of Smad1 transcriptional activity, as determined by changes in Smad1 mRNA levels, in primary cultures that were allowed to mature for 1, 3, and 9 days prior to isolation of RNA. Cells at the 1 day stage are completely untransformed, establishing a base-line from where to compare increases in Smad1 mRNA levels. Cells that are allowed to mature for 3 days can be construed to be in the pre-differentiation stage, while cells cultivated for 9 days are completely

transformed. Using the RT-PCR method, where total RNA of cells is converted to cDNA by using the appropriate Smad1 amplification primers, the transcription of Smad1 in hepatic stellate cells could be studying at various stages of the transformation process.

The results of this study indicate that Smad1 transcriptional activity is up-regulated in cells that are preparing to undergo transformation, and that these levels remain high after the transformation is complete. Using arbitrary, computer generated units of expression intensity, Smad1 levels increased from 0.34 at day 1 to 1.03 at day 3, and remained artificially high at 1.07 at day 9. These results would suggest that the transcription of Smad1 might indeed be an initiating factor in the fibrotic response of hepatic stellate cells.

5.2. Cloning of rat Smad1 cDNA

As part of the study of the transcriptional activity of Smad1 in rat HSC, Smad1 cDNA was cloned. The sequence obtained was checked multiple times to ensure accuracy. The sequence shows six nucleotide substitutions over the published Smad1 cDNA sequence available (GenBank Accession Number U66478). When analysed for open reading frames, the longest, continuous frame remains at positions 316 to 1722 of the published sequence, giving a protein of 468 amino acids in length, but with *alanine* substituted in place *proline* at position 185, *tyrosine* in place of *serine* at position 187, *arginine* instead of *alanine* at position 289, and *glutamic acid* instead of *valine* at position 406. In both cloned and published sequences, the SSXS phosphorylation site

that actives the Smad protein through the kinase activity of the type I receptor is observed at the C-terminal of the protein, with the "X" amino acid being *valine*. The significance of the amino acid substitutions, if any, is not known.

5.3. The effect of the TGF-β1 cytokine on the expression of Smad1 mRNA in rat hepatic stellate cells

To further study the effect of Smad1 transcriptional activity in HSC, Smad1 mRNA expression was studied under cell conditions that favour signalling by Smad2. The TGF-β signalling pathway controls Smad signalling through the nature of its ligands: Smad1 is activated by BMP ligands, whereas Smad2 is phosphorylated by TGF-β1 receptor binding. Since TGF-β1 is believed to be a major fibrogenic activator, the effect of this ligand on Smad1 mRNA transcription was studied. The experiment was conducted in a time and dose-dependent fashion where 2 and 5ng/ml TGF-β1 treated cells were examined for Smad1 mRNA expression over a time period of 24 hours. Results show a steady decline for Smad1 mRNA for both concentration groups, with a maximum depression after 3 hours, followed by return to control levels by 24 hours. No correlation could be made regarding the effect of different concentrations of TGF-β1. It would appear that the Smad1 is initially down-regulated in the cell, suggesting a cellular mechanism involving feedback inhibition designed to maximize signalling events through Smad2. Experiments from our lab has shown that Smad4 levels remain constant in pre- and post-transformed cells, hence the down-regulation of Smad1 could be explained to allow for favourable competitive binding of Smad2 with Smad4.

5.4. Cloning of the 5'-flanking region of the rat Smad1 gene

The cloned PCR sequence of the rat Smad1 gene was constructed from overlapping sequences obtained from full-length sequencing. The sequence is 1078bp long, and aligns at position 138 of the Smad1 sequence. This would suggest that position 137 represents boundary between exon 1 and intron 1 of the rat Smad1 gene. The sequence obtained thus represents part of intron1 of the rat Smad1 gene. Further PCR and cloning is required to identify elements upstream of exon1. The identification of intron 1 will be of assistance for cloning of the promoter region, and may allow for future database searches to identify the rat Smad1 promoter region from *established sequence tags (ESTs)*, and unordered sequences in the GenBank database.

5.5. Concluding remarks

A proposed model of Smad signalling in HSC using the existing data is proposed. In this model, an increase in TGF-β1 causes Smad2 to act as a second messenger in mediating the cytokine effect, first by being phosphorylated by the cell surface receptor, then by associating with Smad4 and translocating into the nucleus, where the complex binds to DNA and causes the transcription of target genes. This is accompanied by the binding of Smads to the SBE of the Smad7 promoter region, causing Smad7 to be up-regulated, and the simultaneous binding of transcription factors to Smad1 causing its down-regulation. The down-regulation of Smad1 enables Smad2 to successfully compete for available Smad4, which has been shown to remain at constant levels in HSC (unpublished results), while the up-regulation of Smad7 mediates the negative feedback inhibition response that has been well-

documented in the literature, whereby a progressive increases in Smad7 blocks type I receptor phosphorylation sites, inhibiting further signalling by Smad2, and bringing the cell pathway to a halt.

VI. References

1. Friedman, S.L., *The cellular basis of hepatic fibrosis.* NEJM, 1993. **328**(25): p. 1828-1853.
2. *The Merck Manual of Diagnosis and Therapy.* 1999, <http://www.merck.com/pubs/mmanual/section4/chapter36/36a.htm>
3. Masaki Matsuoka, H.T., *Stimulation of Hepatic Lipocyte Collagen Production by Kupffer Cell-derived Transforming Growth Factor-beta: Implication for a Pathogenetic Role in Alcoholic Liver Fibrogenesis.* Hepatology, 1990. **11**(4): p. 599 - 606.
4. Bissel, D.M., *Hepatic fibrosis as would repair: A progress report.* Journal of Gastroentrology, 1998. **33**: p. 295 - 302.
5. Friedman, S.L., *Cellular Networks in Hepatic Fibrosis.* Digestion, 1998. **59**: p. 368 - 371.
6. Hidekazu Tsukamoto, W.H., Seiichiro Kamimura, Onni Niemela, Seppi Parkkila, Seppo Yla-Hettuala, *Experimental Liver Cirrhosis Induced by Alcohol and Iron.* J. Clin. Invest., 1996. **96**: p. 620 - 630.
7. Richard A. Rippe, L.W.S., Branko Stefanovic, Jose A. Solis-Herruzo, David A. Brenner, *NF-kB Inhibits Expression of the alpha1 (I) Collagen Gene.* DNA and Cell Biology, 1999. **18**(10): p. 751 - 761.
8. Natalia Nieto, S.L.F., Patricia Greenwel, Arthur I. Cederbaum, *CYP2E1-Mediated Oxidative Stress Induces Collagen Type I Expression in Rat Hepatic Stellate Cells.* Hepatology, 1999. **30**: p. 987 - 996.
9. Rockey, D., *The Cellular Pathogenesis of Portal Hypertension: Stellate Cell Contractility, Endothelin, and Nitric Oxide.* Hepatology, 1997. **25**: p. 2-5.
10. S. C. G. Tseng, E.A.S., R. Stern, *Types of collagen synthesized by normal rat liver hepatocytes in primary culture.* Hepatology, 1983. **3**: p. 955 - 963.
11. Jacquelyn J. Maher, D.M.B., Scott L. Friedmann, F. Joseph Roll, *Collagen Measured in Primary Cultures of Normal Rat Hepatocytes Derives from Lipocytes within the Monolayer.* J. Clin. Invest., 1988. **82**: p. 450 - 459.

12. R.-I. Hata, Y.N., J. Sano, H. Konomi, H. Hori, H. Sunada, S. Tanaka, K. Kabuki, Y. Nagai, Y. Tsukada, *Activation of collagen synthesis in primary culture of rat liver paranchymal cells (hepatocytes).* J. Cell Phys., 1985. **122**: p. 333 - 342.

13. Sheila Sherlock, J.D., *Diseases of the Liver and Biliary System*. 10 ed. 1997, Boston: Blackwell.

14. Gressner, A.M., *Transdifferentiation of hepatic stellate cells (Ito cells) to myofibroblasts: A key event in hepatic fibrosis.* Kidney International, 1996. **49 Suppl 54**: p. S-39 - S-45.

15. V. Paradis, P.M., A. Laurent, F. Charlotte, M. Vidaud, T. Poynard, C. Hoang, *Histological features predictive of liver fibrosis in chronic hepatitis C infection.* Journal of Clinical Pathology, 1996. **49**: p. 998 - 1004.

16. Gulcin Demirci, B.N., Rudolf Pichlmayr, *Fibrosis In Chronic Rejection of Human Liver Allografts.* Transplantation, 1996. **62**(12): p. 1776 - 1783.

17. P. van Eyken, R.S., V. J. Desmet, *Expression of the novel ECM component tenascin in normal and diseased human liver. An immunohistochemical study.* J. Hepatology, 1990. **11**(43).

18. G. Ramadori, T.V., S. Schwogler, H. P. Dienes, T. Knittel, H. Reider, K.-H. Meyer zum Bushenfelde, *Expression of the gene of the alpha-smooth muscle-actin isoform in rat liver and in rat-storing (ITO) cells.* Vichows Archiv B Ccell Pathol., 1990. **59**: p. 349 - 357.

19. S. L. Friedman, F.J.R., J. Boyles, D. M. Arenson, D. M. Bissell, *Maintenance of differentiated phenotype of cultured rat hepatic lipocytes by basement membrane matrix.* J. Biol. Chem, (264): p. 10756 - 10762.

20. Clement Bruno, J.-A.G., Jean-Pierre Campion, Yves Deugner, Andre Guillouzo, *Cell Types Involved in Collagen and Fibronectin Production in Normal and Fibrotic Human Liver.* Hepatology, 1986. **6**(2): p. 225 - 234.

21. Bernard H. Davis, U.R.R., Nicholas O. Davidson, *Retinoic acid and transforming growth factor beta differentially inhibit platelet-derived-growth-factor-induced Ito-cell activation.* Biochem J, 1991. **278**: p. 43-47.

22. Bernard H Davis, U.R.R., Nicholas O Davidson, *Retinoic acid and transforming growth factor beta differentially inhibit platelet-derived-growth-factor-induced Ito-cell activation.* Biochem J, 1991. **278**: p. 43-47.

23. Rune Blomhoff, K.W., *Perisinusoidal stellate cells of the liver: important roles in retinol metabolism and fibrosis.* The FASEB Journal, 1991. **5**(272): p. 271 - 277.

24. H. Enzan, H.H., S. Iwamura, T. Saibara, S. Onishi, Y. Yamamoto, H. Hara, *Immunohistological identification of Ito cells and their myofibroblastic transformation in adult human liver.* Vichows Archiv, 1994. **424**: p. 249 - 256.

25. Yujiro Tanaka, T.N., Michio Yamane, Tetsuya Irie, Happei Miyakawa, Chifumi Sato, Fumiaki Marumo, *Phenotypic Modulation in Lipocytes in Experimental Liver Fibrosis.* Journal of Pathology, 1991. **164**: p. 273 - 278.

26. Massimo Pinzani, L.G., Ghaleb M. Sabbah, Hanna E. Abboud, *Effects of Platelet-derived Growth Factor and Other Polypeptide Mitogens on DNA synthesis and Growth of Cultured Rat Liver Fat-stroring Cells.* The Journal of Clinical Investigation, 1989. **84**: p. 1786 - 1793.

27. D. Montgomery Bissel, S.-S.W., William R. Jarnagin, F. Joseph Roll, *Cell-specific Expression of Transforming Growth Factor-beta in Rat Liver.* J. Clin. Invest., 1995. **96**: p. 447 - 455.

28. Jeffery L. Wrana, L.A., Rotraud Wieser, Francesc Ventura, Joan Massague', *Mechanism of activation of the TGF-beta receptor.* Nature, 1994. **370**: p. 341-347.

29. S. K. Masur, H.S.D., T. T. Dinh, I. Erenburg, S. Petridou, *Myofibroblasts differentiate from fibroblasts when plated at low density.* Proc. Natl. Acad. Sci USA, 1996. **93**: p. 4219 - 4223.

30. Gressner, A.M., *Persinusoidal lipocytes and fibrosis.* Gut, 1994. **35**: p. 1331 - 1333.

31. Susumu Itoh, F.I., Marie-Jose' Goumanns, Peter ten Dijke, *Signalling of transforming growth factor-beta family members through Smad proteins.* Eur. J. Biochem, 2000. **267**: p. 6954 - 6967.

32. Marie-Jose' Goumanns, C.M., *Functional analysis of the TGF-beta receptor / Smad pathway through gene ablation in mice.* International Journal of Developmental Biology, 2000. **44**: p. 253 - 265.

33. Jiano Yue, M.T.H., Randall S. Frey, Thomas Frielle, Kathleen M. Mulder, *Cloning and Expression of a Rat Smad1: Regulation by TGF-beta and Modulation by the Ras/MEK Pathway.* Journal of Cellular Physiology, 1999. **178**: p. 387-396.

34. Thomas Brand, M.D.S., *Transforming Growth Factor- beta Signal Transduction.* Circulation Research, 1996. **78**(2): p. 173-179.

35. Pasche, B., *Role of Transforming Growth Factor Beta in Cancer.* Journal of Cellular Physiology, 2001. **186**: p. 153 - 168.

36. Massague', J., *TGF-beta signal transduction.* Annu. Rev. Biochem, 1998. **67**: p. 753-791.

37. W. Robb MacLellan, T.B., Micheal D. Schneider, *Transforming Growth Factor-beta in Cardiac Ontegeny and Adaptation.* Circulation Research, 1993. **73**(5): p. 783-789.

38. Shibin Zhou, K.W.K., Bert Vogelstein, *Going mad with Smads.* NEJM, 1999. **341**(15): p. 1144-1145.

39. Shi, Y., *Structural insights on Smad function in TGF-beta signaling.* BioEssays, 2001. **23**(223 - 232).

40. Richard W. Padgett, P.D., Sirkant Krishna, *TGF-beta signaling, Smads, and tumor suppressors.* BioEssays, 1998. **20**: p. 382-391.

41. Carl-Henrik Heldin, K.M., Peter ten Dijke, *TGF-beta signalling from cell membrane to nucleus through SMAD proteins.* Nature, 1997. **390**(4): p. 465-471.

42. Wayne A. Border, N.A.N., *Transforming Growth Factor beta in Tissue Fibrosis.* NEJM, 1994. **331**(19): p. 1286 - 1292.

43. S. Sinha, C.N., C. A. Shuttleworth, C. M. Kielty, *Cellular and extracellular biology of the latent transforming growth factor-beta binding proteins.* Matrix Biol., 1998. **17**: p. 529 - 545.

44. Laurel A. Raferty, D.S., *TGF-beta Family Signal Transduction in Drosophilia Development: From Mad to Smads.* Developmental Biology, 1999. **210**: p. 251-268.

45. Robert Flaumenhaft, M.A., Yasufumi Sato, Kohei Mayazono, John Harpel, Carl-Henrik Heldin, Daniel B. Rifkin, *Role of Latent TGF-beta Binding Protein in the Activation of Latent TGF-beta by Co-Cultures of Endothelial and Smooth Muscle Cells.* The Journal of Cell Biology, 1993. **120**(4): p. 995 - 1002.

46. S. Schultz-Cherry, H.C., D.F. Mosher, T.M. Misenheimer, H.C. Krutzsch, D.D. Roberts, J.E. Murphy-Ullrich, *Regulation of transforming growth factor-beta activation by discrete sequences of thromobospondin-1.* J. Biol. Chem, 1995. **270**: p. 7304 - 7310.

47. S.E. Crawford, V.S., J.E. Murphyullrich, S.F. Ribeiro, J. Lawler, R.O. Hynes, G.P. Biovin, N. Bouck, *Thrombospondin-1 is a major activator of TGF-beta-1 in vivo.* Cell, 1998. **93**: p. 1159 - 1170.

48. Makoto Osaki, T.T., Akihiko Yonekura, Yasuhiro Hirota, Youichi Miyazaki, Hiroyuki Shindo, Shin-ichi Sonta, Shunichi Yamashita, *cDNA cloning and Chromosomal Mapping of Rat Smad2 and Smad4 and Their Expression in Cultured Rat Articular Chondrocytes.* Endocrine Journal, 1999. **46**(5): p. 695-701.

49. Fang Liu, A.H., Julie C. Baker, Jacqueline Doody, Juan Carcamo, Richard M. Harland, Joan Massague', *A human Mad protein acting as a BMP-regulated transcriptional activator.* Nature, 1996. **381**: p. 620-623.

50. R. Derynck, J.A.J., E. Y. Chen, D. H. Eaton, J. R. Bell, R. K. Assoian, A. B. Roberts, M. B. Sporn, D. V. Goeddel, *Human transforming growth factor beta complementary DNA sequence and expression in normal and transformed cells.* Nature, 1995. **316**: p. 701 - 705.

51. M. B. Sporn, A.B.R., L. M. Wakefield, R. K. Assoian, *Transforming growth factor -beta: biological function and chemical structure.* Science, 1986. **233**: p. 532 - 534.

52. M. Pinzani, F.M., V. Carloni, *Signal transduction in hepatic stellate cells.* Liver, 1998. **18**: p. 2-13.

53. Anita B. Roberts, M.A.A., Lois C. Lamb, Joseph M. Smith, Micheal B. Sporn, *New class of transforming growth factors potentiated by epidermal growth factor: Isolation from non-neoplastic tissues.* Proc. Natl. Acad. Sci. USA, 1981. **78**(9): p. 5339 - 5343.

54. MB Sporn, A.R., JH Shull, JM Smith, JM Ward, J Sodek, *Polypeptide transforming growth factor isolated from bovine sources and used for wound healing in vivo.* Science, 1983. **219**: p. 1329 - 1331.

55. Max G. Bachem, D.M., Ralph Melchior, Klaus-Martin Sell, Axel M. Gressner, *Activation of Rat Liver Perisinusoidal Lipocytes by Transforming Growth Factors Derived from Myofibroblastlike Cells.* J. Clin. Invest., 1992. **89**: p. 19 - 27.

56. S. L. Friedman, D.C.R., R. F. McGuire, J. J. Maher, J. K. Boyles, G. Yamasaki, *Isolated hepatic lipocytes and Kupffer cells from normal human liver: morphological and functional characteristics in primary culture.* Hepatology, 1992. **15**: p. 234 - 243.

57. Domique Roulot, A.-M.S., Thierry Coste, A. Donny Stronsberg, Stefano Marullo, *Role of Transforming Growth Factor beta Type II Receptor in Hepatic Fibrosis: Studies of Human Chronic Hepatitis C and Experimental Fibrosis in Ratss.* Hepatology, 1999. **29**: p. 1730 - 1738.

58. Massague', J., *TGF-beta Signalling: Receptors, Transducers, and Mad proteins.* Cell, 1996. **85**: p. 947-950.

59. Laurel A. Raferty, D.S., *TGF-beta Family Signal Transduction in Drosophilia Development: From Mad to Smads.* Developmental Biology, 1999. **210**: p. 251-268.

60. F.A. Spencer, F.M.H., W. M. Gelbert, *Decapentaplegic: A gene complex affecting development in Drosophilia Melanogaster.* Cell, 1982. **28**: p. 451 - 461.

61. Jeff J. Sekelsky, S.J.N., Laurel A. Raferty, Elena H. Chartoff, William M. Gelbert, *Genetic Characterization and Cloning of Mothers against dpp, a Gene Required for decapentaplegic Function in Drosopilia Melanogaster.* Genetics, 1995. **139**: p. 1347-1358.

62. Gregory J. Riggins, S.T., Ester Rozenblum, Craig L. Weinstein, Scott E. Kern, Stanley R. Hamilton, James K.V. Willson, Sanford D. Markowitz, Kenneth W.

Kinzler, Bert Vogelstein, *Mad-related genes in the human.* Nature Genetics, 1996: p. 347-349.

63. Volker Wiersdorff, T.L., Stephan M. Cohen, Marek Mlodzik, *Mad acts downstream of Dpp receptors, revealing a differential requirement for dpp signalling in initiation and propagation of morphogenesis in the Drosophilia eye.* Development, 1996. **122**: p. 2153 - 2162.
64. Stuart J. Newfeld, E.H.C., Jonathan M. Graff, Douglas A. Melton, William M. Gelbart, *Mothers against dpp encodes a conserved cytoplasmic protein required in DPP/TGF-beta responsive cells.* Development, 1996. **122**: p. 2099 - 2108.
65. Masahiro Kawabata, K.M., *Signal transduction of the TGF-beta Superfamily by Smad proteins.* Journal of Biochemistry, 1999. **125**(9): p. 9 - 16.
66. Jonathan M. Graff, A.B., *Xenopus Mad Proteins Transduce Distinct Subsets of Signals for the TGF-beta Superfamily.* Cell, 1996. **85**: p. 479-487.
67. Yan Chen, J.-J.L., Wyle Vale, *Regulation of transforming growth factor-beta and activin-induced transcription by mammalian Mad proteins.* Proc. Natl. Acad. Sci USA, 1996. **93**: p. 12992-12997.
68. Marcus Kretzschmar, F.L., Akiko Hata, Jacqueline Doody, Joan Massague', *The TGF-beta family mediator Smad1 is phosphorylated directly and activated functionally by the BMP receptor kinase.* Genes and Development, 1997. **11**: p. 984-995.
69. Xiaojie Liu, J.Y., Randall S. Frey, Qichao Zhu, Kathleen M. Mulder, *Transforming Growth Factor-beta Signalling through Smad1 in Human Breast Cancer Cells.* Cancer Research, 1998. **58**: p. 4752-4757.
70. Ye-Guang Chen, J.M., *Smad1 Recognition and Activation by the ALK1 Group of Transforming Growth Factor-beta Receptors.* The Journal of Biological Chemistry, 1999. **272**(6): p. 3672-3677.
71. Atsuhito Nakao, T.I., Serhiy Souchenytskyi, Masahiro Kawabata, Akira Ishisaki, Eiichi Oeda, Kiyoshi Tamaki, Jun-ichi Hanai, Carl-Henrik Heldin, Kohei Miyazono, Peter ten Dijke, *TGF-beta receptor-mediated signalling through Smad2, Smad3 and Smad4.* The EMBO Journal, 1997. **16**(17): p. 5353-5362.

72. Giorgio Lagna, A.H., Ali Hemmati-Brivanlou, Joan Massague', *Partnership between DPC4 and SMAD proteins in TGF-beta signalling pathways.* Nature, 1996. **383**: p. 832-836.

73. T. Tsukazaki, T.A.C., A.F. Davison, L. Attisano, J. L. Wrana, *SARA, a FYVE domain protein that recruits Smad2 to the TGF-beta receptor.* Cell, 1998. **95**: p. 779 - 791.

74. M. Nishita, M.K.H., S. Ogata, M. N. Laurent, N. Ueno, H. Shibuya, K. W. Y. Cho, *Interaction of Wnt and TGF-beta signalling pathways during signalling formation of Spemann's organizer.* Nature, 2000. **403**: p. 781 - 785.

75. Z Xiao, X.L., H.F. Lodfish, *A distinct nuclear localization signal in the N-terminus of Smad3 determines its ligand-induced nuclear translocation.* Proc. Natl. Acad. Sci USA, 2000. **97**: p. 23425-23428.

76. L. Xu, Y.-G.C., J. Massauge', *The nuclear import function of Smad2 is masked by SARA and unmasked by TGF-beta-dependent phosphorylation.* Nat. Cell Biol., 2000. **2**: p. 559-562.

77. Shannon L. Stroschein, W.W., Kunxin Luo, *Cooperative Binding of Smad Proteins to Two Adjacent DNA Elements in the Plasminogen Activator Inhibitor-1 Promoter Mediates Transforming Growth Factor-beta-induced Smad-dependent Transcriptional Activation.* The Journal of Biological Chemistry, 1999. **272**(14): p. 9431-9441.

78. X. H. Feng, Y.Z., R. Y. Wu, R. Derynck, *The tumor suppressor Smad4/Dpc4 and transcriptional adaptor CBP/p300 are conactivators for Smad3 in TGF-beta-induced transcriptional activation.* Genes and Development, 1998. **12**: p. 2153 - 2163.

79. R. Janknecht, N.J.W., T. Hunter, *TGF-beta-stimulated cooperation of Smad proteins with the coactivators CBP/p300.* Genes and Development, 1998. **12**: p. 2114 - 2119.

80. Jan L. Christian, T.N., *Can't get no SMADisfaction: Smad proteins as positive and negative regulators of TGF-beta family signals.* BioEssays, 1999. **21**: p. 382-390.

81. Wei Li, Feiei Chen, Raman P. Nagarajan, Xubao Lui, Yan Chen, *Characterization of the DNA-Binding Property of Smad5.* Biochemical and Biophysical Research Communications, 2001. **286:** p. 1163 – 1169

82. Unpublished results, Liver Diseases Unit, Department of Internal Medicine, University of Manitoba.